

CRES

REMOTE SENSING LABORATORY

NASA CR-

141869

ROUGH SURFACE SCATTERING BASED ON FACET MODEL

(NASA-CR-141869) · ROUGH SURFACE SCATTERING
BASED ON FACET MODEL (Kansas Univ. Center
for Research, Inc.) · 158 p HC \$6.25 CSCL 20F

N75-26478

Unclas

G3/43 26668

Remote Sensing Laboratory
RSL Technical Report 177-52

H. R. Khamsi

A. K. Fung

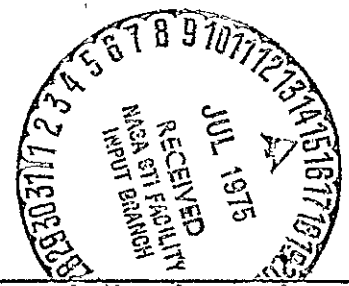
F. T. Ulaby

November, 1974

Supported by:

NATIONAL AERONAUTICS AND SPACE ADMINISTRATION
Lyndon B. Johnson Space Center
Houston, Texas 77058

CONTRACT NAS 9-10261



THE UNIVERSITY OF KANSAS CENTER FOR RESEARCH, INC.

2291 Irving Hill Drive—Campus West Lawrence, Kansas 66045



THE UNIVERSITY OF KANSAS SPACE TECHNOLOGY CENTER

Raymond Nichols Hall CENTER FOR RESEARCH, INC.

2291 Irving Hill Drive—Campus West Lawrence, Kansas 66045

Telephone:

ROUGH SURFACE SCATTERING BASED ON FACET MODEL

Remote Sensing Laboratory
RSL Technical Report 177-52

H. R. Khamsi

A. K. Fung

F. T. Ulaby

November, 1974

Supported by:

NATIONAL AERONAUTICS AND SPACE ADMINISTRATION
Lyndon B. Johnson Space Center
Houston, Texas 77058

CONTRACT NAS 9-10261

TABLE OF CONTENTS

	<u>Page</u>
ABSTRACT	v
1.0 INTRODUCTION	1
2.0 TECHNICAL REVIEW	2
2.1 Specular Point Model	2
2.2 Small Scatterers Model	6
2.2.1 Spetner's Random-Scatterer Model	6
2.2.2 Waite's Model	7
2.3 Facet Model	9
2.3.1 Spetner's Model	9
2.3.2 Katzin's Model	12
2.3.2.1 Katzin's First Model: Grazing Angles	12
2.3.2.2 Katzin's Second Model: High Depression Angle	17
3.0 PROPOSED FACET MODEL	20
3.1 Large Facets	23
3.2 Medium Size Facets	31
3.3 Small Facets	34
4.0 PROPERTIES OF THE SYSTEM	38
4.1 System and Frequency Spectrum	38
4.1.1 Radar	38
4.1.2 Frequency Spectrum of the Signal	40
4.2 Frequency Averaging	47
4.2.1 Uniform Scatterer Model	47
4.2.1.1 Uniform Scatterer Model with no Penetration	47
4.2.1.2 Uniform Scatterer Model with Penetration	62
4.2.2 Number of Independent Samples Based on Facet Model	75
4.2.2.1 Mean and Variance of the Return	76
4.2.2.2 Number of Independent Samples	81
4.2.3 Comparison of the Results with Measured Data	91
4.2.3.1 Alfalfa	91
4.2.3.2 Bare Ground	91

TABLE OF CONTENTS (CONTINUED)

	<u>Page</u>
5.0 RESULTS	95
5.1 Reflection Coefficient	95
5.1.1 Large Facets	95
5.1.2 Small Facets	99
5.1.3 Medium Facets	100
5.2 Comparison of the Results of the Theory with Data	100
5.3 Comparison of Facet Model with Katzin's Facet Model	128
6.0 CONCLUSION	136
REFERENCES	138
APPENDIX A: Katzin's Assumption	140
APPENDIX B: RMS Height for Small Facets	142
APPENDIX C: Correlation Radius of Small Facets	148
APPENDIX D: Evaluation of the Integral for Large Facets	153

LIST OF FIGURES

		Page
Figure 1.	Average number of specular points from Eq. (2-2).	5
Figure 2.	Average backscattering cross-section per unit area σ° . From Eq. (2-6).	5
Figure 3.	Wavelength dependence of normalized radar cross-section (random scatterer model) from Spetner and Katz, 1960.	8
Figure 4.	Effective slope as a function of incidence wavelength from Spetner and Katz, 1960.	11
Figure 5.	Wavelength dependence of σ° , from Eq. (2-19).	11
Figure 6.	Average σ° for small and large facets.	14
Figure 7.	RCS of a disk as a function of dimension/wavelength.	21
Figure 8.	Measured σ° for small and medium facets.	32
Figure 9.	Measured σ° for small, medium and large facets.	32
Figure 10.	Measured VV polarization backscatter cross-section versus the angle of incidence for perfectly conducting rectangular planes with heights of $2\lambda_0$ and lengths of $0.5\lambda_0$ and λ_0 .	32
Figure 11.	Illustration showing frequency relationship between transmitted and received signals.	39
Figure 12.	Basic block diagram of 8-18 GHz radar spectrometer.	41
Figure 13.	Frequency of the transmitted signal as a function of time.	42
Figure 14.	Frequency spectrum of the radar.	46
Figure 15.	Radar illuminated area.	49
Figure 16.	Power spectrum of transmitted wave.	58
Figure 17.	Variance reduction with rectangular spectrum panchromatic illumination. From Eq. (4-56).	61
Figure 18a.	Uniform scatterer model with penetration.	63
Figure 18b.	Uniform scatterer model with penetration.	69
Figure 19.	Time delay based on facet model.	84
Figure 20.	Number of independent samples for alfalfa.	92
Figure 21.	Number of independent samples for bare ground.	93
Figure 22.	Measured dielectric constant data of loamy soil as a function of moisture content by weight around 10 GHz. Solid curves were drawn to fit the data points and the broken curves were extrapolated [25].	97
Figure 23.	Reflection coefficient for large size facets.	98
Figure 24.	Reflection coefficient for medium size facets.	101
Figure 25.	Reflection coefficient for small size facets.	102
Figure 26.	Contribution of the large facets to the return.	103
Figure 27.	Contribution of the large facets to the return.	104
Figure 28.	Contribution of the large facets to the return.	105
Figure 29.	Contribution of medium size facets to the return for HH polarization.	106
Figure 30.	Contribution of medium size facets to the return for VV polarization.	107
Figure 31.	Contribution of small facets to the return.	108
Figure 32.	RCS of bare ground; moisture content = 5.9%, frequency = 9 GHz, polarization = HH.	110
Figure 33.	RCS of bare ground; moisture content = 5.9%, frequency = 9 GHz, polarization = VV.	111
Figure 34.	RCS of bare ground; moisture content = 5.9 %, frequency = 14.2 GHz, polarization = HH.	112

LIST OF FIGURES (CONTINUED)

	<u>Page</u>
Figure 35. RCS of bare ground; moisture content = 5.9%, frequency = 14.2 GHz, polarization = VV.	113
Figure 36. RCS of bare ground; moisture content = 9.4%, frequency = 9 GHz, polarization = HH.	114
Figure 37. RCS of bare ground; moisture content = 9.4%, frequency = 9 GHz, polarization = VV.	115
Figure 38. RCS of bare ground; moisture content = 9.4%, frequency = 14.2 GHz, polarization = HH.	116
Figure 39. RCS of bare ground; moisture content = 9.4%, frequency = 14.2 GHz, polarization = VV.	117
Figure 40. RCS of bare ground; moisture content = 17.8%, frequency = 9 GHz, polarization = HH.	118
Figure 41. RCS of bare ground; moisture content = 17.8%, frequency = 9 GHz, polarization = VV.	119
Figure 42. RCS of bare ground; moisture content = 17.8%, frequency = 14.2 GHz, polarization = HH.	120
Figure 43.] RCS of bare ground; moisture content = 17.8%, frequency = 14.2 GHz, polarization = VV.	121
Figure 44. RCS of bare ground; moisture content = 21.1%, frequency = 9 GHz, polarization = HH.	122
Figure 45. RCS of bare ground; moisture content = 21.1%, frequency = 9 GHz, polarization = VV.	123
Figure 46. RCS of bare ground; moisture content = 21.1%, frequency = 14.2 GHz, polarization = HH.	124
Figure 47. RCS of bare ground; moisture content = 21.1%, frequency = 14.2 GHz, polarization = VV.	125
Figure 48. Four samples of ground contour. Moisture content = 17.8%.	126
Figure 49. RCS based on Katzin's derivation.	134
Figure 50. RCS based on Katzin's derivation.	135
Figure A-1. Radar cross section of a large circular disk.	141
Plate 1. Photographs of bare fields at four different dates.	127

ABSTRACT

A theoretical investigation was performed to develop a model for the radar return from bare ground. The validity of the model was tested by comparing its theoretical prediction with measured data collected by the University of Kansas Remote Sensing Laboratory 8-18 GHz radar spectrometer system.

It was assumed that the target area consists of a collection of small, medium and large size facets. Then this model was used to calculate the radar cross section of bare ground and the effect of the frequency averaging on the reduction of the variance of the return.

It was shown that by assuming that the distribution of the slope to be Gaussian, and by assuming that the distribution of the length of the facet to be in the form of the positive side of a Gaussian distribution, the results are in better agreement with experimental data than the results of previous facet models. It was also shown that for this calculation we do not need to know the exact correlation length of the small structure on the ground, instead an effective correlation length was calculated based on the facet model and the wavelength of the incident wave. Hence, the parameters necessary to specify the surface are: standard derivations of slope in x and y directions, standard deviation of the distribution of the facet size, and the dielectric constants of the target.

For investigating the effect of the frequency averaging we expanded the previously available results based on the uniform scatterer model and took into consideration the penetration effect. It was shown that at small incidence angles, the number of independent samples predicted is significantly larger and in better agreement with measured data from alfalfa.

It was also shown that based on the facet model assumption the reduction in the variance of the return is not only a function of the product of the sweep band and the time span of the target, as the uniform scatterer model indicates, but it is also a function of the geometrical properties of the surface, center frequency of the incident wave and the polarization.

1.0 INTRODUCTION

The purpose of this investigation is to develop a theoretical model for the radar return from bare ground. The validity of the model is to be tested by comparing its theoretical predictions with measured data collected by the University of Kansas Remote Sensing Laboratory 8-18 GHz radar spectrometer system.

In 1956 Katzin [7] proposed that the surface of an area-extended target can be assumed to be composed of a collection of independent facets of varying sizes and slopes. This facet model was developed for predicting sea backscatter at large angles of incidence. Over its range of validity ($>85^\circ$), Katzin reports good agreement with experimental data. Using the same facet backscatter approach, Katzin later developed a second model [8] to cover the other end of the incidence angle range (0° to 40°). In both models Katzin divides his facet sizes into small and large facets and assumes certain facet size and facet slope distributions.

A study of the backscatter from circular disks indicates that the variation of the radar cross section of a disk as a function of its radius (measured in wavelengths) suggests that facets should be separated into three different size ranges rather than two. Thus, in the present study a medium size facet group is introduced along with other modifications of Katzin's models. The results indicate a significant improvement over Katzin's two scale model in terms of agreement with experimental data. Furthermore, the proposed model does not have any inherent incidence angle range limitations.

Prior to developing the model proposed in this study (Chapter 3), a detailed discussion of Katzin's models is presented in Chapter 2 in order to facilitate the understanding of the modifications made in Chapter 3. Chapter 4 describes the properties of the 8-18 GHz radar spectrometer used to collect the experimental data. Two types of experiments were performed; the first experiment consisted of making about 140 independent backscatter measurements of different illuminated cells of alfalfa and bare-soil fields. Measurements were made at 9 GHz with VV polarization at incidence angles of 0° (nadir), 10° , 20° , 30° , 50° and 70° . At each angle, the mean and variance of the backscattering coefficient were calculated and used to calculate the number of independent samples assuming an χ^2 fading distribution. In the second experiment, the radar return from a bare ground field was measured under several soil moisture conditions. Along with the moisture changes, the surface texture changed as well. Comparison of theoretical predictions with measured data is presented in Chapter 5.

2.0 TECHNICAL REIVEW

It is possible to categorize the modeling of extended targets by facets into those different types:

- i) Modeling by a collection of plane facets of infinite size each of which generates a specular type pattern.
- ii) Modeling by a collection of small facets with a uniform pattern and size distribution.
- iii) Modeling by facets of finite dimensions with some assumed patterns and size distributions.

2.1 Specular Point Model

The basic assumption of this model is that the radar return comes only from specular points; in other words, it is assumed that we can ignore all the facets which are not normal to the direction of propagation.

This geometrical optics solution has been shown by Kodis [9] to be equivalent to the physical optics solution when the principle of stationary phase is used to evaluate the Helmholtz integral. In order to show this he performs the integration at a typical stationary phase point and averages the result following integration. Then the problem resolves itself into one of determining the average number of stationary phase points per unit area and the average contribution from each point.

Kodis applied his method to a rough surface. Then by assuming that the return from each specular point has a random phase, he showed that each illuminated specular point scatters like a tangent sphere whose radius is the mean of the two principal radii of the surface at the specular point. Then, because the radar cross section of a perfect conducting sphere of radius r is equal to πr^2 (high frequency), the return from the target is:

$$\bar{\sigma} = \pi \langle |r_1 r_2| \rangle n_A \quad (2-1)$$

where r_1 and r_2 are the principal radii of curvature of the surface and n_A is the number of illuminated specular points.

Barrick [2] examined the geometrical considerations relevant to the occurrence of stationary phase points. His analysis is similar to the zero-crossing problem in communication theory and his approach follows the same approach that can be found in Rice [16]. For a two dimensional Gaussian distributed surface Barrick [2] found the average points per unit surface area to be

$$n_A = \frac{7.255}{\pi^2 \ell^2} \exp \left[-\tan^2 \theta / s^2 \right] \quad (2-2)$$

where

h^2 = mean square height

ℓ = correlation distance of the surface

θ = local incident angle

n_A = number of specular points per unit area

From the geometry of the surface, the product of the principal radii of curvature can be expressed in terms of the derivatives of the surface of the target, $\xi(x,y)$, as follows [24]:

$$|r_1 r_2| = \frac{(1 + \xi_x^2 + \xi_y^2)^2}{|\xi_{xx} \xi_{yy} - \xi_{xy}^2|} \quad (2-3)$$

From the use of the stationary phase technique ξ_x and ξ_y are known quantities. Hence, the variables in Eq. (2-3) only appear in the denominator.

Barrick argued that because in getting Eq. (2-1) we use the stationary phase technique, it follows that the denominator of Eq. (2-3) is not very small. Hence, he assumed that

$$\langle |r_1 r_2| \rangle = \frac{(1 + \xi_x^2 + \xi_y^2)^2}{\langle |\xi_{xx} \xi_{yy} - \xi_{xy}^2| \rangle} \quad (2-4)$$

Then by averaging the denominator he obtained

$$\langle |r_1 r_2| \rangle = 0.138 \pi \frac{l^2}{s^2} \sec^4 \theta \quad (2-5)$$

where

l = correlation distance

S = rms slope

θ = incident angle

Then he substituted $\langle |r_1 r_2| \rangle$ and n_A in Eq. (2-1) and obtained an expression for scattering coefficient, σ^0 given by:

$$\sigma_0 = \frac{\sec^4 \theta}{s^2} \exp \left[-\tan^2 \theta / s^2 \right] \quad (2-6)$$

Barrick's method of calculating n_A differs from Longuet-Higgin's [12] method in that the latter examines the average total number of specular points rather than the average number per unit area.

Longuet-Higgin [11] in a special case, assumes that the surface is isotropically Gaussian. Then he calculated the joint probability distribution function of the first and second derivatives of the surface. By using this probability in a method similar to zero crossing technique he calculates the probability of having a specular point in an area equal to $dx dy$. Then by integrating this probability he calculates the total number of specular points on the surface. His result is as follows:

$$N_{total} = \frac{(m_{04} + 2m_{02} + m_{40})^2}{8\sqrt{3}} \quad (2-7)$$

where

$$m_{pq} = \iint_0^{\infty} E(u, v) u^p v^q du dv \quad (2-8)$$

$E(u, v)$ = power spectrum of the surface

h = the distance between source and surface

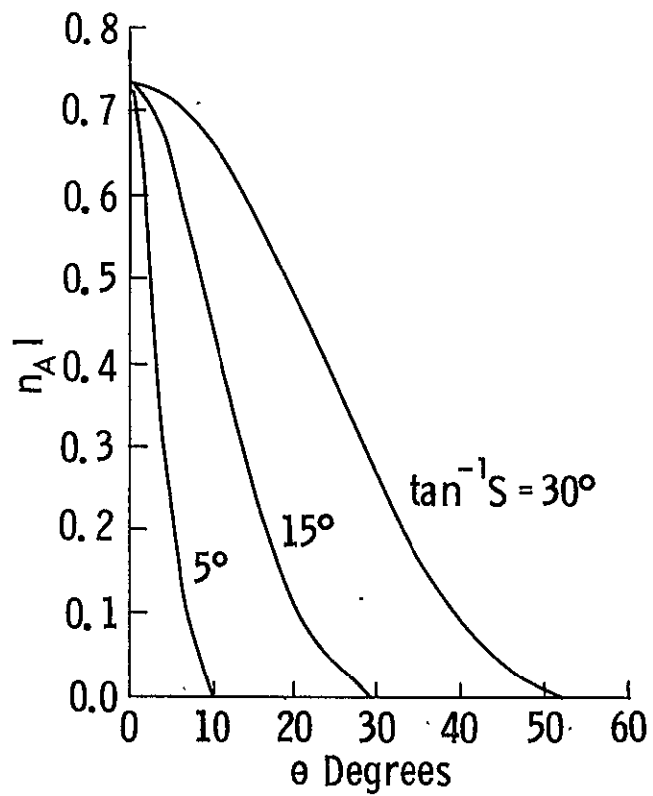


Figure 1. Average number of specular points from Eq. (2-2).

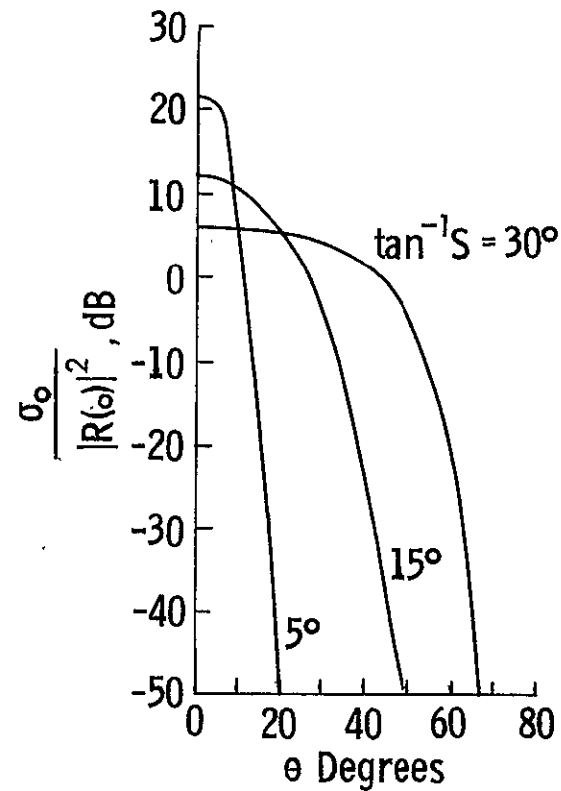


Figure 2. Average backscattering cross-section per unit area σ_0 . From Eq. (2-6).

Barrick [2] in his investigation assumes that the surface height and its second derivatives, (ξ, ξ_{xx}) , are uncorrelated. Seltzer [20] improves Barrick's derivation by first using a correlated distribution function to calculate the probability of having a specular point for a given height. Then by averaging this conditional probability for a given height distribution he calculates the average number of specular points per unit area. For a one dimensional surface, he obtained

$$N = \frac{\sqrt{b}}{\pi l} \exp\left[-\tan^2 \theta / s^2\right] \quad (2-9)$$

where

$$s^2 = \frac{4h^2}{l^2}$$

N = number of specular points

l = correlation distance

h^2 = mean square height

2.2 Small Scatterers Model

2.2.1 Spetner's Random-Scatterer Model [22]

In this model it is assumed that the radar return is composed of the summation of the returns from a collection of randomly located scatterers. Then

$$\bar{\sigma}_0 = p_s \bar{\sigma}_1 \quad (2-10)$$

where

p_s = the density of the scatterer

$\bar{\sigma}_1$ = the average RCS of each scatterer

It is further assumed that the density of the scatterers remains a constant up to a cutoff wavelength λ_c and then decreases as λ^{-2} for $\lambda > \lambda_c$:

$$p_s = \begin{cases} p_0 & \lambda < \lambda_c = (c_1/p_0)^{1/2} \\ c_1/\lambda^2 & \lambda > \lambda_c \end{cases} \quad (2-11)$$

where

P_o = the actual density of scatterers

c_1 = a constant which is a function of surface properties

If the effective area of the scatterer is large in comparison to wavelength then:

$$\bar{\sigma}_1 = \frac{4\pi}{\lambda^2} A_s^2 \quad (2-12)$$

where

λ = wavelength

A_s = effective area of the scatterer

But if A_s is small then the RCS will obey the Rayleigh law and will be

$$\bar{\sigma}_1 = C_2 / \lambda^4 \quad (2-13)$$

where C_2 is a function of the scatterer size. So the average RCS of a scatterer will be

$$\bar{\sigma}_1 = \begin{cases} \frac{4\pi}{\lambda^2} A_s^2 & \lambda < \lambda_0 \\ C_2 / \lambda^4 & \lambda > \lambda_0 \end{cases} \quad (2-14)$$

where λ_0 is the transition wavelength.

By substituting Eq. (2-11) through Eq. (2-14) into Eq. 2-10, the results shown in Table 1 are obtained. Graphically σ^o vs. wavelength is shown in Figure 3.

2.2.2 Waite's Model [26]

In this model it is assumed that 1) the target may be represented by a collection of scatterers which are located randomly on the target, 2) amplitude of the return from each scatterer is a sample of a Gaussian distribution function with zero mean, and 3) it is further assumed that RCS of scatterers are independent of the frequency of the incident wave.

TABLE 1

	$\lambda < \lambda_0$	$\lambda > \lambda_0$
$\lambda < (C_1/p_0)^{1/2}$	$\sigma^o = \frac{4\pi p_0 \rho A^2 s}{\lambda^2}$	$\sigma^o = \frac{C_2 p_0 v^2}{\lambda^4}$
$\lambda > (C_1/p_0)^{1/2}$	$\sigma^o = \frac{4\pi C_1 \rho A^2 s}{\lambda^4}$	$\sigma^o = \frac{C_1 C_2 v^2}{\lambda^6}$

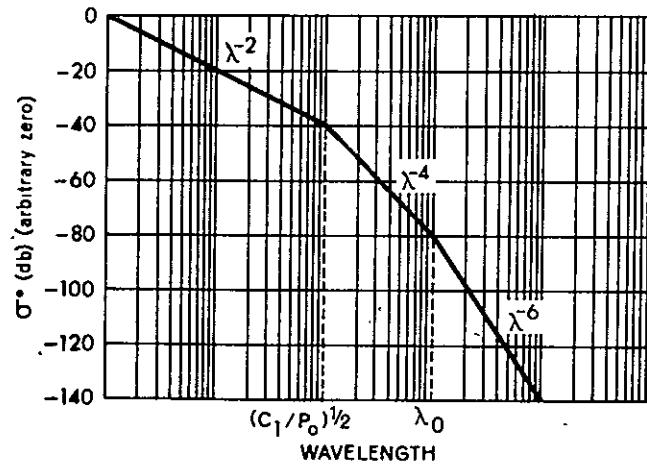


Figure 3. Wavelength dependence of normalized radar cross-section (random scatterer model) from Spetner and Katz, 1960.

Based on these assumptions Waite has shown that the distribution of the returned power will have the form:

$$p(w) = \frac{1}{(2\sigma_c^2)^{N/2} (N/2 - 1)!} w^{(N/2 - 1)} \exp\left[-w/2\sigma_c^2\right] \quad (2-15)$$

where

$$\sigma_c^2 = \sum a_n^2$$

N = number of independent samples which is equal to one for monochromatic case

a_n = amplitude of the return from the n^{th} scatterer

$p(w)$ = probability distribution of the return

He further showed that:

$$N = \frac{\text{transmitted signal bandwidth}}{\text{system resolution bandwidth}}$$

2.3 Facet Model

2.3.1 Spetner's Model

In this model it is assumed that the surface is reflective, continuous, and with continuous derivatives. It is further assumed that :

- i) The effective mean square slope of the surface is constant if we increase the wavelength from zero to some number λ_2 , but if we increase it further, the effective mean square slope starts to get smaller (Figure 4). It is further assumed that the density of the facets at normal incidence, $d_{SL}(0)$, varies with the wavelength as follows

$$d_{SL}(0) = \begin{cases} C_3/\lambda_2^2 & \lambda < \lambda_2 \\ C_3/\lambda^2 & \lambda > \lambda_2 \end{cases} \quad (2-16)$$

where C_3 is a constant close to one.

(ii) The radar cross section of a large facet for vertical incidence is equal to

$$\sigma_{1L}(\theta) = \begin{cases} \frac{4\pi A_s}{\lambda^2} & \lambda < \lambda_2 \\ C_4/\lambda^4 & \lambda > \lambda_2 \end{cases} \quad (2-17)$$

where A_s is the area of the facet and C_4 is a constant. Then,

$$\sigma_L^0 = d_{sL} \bar{\sigma}_L = \begin{cases} C_3/\lambda_2^2 \times \frac{4\pi A_s}{\lambda^2} & \lambda < \lambda_2 \\ C_3/\lambda^2 \times C_4/\lambda^4 & \lambda > \lambda_2 \end{cases} \quad (2-18)$$

So from the above assumptions, and when the angular effect is included, the return from a target which consists of small and large facets, assuming a Gaussian slope distribution for the large scatterers, will be in the form of

$$\sigma_0 = \begin{cases} C_3 \frac{4\pi A_s}{\lambda_2^2} \frac{1}{\lambda^2} \exp\left[-\frac{\tan^2 \theta}{2s_0^2}\right] & \lambda < \lambda_2 \\ \frac{C_4}{\lambda^6} \exp\left[\frac{-\tan^2 \theta}{2s_0^2} \frac{\lambda_2/\lambda}{\lambda_2/\lambda}\right] + C_5/\lambda^6 & \lambda > \lambda_2 \end{cases} \quad (2-19)$$

where

- C_3, C_4, C_5 = are only function of surface properties
- A_s = average area of large facets
- λ_2 = transition wavelength which is a function of surface properties
- θ = look angle
- λ = wavelength

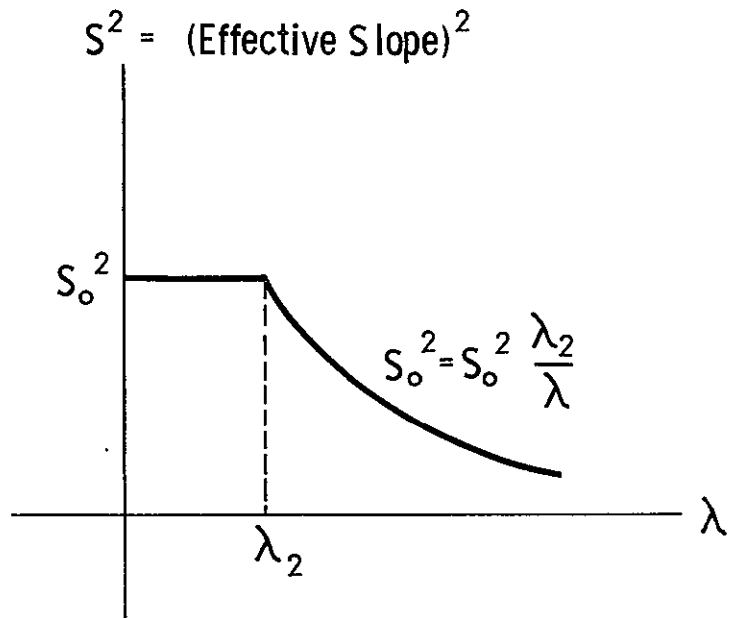


Figure 4. Effective slope as a function of incidence wavelength from Spetner and Katz, 1960.

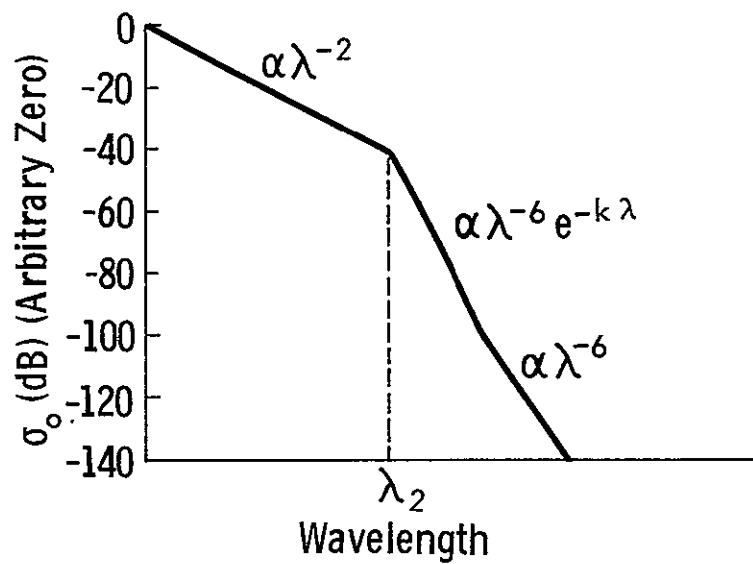


Figure 5. Wavelength dependence of σ_0 , from Eq. (2-19).

$$\begin{array}{ll}
 \sigma_o^2 & = \text{actual mean square slope} \\
 \sigma_o^2 \lambda^2 / \lambda & = \text{effective mean square slope} \\
 C_5 / \lambda^6 & = \text{contribution from small facets}
 \end{array}$$

The wavelength dependence of σ^o at normal incidence is shown in Figure 5.

2.3.2 Katzin's Model [7,8]

This model differs from Spetner's in that he introduces a pattern of finite width for the main beam of large facets, thus large facets which are not located along the specular direction also contribute to the backscattered return.

Katzin's first model [7] is primarily concerned with backscattering at large incident angles. In fact it is only valid for angles larger than about 85° . In his second model the range of validity is broader and it ranges from 0° to 40° incident angles.

2.3.2.1 Katzin's First Model: Grazing Angles [7]

In the first model the facets are divided into two types: 1) large facets, which are large compared to the wavelength so that their return is highly directive and can be predicted by the physical optics method, and 2) small facets, which are so small that the return can be assumed to be proportional to f^4 (f is the incident frequency) and the pattern of the return is uniform. In addition, the following assumptions are made:

- 1) The surface of the target may be considered to be composed of a collection of facets of different sizes distributed around a mean surface in Z direction.
- 2) The facets are randomly located so that the backscatter powers from the two types of facets are additive.
- 3) Shadowing and multiple reflection effects are neglected.
- 4) For a large facet, in small grazing angles, the relation between the average radar cross section per unit area and the actual area may be derived through the following three assumptions [6]

$$(i) \quad \sigma/A \sim (A/\lambda^2)^1 \quad \text{plane of facet lies vertically}$$

$$(ii) \quad \sigma/A \sim (A/\lambda^2)^0 \quad \text{plane tilted at an angle } \theta \text{ from the vertical position}$$

$$(iii) \quad \bar{\sigma}/A \sim (A/\lambda^2)^{-1} \quad \text{plane tilted at an angle } \theta \text{ from the vertical and rotated by an angle } \phi \text{ in azimuth}$$

where $\sigma = \text{RCS}$, $A = \text{area}$, and $\lambda = \text{wavelength}$. From (ii) and (iii) it follows that for facets for which $\theta = \text{constant}$, and $\pi \geq \phi \geq 0$ an average RCS over ϕ may be obtained, i.e.

$$\bar{\bar{\sigma}}/A = \langle \bar{\sigma}/A \rangle \sim (A/\lambda^2)^{-1/2} \quad (2-20)$$

where $\bar{\sigma}$ is the average RCS for a fixed θ .

The mathematical proof for the last result is given in Appendix A.

5) For small facets it can be assumed that the RCS is proportional to λ^{-4} (Rayleigh region). Then from [19]

$$\frac{\bar{\sigma}_{HH}}{A} = \frac{\bar{\sigma}_{HH}}{A} = \frac{4^5}{9} \left[1 + \frac{\cos^2 \theta_g}{2} \right]^2 \frac{A^2}{\lambda^4} \sim (A/\lambda^2)^2$$

$$\frac{\bar{\sigma}_{VV}}{A} = \frac{\bar{\sigma}_{VV}}{A} = \frac{4^5}{9} \sec^4 \theta_g \frac{A^2}{\lambda^4} \sim (A/\lambda^2)^2 \quad (2-21)$$

where θ_g is the grazing angle ($\theta_g = \pi/2 - \theta$).

6) Because $\bar{\sigma}/A$ is an increasing function of A/λ^2 for small facets and it is a decreasing function for the large ones, (assumptions 4 and 5), Katzin assumed that we can extrapolate $\bar{\sigma}/A$ vs. A/λ^2 for large and small facets into the intermediate region with the intersection point serving as the transition point (Figure 6).

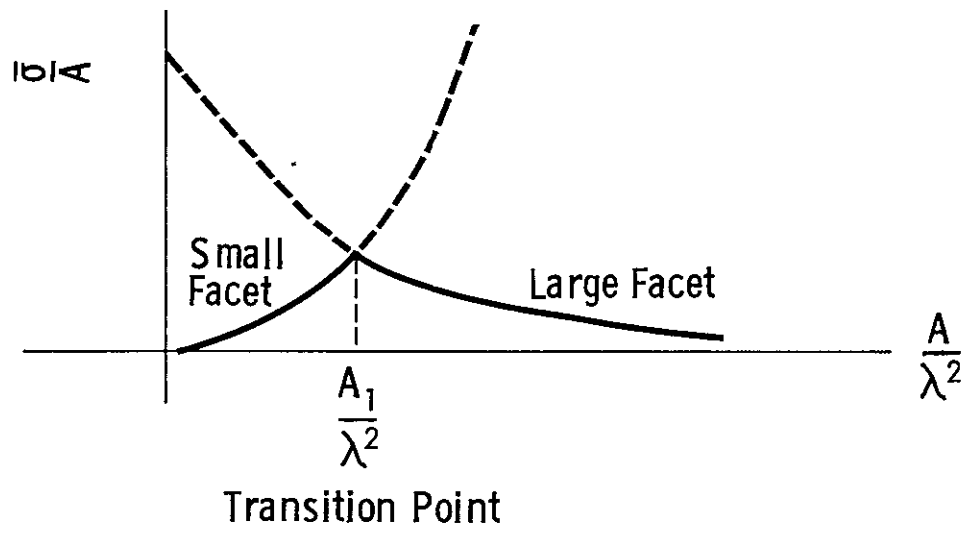


Figure 6. Average σ^o for small and large facets.

By using the physical optics method, it can be shown, (Appendix A) that

$$\bar{\sigma}/A = (4\pi^{3/2})^{-1} \tan^2 \theta_g \sec \theta_g (A/\lambda^2)^{-1/2} \quad (2-22)$$

Consider first the horizontally polarized case. As stated earlier for small facets

$$\frac{\bar{\sigma}_{HH}}{A} = \frac{4^5}{9} \left[1 + \frac{\cos^2 \theta_g}{2} \right]^2 \left(\frac{A}{\lambda^2} \right)^2 \quad (2-23)$$

The transition point is defined by

$$\left(\frac{\bar{\sigma}_{HH}}{A_1} \right) = \left(\frac{\bar{\sigma}}{A_1} \right) \quad (2-24)$$

small facets
from Eq. (2-21)

large facets
from Eq. (2-20)

where A_1 is the transition area for horizontal polarization, given by

$$(A_1)_{HH} = \lambda^2 \left[\frac{\frac{1}{4\pi^{3/2}} \tan^2 \theta_g \sec \theta_g}{\frac{4^5}{9} \left[1 + \frac{\cos^2 \theta_g}{2} \right]^2} \right]^{2/5} \quad (2-25)$$

From the above equation and from the relation between the diameter of a circular facet and its area

$$D = \left(\frac{4}{\pi} A \right)^{1/2}$$

then

$$\pi D_1 = \pi \sqrt{\frac{4}{\pi} A_1} = 4\sqrt{\pi} \frac{\lambda}{2} \left[\frac{\frac{1}{4\pi^{3/2}} \tan^2 \theta_g \sec \theta_g}{\frac{4^5}{9} \left(1 + \frac{\cos^2 \theta_g}{2} \right)^2} \right]^{1/5} \quad (2-26)$$

$$\triangleq \beta \frac{\lambda}{2}$$

where

$$\beta \triangleq 4 \sqrt{\pi} \left[\frac{\frac{1}{4\pi^{3/2}} \tan^2 \theta_g \sec \theta_g}{\frac{4^5}{9} \left(1 + \frac{\cos^2 \theta_g}{2}\right)^2} \right]^{1/5}$$

where D_1 is the diameter for a facet with transition area and β is a number which varies from .4 to 1.2 for grazing angles changing from 10° to 30° .

For vertical polarization we can argue in the same way and get a similar equation for $(A_1)_{VV}$.

Figure 6 shows that the normalized radar cross section for facets with area equal to A_1 is maximum. It follows that the facets for which the diameter is comparable to the wavelength have the largest RCS. So for a target, the bigger the number of facets with a diameter comparable to the wavelength the larger the return will be (Figure 6). Hence there is a direct relation between the distribution of the facet size of a target and the wavelength dependence of the return.

If the distribution of the slope and the distribution of the area of the target face are known we can calculate the backscattering coefficient as follows

$$\begin{aligned} \bar{\sigma}^o &= \bar{\sigma}_s^o + \bar{\sigma}_l^o \\ &= \int_{A_0}^{A_1} N_s(A) P_s(z') \bar{\sigma}_s(z', A) dz' dA + \\ &+ \int_{A_1}^{A_2} N_l(A) P_l(z') \bar{\sigma}_l(z', A) dz' dA \end{aligned} \quad (2-27)$$

where

P_s and P_l = are respectively, the distribution function of slopes for small and large facets

N_s and N_l = are the distribution functions of facet sizes

A_0, A_1, A_2 = are respectively, the areas of the smallest, transition, and largest facets

Z' = slope

$$\begin{aligned}
\sigma_s^o &= \text{return contributed by small facets} \\
\sigma_l^o &= \text{return contributed by large facets} \\
\overline{\sigma_s} &= \text{average RCS of a small facet from Eq. (2-21),} \\
\overline{\sigma_l} &= \text{average RCS of a large facet from Eq. (2-20)}
\end{aligned}$$

2.3.2.2 Katzin's Second Model: High Depression Angle [7]

For near vertical incidence the radar cross section of large facets computed by using the physical optics method is

$$\overline{\sigma}_l = 4\pi \frac{A^2}{\lambda^2} \cos^2 \alpha \left(\frac{\sin \kappa w \delta}{\kappa w \delta} \right)^2 \left(\frac{\sin \kappa l \mu}{\kappa l \mu} \right)^2 \quad (2-28)$$

where

$$\mu = \sin \theta - Z_y \cos \theta$$

$$\delta = -Z_x \cos \theta$$

$$\cos \alpha = -\cos \theta - Z_y \sin \theta$$

and

l, w = are dimensions of the facet

A = the area and is equal to $l \times w$

Z_x, Z_y = are, respectively, slopes of the facet in x and y directions

λ = wavelength

For this model the RCS of the small facets, for small incidence angles, is assumed to be

$$(\overline{\sigma}_s)_{\mu\mu} = 4 \frac{5}{9} A^3 / \lambda^4 \quad (2-29)$$

With the RCS for the two types of facets known, the total RCS can be obtained by averaging each individual RCS over its size and slope distributions and then sum them together, i.e.

$$\overline{\sigma}^o = \overline{\sigma}_s^o + \overline{\sigma}_l^o \quad (2-30)$$

where

$$\bar{\sigma}_s^0 = \frac{4^5}{9 \lambda^4} \int_{A_0}^{A_1} A^3 N(A) dA \quad (2-31)$$

$$\begin{aligned} \bar{\sigma}_l^0 = \frac{4\pi}{\lambda^2} & \int_{-\infty}^{\infty} \int_{A_1}^{A_2} A^2 N(A) P(Z_x, Z_y) \sigma_s^2 \times \left(\frac{\sin K \omega \delta}{K \omega \delta} \right)^2 \\ & \times \left(\frac{\sin Kl \mu}{Kl \mu} \right)^2 dA dz_x dz_y \end{aligned} \quad (2-32)$$

where

A_0, A_1, A_2 = are respectively, the smallest, transition, and the largest are in facet distribution

$P(Z_x, Z_y)$ = distribution function of slope

$N(A)$ = distribution function of area

In order to calculate the above equation Katzin assumes that

- (i) $K \omega \sigma_s \sigma_x / \sqrt{2} > 1$
 - (ii) $Kl \sigma_s \sigma_y / \sqrt{2} > 1$
 - (iii) $2 Kl \sigma_s^2 / \tan^2 \theta > 1$
- (2-33)

where

$$K = 2\pi/\lambda$$

w = width of facet, x direction

l = length of facet, y direction

θ = incident angle

σ_x, σ_y = are respectively, the standard deviation of the slope along x
and y directions

3.0 PROPOSED FACET MODEL

Data taken from disks of different sizes shows that the variation of the RCS as a function of the disks dimensions has the shape shown by the solid line in Figure 7 below; where $Ka \equiv 2\pi/\lambda \times$ radius of the disk [19]. It is apparent from the solid curve in this figure that there are at least three recognizable regions, and hence it appears appropriate to separate the size of facets into the three categories rather than two. Approximately, the following three types of facets may be defined:

- (i) Large facets for which $Ka > \pi$ and the return can be determined by the physical optics method.
- (ii) Medium size facets for which $\pi > Ka > \frac{2\pi}{5}$. For this region the return is almost constant and does not change more than 3 dB for the whole range. It may be assumed that the value of the RCS for the whole range varies with $A^{5/4}$.
- (iii) Small size facets for which $\frac{2\pi}{5} > Ka$. For this case the small perturbation method can be used to evaluate the RCS.

By dividing the facets, according to their sizes, to three instead of two categories, we overcome the problem of extrapolating the curves for large and small facets to intermediate sizes. This should give us an improved result over the two scale model; since the assumptions on facet sizes are less severe. To see this note that in reference 19:

$$\sigma_s^o = \frac{4}{\pi^2} K^4 a^4 \left[\frac{4}{3} + \frac{32}{45} (Ka)^2 \right]^2 \quad (3-1)$$

Hence, for
$$\sigma_l^o = (Ka)^2 \quad (3-2)$$

$$\sigma_s^o = \sigma_l^o \quad (3-3)$$

It follows that $Ka \cong 1$. The dashed line in Figure 7 shows that $Ka=1$ belongs to the small region and by this extrapolation not only the entire intermediate region but part of the small region are grouped into the large size region.

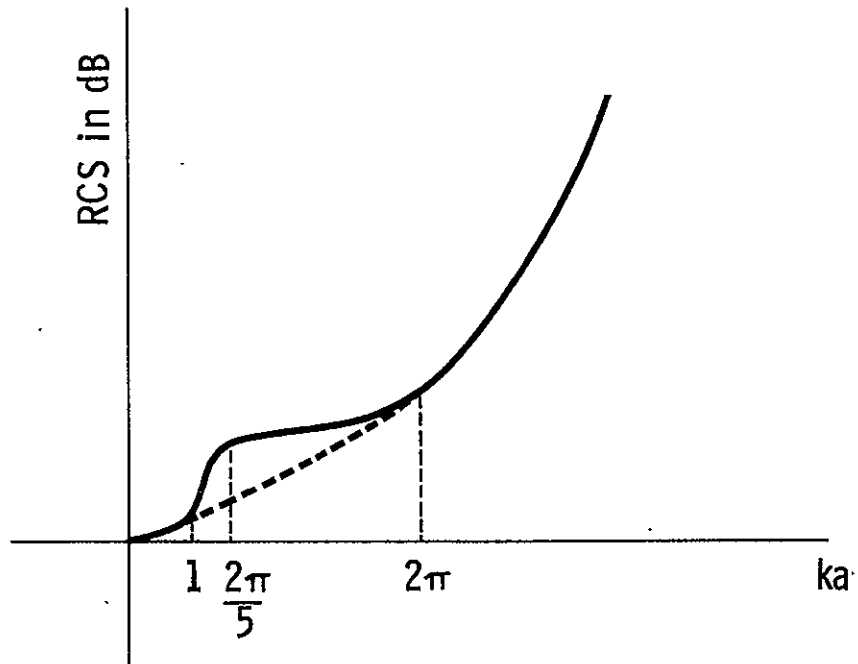


Figure 7. RCS of a disk as a function of deminsion/wavelength.

Katzin assumes that the probability distribution function of the area is in the form of

$$p(A) = N_0 A^{-m} \quad (3-4)$$

where N_0 and m are constants and $P(A)$ is the area probability distribution function.

In order to overcome the problem of determining $P(A)$, we start from the dimensions of the rectangular facets instead of their areas. Then the three regions will be as follows:

- (i) Small facets for which dimensions are smaller than $2\lambda/5$.
- (ii) Medium facets for which dimensions are bigger than $2\lambda/5$ but smaller than λ .
- (iii) Large facets for which dimensions are bigger than λ .

In order to compute the return we have to know the distribution of the dimensions of the facets. This distribution can easily be calculated by using the distribution function for height and slope of the target. Thus, an independent assumption about the facet area distribution can be avoided.

For the facets with dimensions less the $2\lambda/5$ we suggest to use the small perturbation method. In this case it can be shown that (Appendix B)

$$\{ \langle h^2 \rangle \}^{1/2} \cong \lambda/10 \quad (3-5)$$

where

- h^2 mean square height
- l length of facet (max.)

We should add that the answer from this model has the local incident angle and if we want to consider it as a superposition of the small facets over the large ones, we should average it over the variations of the angle due to the variation of the slopes of the large facets.

In what follows we calculate the RCS of the large, medium, and small facets. It is assumed that the distribution of the facet size is in the form of

$$p(l) = \frac{2}{5l\sqrt{2\pi}} \exp\left[-l^2/25l^2\right] \quad l \geq 0$$

$$= 0 \quad l < 0$$

It is also assumed that the slope has a Gaussian distribution with zero mean.

3.1 Large Facets

From physical optics the radar cross-section of a plate with a length of "a" and a width of "b" is equal to

$$\sigma_L(\theta) = \frac{4\pi}{\lambda^2} A^2 = \frac{K^2}{\pi} (ab)^2 \quad (3-6)$$

Now if we assume that the direction of propagation is in YZ plane and has an angle θ with the Z direction, and the plate has a slope Z_x in x direction and Z_y in the y direction than from [7] the cross section of an arbitrarily oriented rectangular plate is

$$\begin{aligned} \sigma_L(\theta) = & \frac{K^2}{\pi} a^2 b^2 \left(\cos\theta + Z_y \sin\theta \right)^2 \left(\frac{\sin Ka(-Z_x \cos\theta)}{Ka(-Z_x \cos\theta)} \right)^2 \times \\ & \times \left(\frac{\sin Kb(\sin\theta - Z_y \cos\theta)}{Kb(\sin\theta - Z_y \cos\theta)} \right)^2 \end{aligned} \quad (3-7)$$

where

$$K = \frac{2\pi}{\lambda}$$

a, b, are respectively length and width of the plate

Z_x, Z_y are respectively the slopes in x and y directions

In order to get contribution of the large facets to the return power we should average $\sigma_L(\theta)$ over all possible slopes and all possible size. We assume that the slope distribution in both x and y directions are Gaussian with zero mean and standard deviation of s_x and s_y . Then

$$\sigma_L(\theta) = \frac{K^2}{\pi} \int_{b_1}^{\infty} b^2 p(b) \int_{a_1}^{\infty} a^2 p(a) \int_{-\infty}^{\infty} (\cos\theta + z_y \sin\theta)^2 \dots$$

$$\left(\frac{\sin(Ka z_x \cos\theta)}{Ka z_x \cos\theta} \right)^2 \left(\frac{\sin Kb (\sin\theta - z_y \cos\theta)}{Kb (\sin\theta - z_y \cos\theta)} \right)^2$$

$$\frac{1}{2\pi s_x s_y} \exp\left[-\frac{z_x^2}{2s_x^2} - \frac{z_y^2}{2s_y^2} \right] dz_y dz_x da db$$

(3-8)

where

$\sigma_L(\theta)$ contribution of the large facets

$p(a), p(b)$ are respectively the probability distribution functions of the length and width of the plate

a_1, b_1 are respectively the smallest length and width for a plate to satisfy the physical optics requirement.

As stated earlier we assume that the distribution of the size of the facet is a Gaussian function. i.e.

$$p(a) = \frac{2}{\sigma_a \sqrt{2\pi}} e^{-\frac{a^2}{2\sigma_a^2}}$$

$$p(b) = \frac{2}{\sigma_b \sqrt{2\pi}} e^{-\frac{b^2}{2\sigma_b^2}} \quad (3-9)$$

By assuming that

- i) $\bar{\sigma}_a = \bar{\sigma}_b = \bar{\sigma}_l$
 ii) $a_1 = b_1 = \alpha$ (3-10)

The contribution of large facets will be

$$\bar{\sigma}_L(\theta) = \frac{K^2}{\pi} \int_{\alpha}^{\beta} \left\{ \frac{2a^2}{\bar{\sigma}_l \sqrt{2\pi}} e^{-\frac{a^2}{2\bar{\sigma}_l^2}} \frac{2b^2}{\bar{\sigma}_l \sqrt{2\pi}} e^{-\frac{b^2}{2\bar{\sigma}_l^2}} \int_{-\infty}^{\infty} \frac{1}{\sqrt{2\pi} S_x} e^{-\frac{z_x^2}{2S_x^2}} \times \left(\frac{\sin Ka z_x \cos \theta}{Ka z_x \cos \theta} \right)^2 \int_{-\infty}^{\infty} \frac{1}{\sqrt{2\pi} S_y} e^{-\frac{z_y^2}{2S_y^2}} (\cos \theta + z_y \sin \theta)^2 \left(\frac{\sin Kb (\sin \theta - z_y \cos \theta)}{Kb (\sin \theta - z_y \cos \theta)} \right)^2 dz_y \right\} dz_x$$

db da

(3-11)

where

β = the size of the largest facet on the target

The integral over Z_x and Z_y have the general form of

$$I = \int_{-\infty}^{\infty} e^{-A^2 u^2} \left(\frac{\sin P(C+Bu)}{P(C+Bu)} \right)^2 du \quad (3-12)$$

where the parameters are as follows:

i) integral over Z_x

$$A = \frac{1}{\sqrt{2} S_x} \quad B = \cos \theta \quad C = 0 \quad P = Ka \quad (3-13)$$

ii) integral over Z_y

$$A = \frac{1}{\sqrt{2} S_y} \quad B = \cos \theta \quad C = \sin \theta \quad P = Kb \quad (3-14)$$

Appendix D shows that the answer to the integral in Eq. (3-12) is

$$I = \frac{\pi}{2Ax^2} e^{-y^2} \left[z \operatorname{erf}(z) + z^* \operatorname{erf}(z^*) - i2y \operatorname{erf}(iy) - \frac{2}{\sqrt{\pi}} e^{y^2} \left(1 - e^{-z^2} \cos 2xy \right) \right] \quad (3-15)$$

where

$$\operatorname{erf}(z) \triangleq \frac{2}{\sqrt{\pi}} \int_0^z e^{-t^2} dt \quad (3-16)$$

$$Z = x + iy$$

$$Z^* = x - iy$$

$$x = PB/A$$

$$y = AC/B$$

From Appendix D

$$\int_{-\infty}^{\infty} U^2 e^{-A^2 U^2} \left(\frac{\sin P(c+BU)}{P(c+BU)} \right)^2 dU = -\frac{\partial I}{\partial A^2}$$

(3-17)

$$\int_{-\infty}^{\infty} U e^{-A^2 U^2} \left(\frac{\sin P(c+BU)}{P(c+BU)} \right)^2 dU \cong 0$$

Now if we consider the last integral of Eq. (3-11) we have

$$\begin{aligned} \text{Integral over } z_y &= \cos^2 \theta \int_{-\infty}^{\infty} e^{-\frac{z_y^2}{2s_y^2}} \left(\frac{\sin kb(\sin \alpha - z_y \cos \alpha)}{kb(\sin \alpha - z_y \cos \alpha)} \right)^2 dz_y \\ &+ 2 \sin \alpha \cos \alpha \int_{-\infty}^{\infty} z_y e^{-\frac{z_y^2}{2s_y^2}} \left(\frac{\sin kb(\sin \alpha - z_y \cos \alpha)}{kb(\sin \alpha - z_y \cos \alpha)} \right)^2 dz_y \\ &+ \sin^2 \alpha \int_{-\infty}^{\infty} z_y^2 e^{-\frac{z_y^2}{2s_y^2}} \left(\frac{\sin kb(\sin \alpha - z_y \cos \alpha)}{kb(\sin \alpha - z_y \cos \alpha)} \right)^2 dz_y \end{aligned} \quad (3-18)$$

We see that the first integral in the right hand side has the form of Eq. (3-12), the second is zero, and the third one has the form of Eq. (3-17). So in order to calculate this integral we first calculate it from Eq. (3-15) then differentiate it vs. A^2 and get $\frac{\partial I}{\partial A^2}$.

For the case when the parameters x of the error function is large i.e. when we are dealing with very large facets in comparison with wavelength, and these are the facets which contribute the most, we can assume that the error function is equal to unity and this will make the computation much easier. For this case

(i) Integral over Z_x

From Eq. (3-11)

integral over $Z_x = I$

where I is defined in Eq. (3-12). Then by using the result of Eq. (3-15) and by assuming that the parameters are as indicated in Eq. (3-13)

$$\text{Integral over } Z_x = \frac{\pi}{2 \times \frac{1}{\sqrt{2} S_x} x^2} \left[x \operatorname{erf}(x) + x \operatorname{erf}(x) - \frac{2}{\sqrt{\pi}} (1 - e^{-x^2}) \right] \quad (3-19)$$

where

$$x = Ka \sqrt{2} S_x \cos \theta$$

K = wavenumber

a = length of facet

S_x = standard deviation of slope in x direction

θ = incidence angle

then from here because it is assumed that $x \geq 2$ so $\operatorname{erf}(2) \cong 1$; $e^{-x^2} \cong 0$,

$$\begin{aligned} \text{Integral over } Z_x &= \frac{\pi}{2 \times \frac{1}{\sqrt{2} S_x} x^2} \left[2x - \frac{2}{\sqrt{\pi}} \right] \\ &= \frac{\pi}{Ka \cos \theta} \left[1 - \frac{1}{\sqrt{2\pi} S_x Ka \cos \theta} \right] \end{aligned} \quad (3-20)$$

Now if we further assume that

$\sqrt{2} S_x K_a \cos\theta \gg 1$, i.e. facet size is large and the standard deviation of the slope is not very small. (3-21)

$$\text{integral over } Z_x = \frac{\pi}{K_a \cos\theta} \quad (3-22)$$

ii) Integral over Z_y

From Eq. (3-18) and by using the results of Appendix D as indicated in Eq. (3-17)

$$\text{Integral over } Z_y = \cos^2\theta I + \sin^2\theta \left(-\frac{\partial I}{\partial R^2} \right) \quad (3-23)$$

where I is defined in Eq. (3-12) and its parameters are given in Eq. (3-14). Then by using the results of Eq. (3-15) with the same procedure as indicated in getting Eq. (3-22)

$$I = \frac{\pi e^{-y^2}}{2 \times \frac{1}{\sqrt{2} S_y} x^2} \left[(x+iy) \operatorname{erf}(x+iy) + (x-iy) \operatorname{erf}(x-iy) - 2iy \times \operatorname{erf}(iy) + \frac{2}{\sqrt{\pi}} e^{y^2} (1 - e^{-x^2} \cos 2xy) \right] \quad (3-24)$$

Now if we assume that

$$1) x \gg 1 \quad (3-25)$$

$$2) x > y \quad (3-26)$$

i.e. consider large facets only near specular direction, then

$$I = \frac{\pi e^{-y^2}}{K_b \cos\theta} = \frac{\pi}{K_b \cos\theta} \exp\left[-\tan^2\theta / 2 S_y^2\right] \quad (3-27)$$

from here

$$\frac{\partial I}{\partial A^2} = \frac{\partial I}{\partial \left(\frac{1}{2s_y^2}\right)} = \frac{-\pi \tan^2 \theta}{kb \cos \theta} \exp\left[-\frac{\tan^2 \theta}{2s_y^2}\right]. \quad (3-28)$$

then by substituting in Eq. (3-23)

$$\begin{aligned} \text{Integral over } z_y &= \cos^2 \theta \frac{\pi}{kb \cos \theta} \exp\left[-\frac{\tan^2 \theta}{2s_y^2}\right] + \sin^2 \theta \frac{\pi \tan^2 \theta}{kb \cos \theta} \exp\left[-\frac{\tan^2 \theta}{2s_y^2}\right] \\ &= \frac{\pi}{kb \cos \theta} \exp\left[-\frac{\tan^2 \theta}{2s_y^2}\right] (\cos^2 \theta + \sin^2 \theta \tan^2 \theta) \\ &= \frac{\pi \cos \theta}{kb} \exp\left[-\frac{\tan^2 \theta}{2s_y^2}\right] (1 + \tan^4 \theta) \end{aligned} \quad (3-29)$$

By substituting these results in Eq. (3-11)

$$\begin{aligned} \sigma_L(\theta) &= \frac{K^2}{\pi} \iint_{\alpha}^{\beta} \frac{4a^2b^2}{2\pi \sigma_L^2} \exp\left[-\frac{a^2+b^2}{2\sigma_L^2}\right] \left\{ \frac{1}{2\pi s_x s_y} \times \frac{\pi^2 (1+\tan^4 \theta)}{K^2 ab} \right. \\ &\quad \left. e^{-\frac{\tan^2 \theta}{2s_y^2}} \left[1 - \frac{1}{\sqrt{2\pi} s_x K a \cos \theta} \right] \left[1 - \frac{1}{\sqrt{2\pi} s_y K b \cos \theta} \right] \right\} \\ &\quad da db \end{aligned} \quad (3-30)$$

assuming that $\beta \rightarrow \infty$, i.e. the size of the largest facet is very large,

$$\sigma_L(\theta) = \frac{e^{-\frac{\tan^2 \theta}{2s_y^2}} (1 + \tan^4 \theta)}{s_x s_y} \times \sigma_L^2 \times \left\{ \frac{\alpha}{\sigma_L \sqrt{2}} e^{-\frac{\alpha^2}{2\sigma_L^2}} + \frac{\sqrt{\pi}}{2} \left(1 - \operatorname{erf} \left(\frac{\alpha}{\sigma_L \sqrt{2}} \right) \right) \right\}^2 \quad (3-31)$$

This result, as it is expected, is in general form of the result that one would get by using the geometric optics method. The only difference is that we have $(1 + \tan^4 \theta)$ rather than $(1 + \tan^2 \theta)^2$. The reason for this is the assumption that is made in Appendix D, i.e.

$$\int u e^{-A^2 u^2} \left(\frac{\operatorname{Im} P(c+Bu)}{P(c+Bu)} \right)^2 \approx 0 \quad (3-32)$$

which is not true for the extreme case when $\beta \rightarrow \infty$ and the angle of incidence is not equal to zero.

It should be noted that in comparing the theory with the measured data we do not use the assumptions indicated in Eqs. (3-25), (3-26) and (3-31). For this purpose we use the result of Eqs. (3-15) and calculate it numerically or digital computer.

3.2 Medium Size Facets

The facets whose dimensions are less than λ but larger than $2\lambda/5$ are considered to be medium size facets.

There is no exact easy solution to the RCS of the medium size facets. Figures 8 and 9^[19] show that for small and large facets, as it is expected, the normalized RCS versus area varies, respectively, with A^2 and A (A is the area). We also see that the slope of the curve for medium size is smaller than the slope for both large and small size, and it varies almost as $A^{1/4}$. Figure 10^[19] gives us the variation of the return versus the local angle of incidence. This variation is in the form of

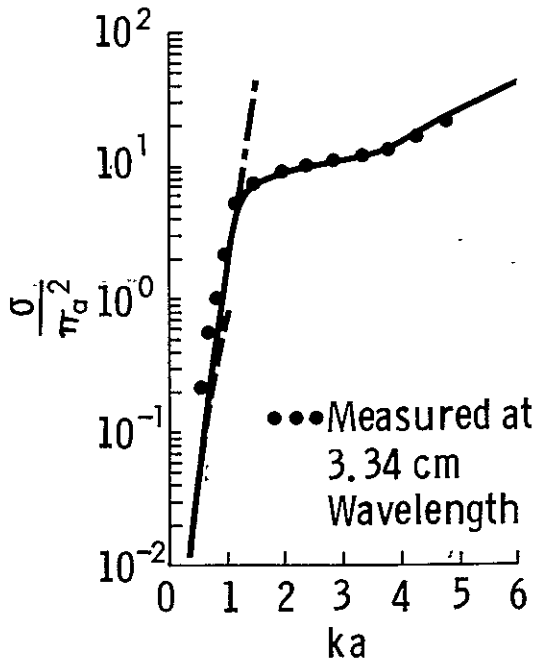


Figure 8. Measured σ^o for small and medium facets.

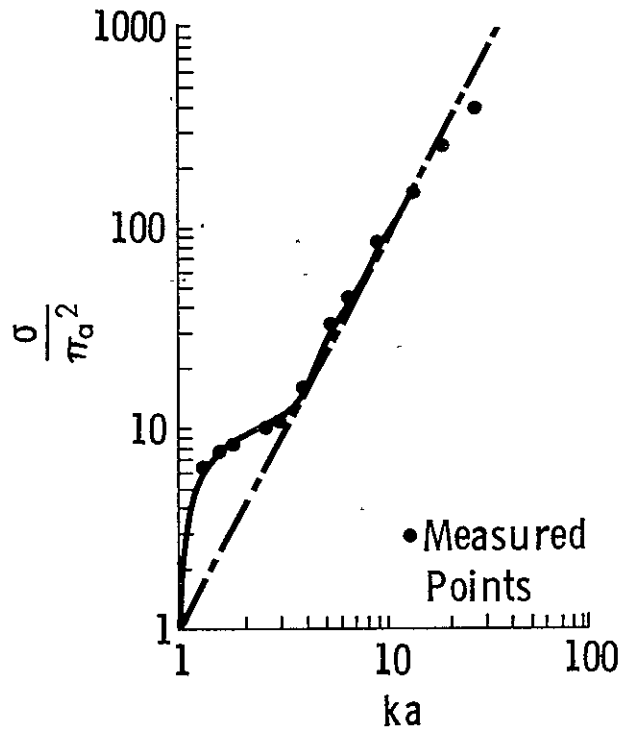


Figure 9. Measured σ^o for small, medium, and large facets.

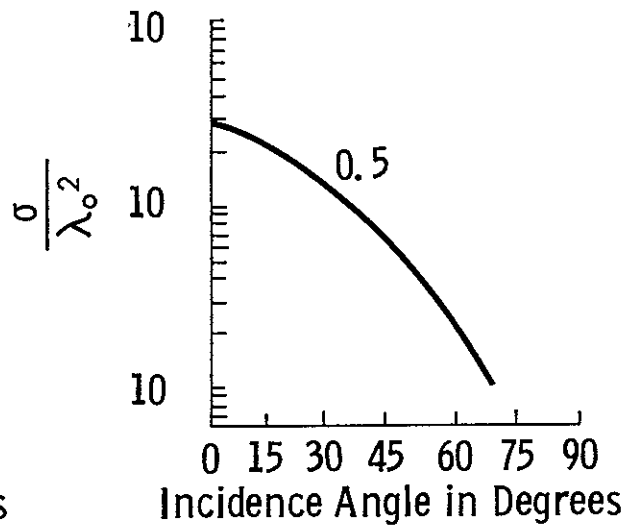
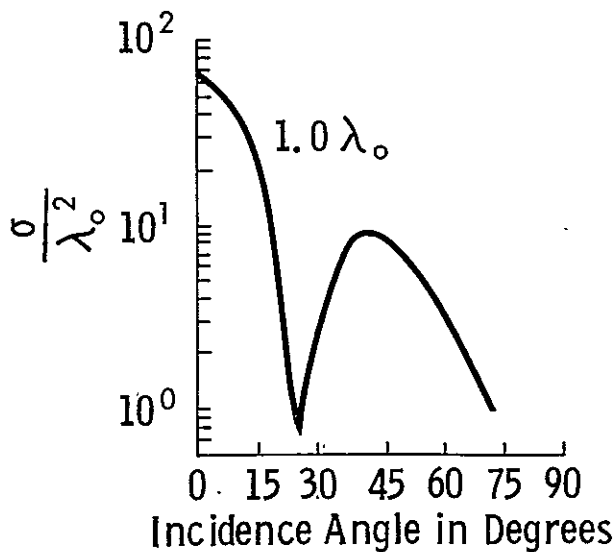


Figure 10. Measured VV polarization backscatter cross-section versus the angle of incidence for perfectly conducting rectangular planes with heights of $2\lambda_o$ and lengths of $0.5\lambda_o$ and λ_o .

$\left(\frac{\sin x}{x}\right)^2$. So in view of the measured data shown in Figures 8, 9, and 10 we assume

$$\bar{\sigma}_M(\theta') = 25 \frac{a^{5/4} b^{5/4}}{\lambda^{1/2}} \left(\frac{\sin(Kb \sin \theta')}{Kb \sin \theta'} \right)^2 \quad (3-33)$$

where

$$K = 2\pi/\lambda$$

λ = wavelength

a = width of the facet

b = length of the facet

θ' = local incidence angle

If we write Eq. (3-33) in terms of incidence angle

$$\bar{\sigma}_M(\theta) = 25 \frac{a^{5/4} b^{5/4}}{\lambda^{1/2}} \left(\frac{\sin Kb (\sin \theta - S \cos \theta)}{Kb (\sin \theta - S \cos \theta)} \right)^2 \quad (3-34)$$

where S is the slope

Because we assume that the slope of the medium size facets are not large and because the slope of the return versus angle is small for the medium size facets, then $s \approx 0$.

Hence Eq. (4-34) will be:

$$\bar{\sigma}_M(\theta) \cong 25 \frac{a^{5/4} b^{5/4}}{\lambda^{1/2}} \left(\frac{\sin(Kb \sin \theta)}{Kb \sin \theta} \right)^2 \quad (3-35)$$

In order to calculate the contribution of the medium size facets we have to average Eq. (3-35) over a and b . Then

$$\sigma_M(\theta) = \frac{25}{\lambda^{1/2}} \int_{\frac{2\lambda}{5}}^{\lambda} a^{5/4} b^{5/4} p(a) p(b) \left(\frac{\sin(Kb \sin \theta)}{Kb \sin \theta} \right)^2 da db \quad (3-36)$$

where

$$K = 2\pi/\lambda$$

λ = wavelength

a = width of the facet

b = length of the facet

$p(a)$ = distribution function of the width of the facet which is assumed to be Gaussian

$p(b)$ = distribution function of the length of the facet which is assumed to be Gaussian

$\sigma_M(\theta)$ = contribution of the medium facets to RCS

In order to compare the result of the theory with the data we have to take into consideration the reflection coefficient of the facets. The assumptions for calculating the reflection coefficient has been explained in Section 5.1.

3.3 Small Facets

In order to calculate the contribution of small facets i.e. facets whose length is less than $2\lambda/5$ we use the perturbation method as first formulated by Rice [17] and then further developed by Peak [14].

In this technique unlike the tangent-plane approximation there is no requirement indicating that the radius of curvature at any point must be large in comparison with the wavelength. So we can easily use it for the return from small facets of the natural surfaces.

The requirement of this model are as follows [19]:

$$i) \quad 2\pi h/\lambda < 1 \quad , \text{ i.e. roughness height is small}$$

$$\text{ii) } \left| \frac{\partial z}{\partial x} \right|, \left| \frac{\partial z}{\partial y} \right| < 1, \text{ i.e. surface slopes are relatively small}$$

$$\text{iii) } \left(\left\langle \frac{\partial z}{\partial x} \right\rangle \right)^2 = \left(\left\langle \frac{\partial z}{\partial y} \right\rangle \right)^2, \text{ i.e. roughness is isotropic}$$

In the previous section we showed that the first requirement is correct for small facets and by assuming that the second and third requirements are also correct, the radar cross section will be [19]

$$\sigma_s(\theta) = \frac{4}{\pi} k^2 h^2 \cos^2 \theta |\alpha|^2 \quad (3-37)$$

where

λ = wavenumber

h = r.m.s. height

θ = angle of incidence

In this equation α for horizontal, cross, and vertical polarization are given, respectively, by

$$\alpha_{hh} = - \frac{(\mu_r - 1) \left[(\mu_r - 1) \sin^2 \theta + \epsilon_r \mu_r \right] - \mu_r^2 (\epsilon_r - 1)}{\left[\mu_r \cos \theta + \sqrt{\epsilon_r \mu_r - \sin^2 \theta} \right]^2} \quad (3-38)$$

$$\alpha_{hv} = \alpha_{vh} = 0$$

$$\alpha_{vv} = \frac{(\epsilon_r - 1) \left[(\epsilon_r - 1) \sin^2 \theta + \epsilon_r \mu_r \right] - \epsilon_r^2 (\mu_r - 1)}{\left[\epsilon_r \cos \theta + \sqrt{\epsilon_r \mu_r - \sin^2 \theta} \right]^2} \quad (3-39)$$

and I is defined as

$$I \triangleq 2\pi \int_0^{\infty} r \rho(r) J_0(2K \sin \theta r) dr \quad (3-40)$$

where $J_0(\cdot)$ is the zero-order Bessel function and $\rho(r)$ is the surface-height correlation coefficient for an isotropically rough surface and is defined as

$$\rho(r) = \frac{\langle z(x, y) z(x', y') \rangle}{h^2} \quad (3-41)$$

where

$$r = \sqrt{(x-x')^2 + (y-y')^2} \quad (3-42)$$

For the case that the surface is not isotropic the result for Eq. (3-40) is given in [5]. Now if we assume that the correlation coefficient has a Gaussian form, i.e.

$$\rho(r) = e^{-r^2/\ell^2} \quad (3-43)$$

then from Eq. (3-40) [19]

$$I = \pi \ell^2 \exp \left[-\frac{K^2 \ell^2}{4} (4 \sin^2 \theta) \right] \quad (3-44)$$

where ℓ is the correlation distance.

By substituting Eq. (3-44) in Eq. (3-37) and assuming $\mu_r = 1$

$$\left. \bar{\sigma}_s^{\circ}(\theta) \right|_{\#H} = 4 K^4 h^2 l^2 \cos^4 \theta \left| \frac{\epsilon_r - 1}{\left[\cos \theta + \sqrt{\epsilon_r - \sin^2 \theta} \right]^2} \right|^2 \times \quad (3-45)$$

$$\exp\left[-K^2 l^2 \sin^2 \theta\right]$$

$$\left. \bar{\sigma}_s^{\circ}(\theta) \right|_{HV} = \left. \bar{\sigma}_s^{\circ}(\theta) \right|_{VH} = 0 \quad (3-46)$$

$$\left. \bar{\sigma}_s^{\circ}(\theta) \right|_{VV} = 4 K^4 h^2 l^2 \cos^4 \theta \left| \frac{(\epsilon_r - 1) \left[(\epsilon_r - 1) \sin^2 \theta + \epsilon_r \right]}{\left[\epsilon_r \cos \theta + \sqrt{\epsilon_r - \sin^2 \theta} \right]^2} \right|^2 \times \quad (3-47)$$

$$\times \exp\left[-K^2 l^2 \sin^2 \theta\right]$$

4.0 PROPERTIES OF THE SYSTEM

In this chapter we explain the principle and the construction of the large time-bandwidth FM-CW radar which is used to collect data from the bare ground.

Section 4.1.1 is devoted to briefly state the principle of the radar. In Section 4.1.2 we have calculated the frequency spectrum of the radar and have shown that it is uniformly spread over the sweeping bandwidth. This result has been used in Section 4.2 to calculate the variance of the return power.

Section 4.2 examines the effect of the frequency averaging. We first show the predicted reduction of variance due to frequency averaging by assuming a uniform scatterer model [26], then we extend this result to take into consideration the penetration effect. Then we calculate the reduction in the variance for the case that the target is assumed to consist of a collection of facets.

Section 4.2.3 compares the theoretical results obtained in Sections 4.2.1 and 4.2.2 to the measured data. It is shown that by considering penetration we can explain the reduction in the variance of the backscatter data from alfalfa. We also show that the facet model can explain the difference between the measured curve from the bare ground and the curve predicted by assuming that the ground consists of small scatterers.

4.1 System and Frequency Spectrum

4.1.1 Radar

The radar used in this investigation is a FM-CW radar which has a very large time-bandwidth product. A FM-CW radar transmits a modulated signal as shown in Figure 11. Then from [21] the IF frequency after the mixer is equal to

$$F_{IF} = \frac{4R}{c} \Delta F F_M \quad (4-1)$$

where

- F_{IF} = intermediate frequency
- R = range
- c = speed of light
- F = RF frequency deviation
- F_M = frequency of modulation

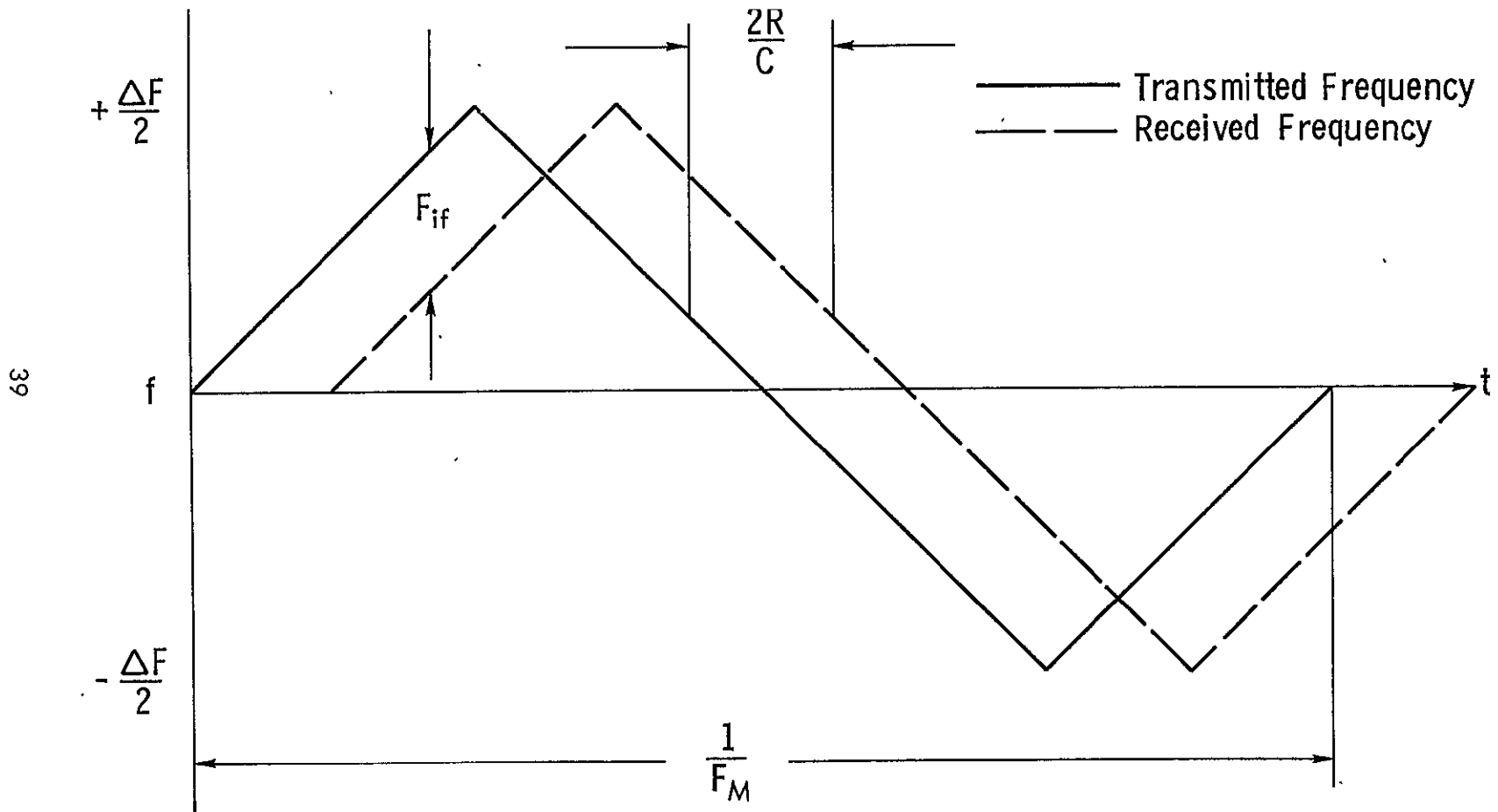


Figure 11. Illustration showing frequency relationship between transmitted and received signals.

A block diagram for the radar used is given in Figure 12 and its characteristics are as follows [3]:

<u>TYPE</u>	FM-CW
Modulating Waveform	Triangular
Frequency	8-18 GHz
FM sweep: Δf	400 MHz
Transmitter Power	10 dBm (10 mW)
Intermediate Frequency	60 kHz
IF Bandwidth	3.58 kHz
Antennas	
Height above ground	26 m
Reflector Diameter	61 cm
Feeds	Cavity backed, log-periodic

Frequency (GHz)	Calculated Antenna Gain (dB)	Effective Beamwidths of Product Patterns (Degrees)	
		Az	EI
8	31.2	2.94	3.43
10	33.0	3.07	3.24
12	34.6	2.42	2.38
14	35.9	2.35	2.34
16	37.1	1.65	1.46
18	38.1	2.02	3.20

4.1.2 Frequency Spectrum of the Signal

In this section we would like to show that the frequency spectrum of the return signal of an FM-CW radar with which the data has been collected is flat over the sweep band. If the frequency of the wave varies with time as shown in Figure 13, then the wave form will be:

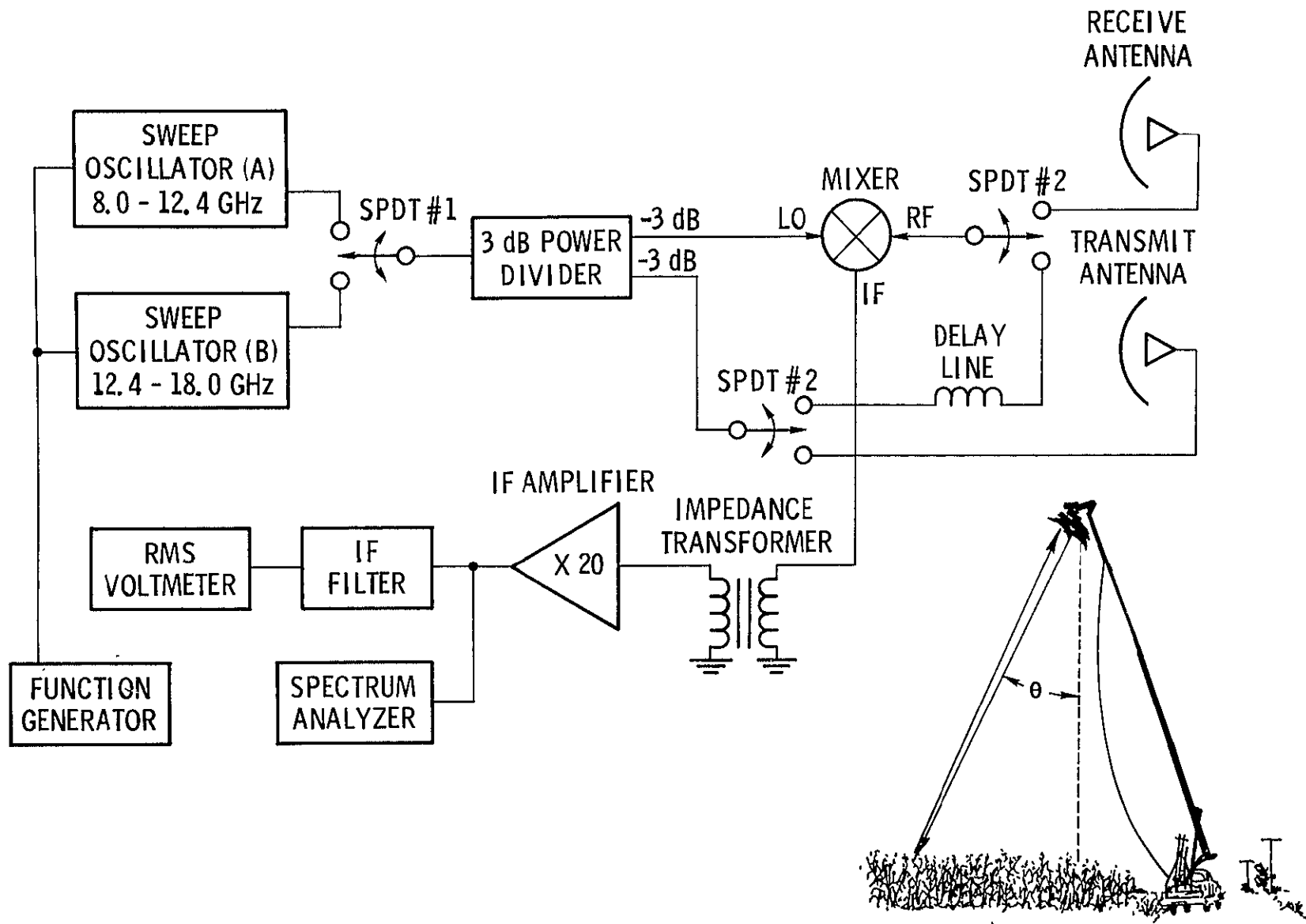


Figure 12. Basic block diagram of 8-18 GHz radar spectrometer.

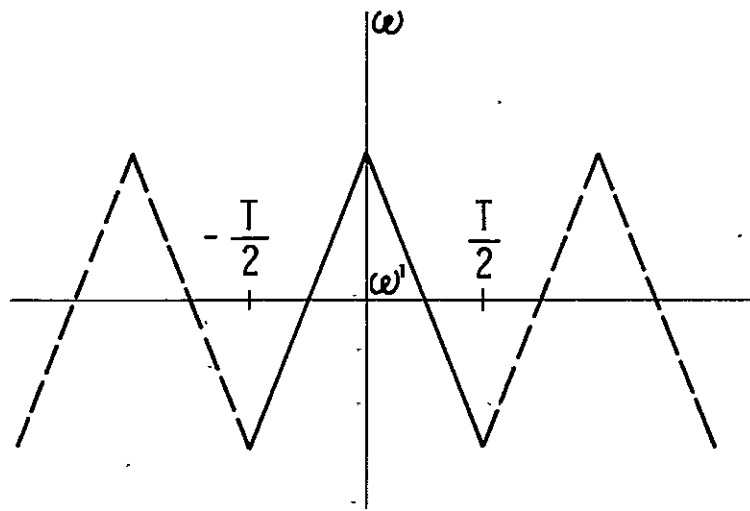


Figure 13. Frequency of the transmitted signal as a function of time.

$$s(t) = \begin{cases} \cos \left[\left(\omega' + \mu \frac{T}{4} \right) t + \frac{\mu t^2}{2} \right] & nT \geq t \geq nT - \frac{T}{2} \\ \cos \left[\left(\omega' + \mu \frac{T}{4} \right) t - \frac{\mu t^2}{2} \right] & nT + \frac{T}{2} \geq t \geq nT \end{cases} \quad (4-2)$$

Because $s(t)$ is a periodic function we can write

$$s(t) = \sum_{n=-\infty}^{\infty} F_n e^{jn\omega_0 t} \quad (4-3)$$

where

$$F_n \triangleq \frac{1}{T} \int_{-T/2}^{T/2} s(t) e^{-jn\omega_0 t} dt \quad (4-5)$$

$$\omega_0 \triangleq \frac{2\pi}{T} \quad (4-6)$$

then

$$s(\omega) = \mathcal{F}[s(t)] = \mathcal{F}\left[\sum_{n=-\infty}^{\infty} F_n e^{jn\omega_0 t} \right] = 2\pi \sum_{n=-\infty}^{\infty} F_n \delta(\omega - n\omega_0) \quad (4-7)$$

First we should calculate F_n . By substituting Eq. (4-2) in Eq. (4-5) we get

$$F_n = \frac{1}{T} \left\{ \int_{-T/2}^0 \cos \left[\left(\omega' + \frac{\mu T}{4} \right) t + \frac{\mu t^2}{2} \right] e^{-jn\omega_0 t} dt + \int_0^{T/2} \cos \left[\left(\omega' + \frac{\mu T}{4} \right) t - \frac{\mu t^2}{2} \right] e^{-jn\omega_0 t} dt \right\} \quad (4-8)$$

By using the relation

$$\cos \alpha = \frac{e^{j\alpha} + e^{-j\alpha}}{2} \quad (4-9)$$

Eq. (4-8) becomes:

$$\begin{aligned} F_n = \frac{\sqrt{\pi k}}{2T} & \left\{ e^{-jA} [c(x_1) + j s(x_1) + c(x_2) + j s(x_2)] + e^{jB} [c(x_3) - j s(x_3) \right. \\ & + c(x_4) - j s(x_4) + e^{jA} [c(x_1) - j s(x_1) + c(x_2) - j s(x_2)] + \\ & \left. + e^{-jB} [c(x_3) + j s(x_3) + c(x_4) + j s(x_4)] \right\} \end{aligned} \quad (4-10)$$

where

$$\begin{aligned} x_1 &= \left[1 - \frac{\omega' - n\omega_0}{\frac{\Delta\omega}{2}} \right] \frac{\sqrt{\Delta\omega T}}{2\sqrt{2\pi}} \\ x_2 &= \left[1 + \frac{\omega' - n\omega_0}{\frac{\Delta\omega}{2}} \right] \frac{\sqrt{\Delta\omega T}}{2\sqrt{2\pi}} \\ x_3 &= \left[1 - \frac{\omega' + n\omega_0}{\frac{\Delta\omega}{2}} \right] \frac{\sqrt{\Delta\omega T}}{2\sqrt{2\pi}} \\ x_4 &= \left[1 + \frac{\omega' + n\omega_0}{\frac{\Delta\omega}{2}} \right] \frac{\sqrt{\Delta\omega T}}{2\sqrt{2\pi}} \end{aligned} \quad (4-11)$$

$$\Delta\omega = \mu T / 2$$

$$C(z) \triangleq \int_0^z \cos\left(\frac{\pi}{2} t^2\right) dt \quad \text{Fresnel cosine integral}$$

$$S(z) \triangleq \int_0^z \sin\left(\frac{\pi}{2} t^2\right) dt \quad \text{Fresnel sine integral}$$

From the Fresnel integral properties

$$C(-x) = -C(x)$$

$$S(-x) = -S(x)$$

$$C(\infty) = 0.5$$

$$S(\infty) = 0.5$$

(4-12)

and because the system used has a very large time-bandwidth product, i.e.

$$\sqrt{\Delta\omega T} \cong \sqrt{4 \times 10^8 \times \frac{1}{400}} \approx 1000$$

(4-13)

It can easily be shown [4] that from Eq. (4-10) the signal has spectrum only around the ω_c carrier frequency, and its magnitude is

$$F_n = \frac{\sqrt{2}}{T} \sqrt{\pi/\mu} \cos \frac{(\mu T/4 + \omega' - n\omega_0)^2}{2\mu} \quad (4-14)$$

So from Eq. (4-7)

$$S(\omega) = \frac{2\pi}{T} \sqrt{\pi/\mu} \sum_{n=-\infty}^{\infty} \cos \frac{(\mu T/4 + \omega' - n\omega_0)^2}{2\mu} \delta(\omega - n\omega_0) \quad (4-15)$$

This spectrum is shown in Figure 14.

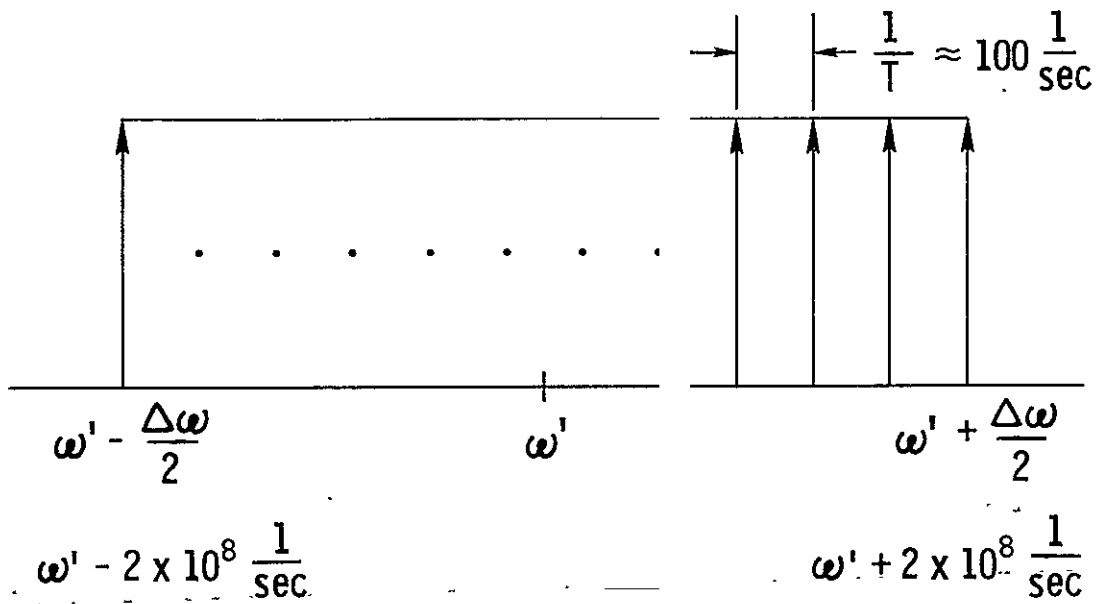


Figure 14. Frequency spectrum of the radar.

4.2 Frequency Averaging

It is a well known fact that radar return from irregular targets may fluctuate due to insufficient averaging. In order to overcome this problem, over the years many techniques have been used, and frequency averaging is one of them. Waite [26] has shown that if we average the return of the target for different frequencies the standard deviation of the average will be much smaller than the standard deviation of the data measured in each frequency. For doing this, Waite assumed that the target is composed of small scatterers for which the pattern is assumed to be uniform.

In Section 4.2.1 we shall first explain the work done by Waite then we shall expand his work by taking into consideration the penetration of the wave into the target.

In Section 4.2.2 we assume that the target is composed of the facets rather than small uniform scatterers. We have shown that if the return from different facets are comparable than the reduction of standard deviation of the return due to frequency averaging will be the same as predicted by Waite. But if the return from different facets are not comparable, then we have to have some information, about the facets whose contribution to the return is very large, in order to be able to determine the reduction of the standard deviation of the return.

In Section 4.2.3 we compare the theoretical results obtained in this chapter by the actual measurement and show that alfalfa is a good example of a target composed of layers of small scatterers. We then use the results of the facet model to explain the number of independent samples in the RCS measurement of the bare ground.

4.2.1 Uniform Scatterer Model

4.2.1.1 Uniform Scatterer Model with no Penetration [26]

In this model it is assumed that the target may be represented by a random collection of discrete independent scatterers. Each scatterer has a uniform pattern and its reradiation amplitude is a sample of a Gaussian random process with zero mean and standard deviation.

As Figure 15 shows the illuminated area of the target is a function of D and β , then the returned signal will be in the form of

$$S_{rn}(t) = a_n s(t - t_n) \quad (4-16)$$

where

$s(t)$ = transmitted waveform

t_n = roundtrip time delay of n^{th} scatterer and is equal to $\frac{2R_n}{c}$

a_n = scattering amplitude of n^{th} scatterer

The total return from the illuminated area is:

$$S_r(t) = \sum a_n s(t - t_n) \quad (4-17)$$

From the characteristic of delta function we can write the transmitted signal as

$$s(t) = \int_{-\infty}^{\infty} s(\alpha) \delta(t - \alpha) d\alpha \quad (4-18)$$

or

$$s(t - t_n) = \int_{-\infty}^{\infty} s(\alpha) \delta(t - t_n - \alpha) d\alpha \quad (4-19)$$

Hence, the return signal may be written as

$$\begin{aligned} S_r(t) &= \sum a_n \int_{-\infty}^{\infty} s(\alpha) \delta(t - t_n - \alpha) d\alpha \\ &= \int_{-\infty}^{\infty} s(\alpha) \sum a_n \delta(t - t_n - \alpha) d\alpha \\ &= s(t) \otimes \sum a_n \delta(t - t_n) \end{aligned} \quad (4-20)$$

where the symbol \otimes denotes convolution of two function [10].

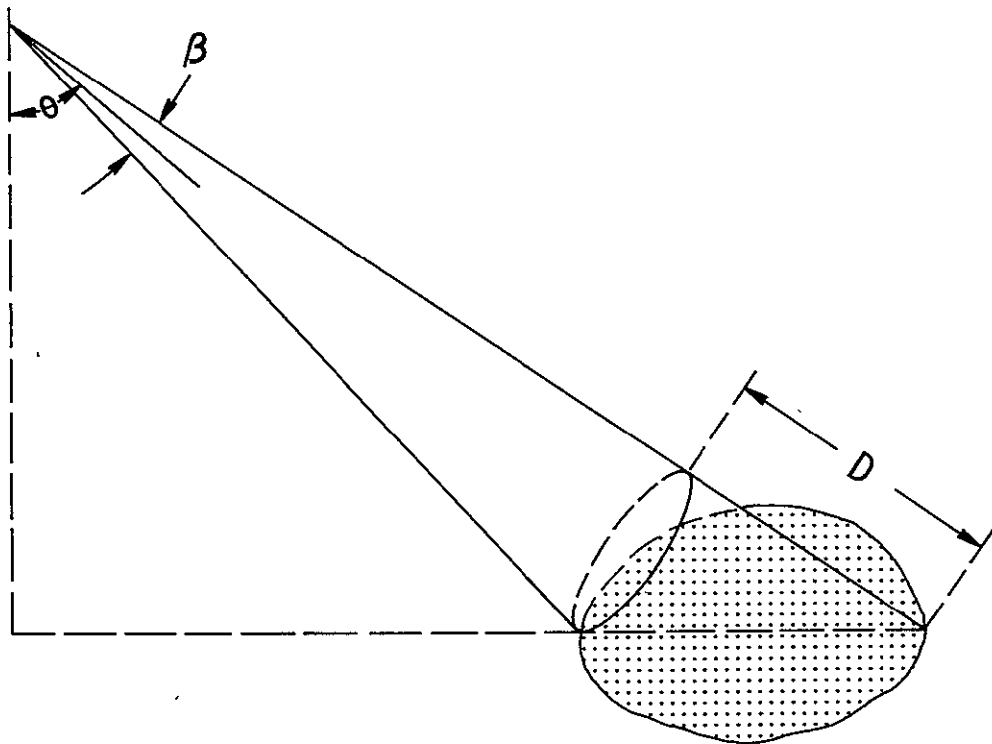


Figure 15. Radar illuminated area.

The target effect is only introduced in the second term of this convolution so if we define $c(t)$ as

$$c(t) \triangleq \sum a_n \delta(t-t_n) \quad (4-21)$$

then $c(t)$ will be the target impulse response.

In order to obtain the reduction in the standard deviation of the return signal due to frequency averaging, consider the Fourier transform of $c(t)$,

$$\begin{aligned} c(f) = \mathcal{F}[c(t)] &= \int_{-\infty}^{\infty} \sum a_n \delta(t-t_n) e^{-j\omega t} dt \\ &= \sum a_n e^{-j\omega t_n} \\ &= \sum a_n e^{-j2\pi f t_n} \end{aligned} \quad (4-22)$$

From Eq. (4-22) the autocorrelation of the response of the target in the frequency domain can be calculated as:

$$\begin{aligned} R(\nu) &= E \left[c(f) c^*(f-\nu) \right] \\ &= E \left[\sum a_n e^{-j2\pi f t_n} \sum a_m e^{j2\pi f t_m} \right] \end{aligned} \quad (4-23)$$

or

$$R(\nu) = E \left[\sum a_n a_m e^{-j2\pi f (t_n - t_m)} e^{j2\pi \nu t_m} \right] \quad (4-24)$$

From the requirement of the model that the scatterers are independent samples of a Gaussian process with zero mean we obtain:

$$E[a_n a_m] = E[a_n] E[a_m] = 0 \quad (4-25)$$

Hence

$$R(\nu) = E\left[\sum a_n^2 e^{-j2\pi\nu t_n}\right] \quad (4-26)$$

By the assumption that a_n and t_n are independent

$$R(\nu) = \sum E[a_n^2] E\left[e^{-j2\pi\nu t_n}\right] \quad (4-27)$$

By assuming a uniform distribution for time delay i.e.

$$p(t_n) = \frac{1}{T} \quad \frac{T}{2} \geq t_n \geq -\frac{T}{2} \quad (4-28)$$

$$\begin{aligned} E\left[e^{-j2\pi\nu t_n}\right] &= \int_{-\infty}^{\infty} p(t_n) e^{-j2\pi\nu t_n} dt_n \\ &= \int_{-\frac{T}{2}}^{\frac{T}{2}} \frac{1}{T} e^{-j2\pi\nu t_n} dt_n \\ &= \frac{\sin \pi\nu T}{\pi\nu T} \end{aligned} \quad (4-29)$$

So,

$$R(\nu) = \left\{ \sum E[a_n^2] \right\} \frac{\sin \pi \nu T}{\pi \nu T} \quad (4-30)$$

where T is the time span of the target and is equal to $\frac{2D}{c}$ (c is the speed of light and D is shown in Figure 15). In Eq. (4-30) if we put $\nu = \frac{1}{T}$ then

$$R(\nu = \frac{1}{T}) = \frac{\sin \pi}{\pi} = 0 \quad (4-31)$$

which indicates that for two frequencies $\frac{1}{T}$ Hz apart the target effect will be uncorrelated.

In what follows we will obtain the mean and the variance of the returned power and by using the correlation of the target in frequency domain from Eq. (4-30), we will calculate the reduction in the variance of returned power due to the frequency averaging.

Variance of the Returned Power

As stated earlier in Eqs. (4-20) and (4-21)

$$s_r(t) = s(t) \otimes c(t) \quad (4-32)$$

Hence, the Fourier transform of $s_r(t)$ is

$$s_r(f) = s(f) c(f) \quad (4-33)$$

then the received power will be equal to

$$\begin{aligned} W_r &= \int_{-\infty}^{\infty} |s_r(t)|^2 dt = \int_{-\infty}^{\infty} |s_r(f)|^2 df \\ &= \int_{-\infty}^{\infty} |s(f)|^2 |c(f)|^2 df \end{aligned} \quad (4-34)$$

Now by using this relation we will calculate the variance of the return power,

$$\sigma_{w_r}^2$$

$$\sigma_{w_r}^2 = E[w_r^2] - E^2[w_r] \quad (4-35)$$

Now we calculate each term separately

i) Mean

$$\begin{aligned} E[w_r] &= E \left[\int_{-\infty}^{\infty} |s(f)|^2 |c(f)|^2 df \right] \\ &= \int_{-\infty}^{\infty} E[|c(f)|^2] |s(f)|^2 df \end{aligned} \quad (4-36)$$

ii) Expected value of w_r^2

$$\begin{aligned} w_r^2 &= \int_{-\infty}^{\infty} |s(f)|^2 |c(f)|^2 df \int_{-\infty}^{\infty} |s(f')|^2 |c(f')|^2 df' \\ &= \iint_{-\infty}^{\infty} |c(f)|^2 |c(f')|^2 |s(f)|^2 |s(f')|^2 df df' \end{aligned} \quad (4-37)$$

In order to calculate this integral we use the procedure as stated in reference [10] i.e.

$$f' = f - \nu \quad (4-38)$$

Then

$$w_r^2 = \iint_{-\infty}^{\infty} |c(f)|^2 |c(f-\nu)|^2 |s(f)|^2 |s(f-\nu)|^2 df d\nu \quad (4-39)$$

then

$$E[w_r^2] = \iint_{-\infty}^{\infty} E[|c(f)|^2 |c(f-\nu)|^2] |s(f)|^2 |s(f-\nu)|^2 df d\nu \quad (4-40)$$

Now by using the results of Eqs. (4-36) and (4-40) we calculate the variance of the returned power, $\sigma_{w_r}^2$.

$$\begin{aligned} \sigma_{w_r}^2 &= E[w_r^2] - E^2[w_r] \\ &= \iint_{-\infty}^{\infty} \left\{ E[|c(f)|^2 |c(f-\nu)|^2] - E^2[|c(f)|^2] \right\} \times \\ &\quad |s(f)|^2 |s(f-\nu)|^2 df d\nu \end{aligned} \quad (4-41)$$

Because, as shown in Eqs. (4-46) and (4-47) $\left\{ E \left[|c(f)|^2 |c(f-\nu)|^2 \right] - E^2 \left[|c(f)|^2 \right] \right\}$ is not a function of frequency

$$\begin{aligned} \bar{\sigma}_{WR}^2 &= \int_{-\infty}^{\infty} \left\{ E \left[|c(f)|^2 |c(f-\nu)|^2 \right] - E^2 \left[|c(f)|^2 \right] \right\} \cdot \\ &\quad \times \int_{-\infty}^{\infty} |s(f)|^2 |s(f-\nu)|^2 d f d \nu \end{aligned} \quad (4-42)$$

then by letting

$$p(\nu) \triangleq \int_{-\infty}^{\infty} |s(f)|^2 |s(f-\nu)|^2 d f \quad (4-43)$$

$$\bar{\sigma}_{WR}^2 = \int_{-\infty}^{\infty} \left\{ E \left[|c(f)|^2 |c(f-\nu)|^2 \right] - E^2 \left[|c(f)|^2 \right] \right\} p(\nu) d \nu \quad (4-44)$$

In what follows we will calculate this integral by using the assumption that the target is composed of small scatterers with uniform pattern. In reference [26] it is stated that in this case

$$E \left[|c(f)|^2 |c(f-\nu)|^2 \right] = E^2 \left[|c(f)|^2 \right] + E^2 \left[c(f) c^*(f-\nu) \right] \quad (4-45)$$

This result is correct if the following assumptions are satisfied:

- i) Number of the scatterers contributing to the return is large.
- ii) fT , where f is the frequency and T is the time span of the target is very large.

Then by using Eqs. (4-23) and (4-30) we obtain

$$E \left[|c(f)|^2 \right] = \sum E[a_n^2] \quad (4-46)$$

and

$$E \left[c(f) c^*(f-\nu) \right] = R(\nu) = \left\{ \sum E[a_n^2] \right\} \frac{\sin \pi \nu T}{\pi \nu T} \quad (4-47)$$

Because both of these results are independent of the frequency we can use Eq. (4-44) to obtain the variance of the returned power

$$\begin{aligned} \sigma_{wr}^2 &= \int_{-\infty}^{\infty} \left\{ \sum E[a_n^2] \right\}^2 \frac{\sin^2 \pi \nu T}{(\pi \nu T)^2} \int_{-\infty}^{\infty} |S(f)|^2 |S(f-\nu)|^2 d\phi d\nu = \\ &= \left\{ \sum E[a_n^2] \right\}^2 \int_{-\infty}^{\infty} \left(\frac{\sin \pi \nu T}{\pi \nu T} \right)^2 p(\nu) d\nu = \\ &= \int_{-\infty}^{\infty} R^2(\nu) p(\nu) d\nu \end{aligned} \quad (4-48)$$

where $p(\nu)$ is defined in Eq. (4-43).

Now in order to calculate the improvement due to the frequency averaging we compare the standard deviation of the return when the frequency is swept over f_m with the case when the sweep is zero.

$$I = \frac{\sigma_{wr}^2 \mid \text{freq. Averaging}}{\sigma_{wr}^2 \mid \text{no Averaging}} \quad (4-49)$$

In Section 4.1.2 it was shown that the signal has a frequency spectrum as shown in Figure 16, where the power of the incident signal is assumed to be one

$$\int_{-\infty}^{\infty} |s(f)|^2 df = \int_{f - \frac{f_m}{2}}^{f + \frac{f_m}{2}} \frac{1}{f_m} df = 1 \quad (4-50)$$

then from Eq. (4-43)

$$p(\nu) = \int_{-\infty}^{\infty} |s(f)|^2 |s(f-\nu)|^2 df$$

$$= \begin{cases} \frac{1}{f_m^2} \int_{f - \frac{f_m}{2}}^{f + \frac{f_m}{2} - \nu} df = \frac{1}{f_m^2} [f_m - \nu] & \nu > 0 \\ \frac{1}{f_m^2} \int_{f - \frac{f_m}{2} - \nu}^{f + \frac{f_m}{2}} df = \frac{1}{f_m^2} [f_m + \nu] & \nu < 0 \end{cases} \quad (4-51)$$

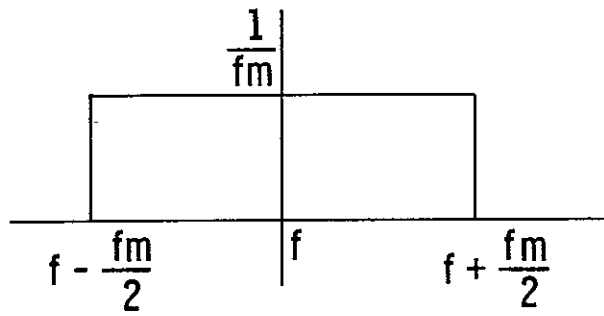


Figure 16. Power spectrum of transmitted wave.

or

$$p(\nu) = \frac{1}{f_m} \left[1 - \frac{|\nu|}{f_m} \right] \quad (4-52)$$

In order to calculate Eq. (4-49), we first calculate the standard deviation of the return signal by substituting Eq. (4-52) in Eq. (4-48)

$$\sigma_{wr}^2 = \left\{ \sum E[a_n^2] \right\}^2 \int_{-f_m}^{f_m} \left(\frac{\sin \pi \nu T}{\pi \nu T} \right)^2 \frac{1}{f_m} \left[1 - \frac{|\nu|}{f_m} \right] d\nu \quad (4-53)$$

For the case, when there is no frequency averaging $f_m \rightarrow 0$, i.e.

$$\begin{aligned} \sigma_{wr}^2 \Big|_{\text{no Ave}} &= \left\{ \sum E[a_n^2] \right\}^2 \int_{-f_m}^{f_m} \left(\frac{\sin \pi \nu T}{\pi \nu T} \right)^2 \frac{1}{f_m} \left[1 - \frac{|\nu|}{f_m} \right] d\nu \\ &= \left\{ \sum E[a_n^2] \right\}^2 \times \int_{-f_m}^{f_m} \frac{1}{f_m} \left[1 - \frac{|\nu|}{f_m} \right] d\nu \\ &= \left\{ \sum E[a_n^2] \right\}^2 \times \left\{ \left[\frac{1}{f_m} \left(\nu - \frac{\nu^2}{2f_m} \right) \right]_0^{f_m} + \left[\frac{1}{f_m} \left(\nu + \frac{\nu^2}{2f_m} \right) \right]_{-f_m}^0 \right\} \\ &= \left\{ \sum E[a_n^2] \right\}^2 \end{aligned} \quad (4-54)$$

Therefore, from Eq. (4-49)

$$I = \frac{\sigma_{wr}^2 \Big|_{\text{Freq. Ave}}}{\sigma_{wr}^2 \Big|_{\text{no Ave}}} = \frac{\left\{ \sum E[a_n^2] \right\}^2 \int_{-\frac{f_m}{2}}^{\frac{f_m}{2}} \left(\frac{\sin \pi \nu T}{\pi \nu T} \right)^2 \frac{1}{f_m} \left[1 - \frac{|\nu|}{f_m} \right] d\nu}{\left\{ \sum E[a_n^2] \right\}^2} \quad (4-55)$$

So

$$I = \int_{-\frac{f_m}{2}}^{\frac{f_m}{2}} \left(\frac{\sin \pi \nu T}{\pi \nu T} \right)^2 \frac{1}{f_m} \left[1 - \frac{|\nu|}{f_m} \right] d\nu \quad (4-56)$$

Where I is the reduction ratio of the variance that we get when we perform frequency averaging (Figure 17). Note that from Eq. (4-54) and Eq. (4-44)

$$\sigma_{wr}^2 \Big|_{\text{no Ave}} = \left\{ \sum E[a_n^2] \right\}^2 = E^2[w_r] \quad (4-57)$$

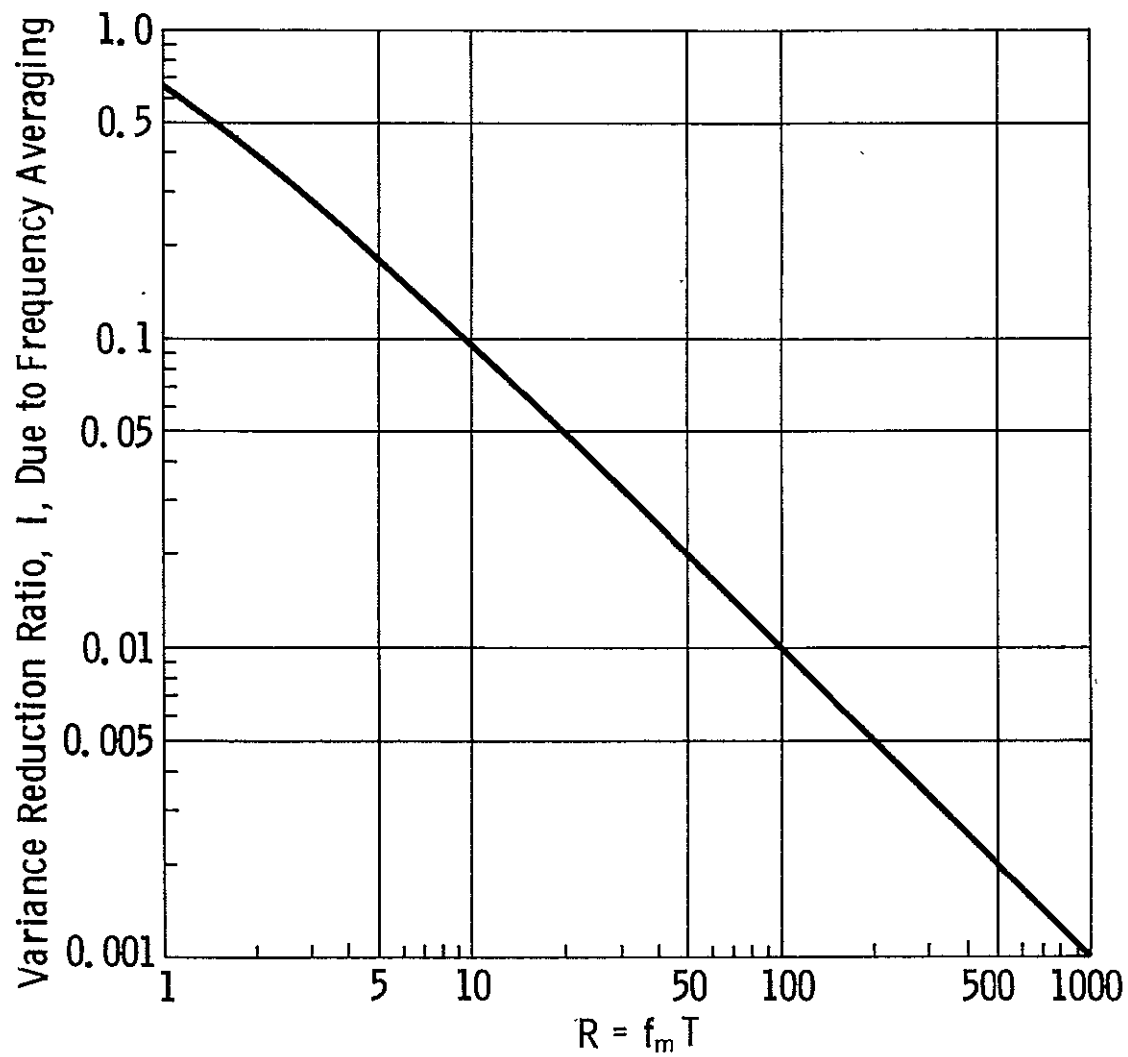


Figure 17. Variance reduction with rectangular spectrum panchromatic illumination. From Eq. 4 - 56.

so Eq. (4-55) can be written as

$$I = \frac{\sigma_{wr}^2 \Big|_{\text{Freq. Ave}}}{E^2[w_r]} \quad (4-58)$$

So by the assumption of small scatterers we can calculate the average μ and the deviation σ of the data taken by a FM-CW radar, and then the variance reduction due to the frequency averaging will be

$$I = \sigma^2 / \mu^2 \quad (4-59)$$

4.2.1.2 Uniform Scatterer Model with Penetration

In this section it is assumed that the target can be represented by independent scatterers located in layers. The pattern for each scatterer is uniform and its return is a sample of a Gaussian random process with zero mean and σ standard deviation.

The procedure for calculating the variance reduction due to frequency averaging is very close to the method used in Section 4.2.1.1. We first calculate the correlation of the target return in frequency domain then use this correlation to calculate the variance of the return signal.

From Figure 18a

$$R_{i1} = h_i / \cos(\theta - \beta/2) \quad (4-60)$$

$$R_{i2} = h_i / \cos(\theta + \beta/2) \quad (4-61)$$

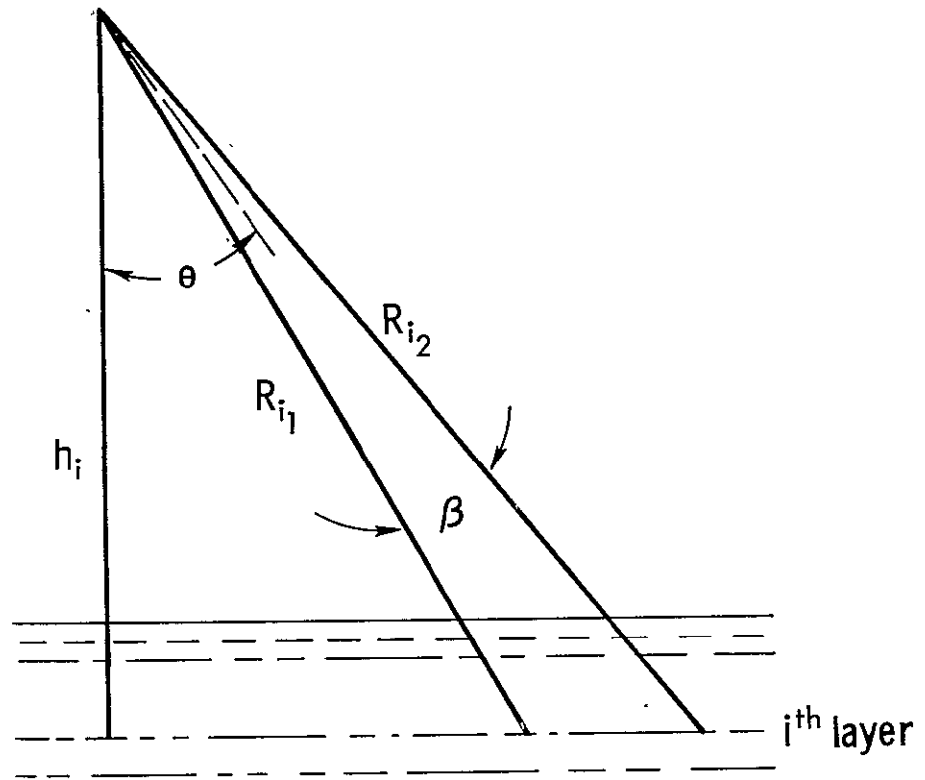


Figure 18a. Uniform scatterer model with penetration.

where

- θ = incidence angle
- β = beamwidth of antenna
- h_i = height of the source from the i^{th} layer
- R_{i1} = smallest distance between the source and the illuminated area of the i^{th} layer
- R_{i2} = largest distance between the source and the illuminated area of the i^{th} layer

then

$$T_{i1} = \frac{2h_i}{c \cos(\theta - \beta/2)} \quad (4-62)$$

$$T_{i2} = \frac{2h_i}{c \cos(\theta + \beta/2)} \quad (4-63)$$

where

- c = speed of a light
- T_{i1} = smallest time required for travel, a roundtrip distance, between the source and the i^{th} layer
- T_{i2} = largest time required for travel, a roundtrip distance, between the source and the i^{th} layer

As stated in Eq. (4-1) the return from the n^{th} scatterer of the i^{th} layer is

$$S_{r,i}(t) = a_{in} S(t - t_{in}) \quad (4-64)$$

Then the total return will be

$$S_r(t) = \sum_i \sum_n a_{in} S(t - t_{in}) \quad (4-65)$$

with the same procedure that is used to get Eq. (4-22)

$$c(f) = \sum_i \sum_n a_{in} e^{-j2\pi f t_{in}} \quad (4-66)$$

then by the definition of Eq. (4-23)

$$R(\nu) = E \left[c(f) c^*(f-\nu) \right] \quad (4-67)$$

or

$$R(\nu) = E \left[\sum_i \sum_n a_{in} e^{-j2\pi f t_{in}} \sum_j \sum_m a_{jm} e^{j2\pi f t_{jm}} \right] \quad (4-68)$$

then by the assumption

$$E \left[a_{in} a_{jm} \right] = E \left[a_{in} \right] E \left[a_{jm} \right] = 0 \quad (4-69)$$

$i \neq j \text{ or } n \neq m$

we have

$$R(\nu) = E \left[\sum_i \sum_n a_{in}^2 e^{-j2\pi \nu t_{in}} \right] \quad (4-70)$$

or

$$R(\nu) = E \left[\sum a_{1n}^2 e^{-j2\pi\nu t_{1n}} + \sum a_{2n}^2 e^{-j2\pi\nu t_{2n}} + \dots + \sum a_{in}^2 e^{-j2\pi\nu t_{in}} + \dots \right] \quad (4-71)$$

where

$R(\nu)$ is the correlation function of the return in frequency domain and

$\sum_n a_{in}^2 e^{-j2\pi\nu t_{in}}$ is the contribution of i^{th} layer

By assuming that the time delay of the return from each scatterer is a sample of a uniform distribution, i.e.

$$p(t_{in}) = \frac{1}{T_{i2} - T_{i1}} \quad (4-72)$$

$$= 0 \quad \text{otherwise} \quad (4-73)$$

and by assuming that the return from the scatterers of each layer are comparable in size before attenuation through layers above them is accounted for, we obtain from Eq. (4-71)

$$\begin{aligned} E \left[\sum_n a_{in}^2 e^{-j2\pi\nu t_{in}} \right] &= \sum_n E \left[a_{in}^2 e^{-j2\pi\nu t_{in}} \right] \\ &= \sum_n \left\{ E[a_{in}^2] \right\} E \left[e^{-j2\pi\nu t_{in}} \right] \end{aligned} \quad (4-74)$$

by the same procedure as stated in Eq. (4-29)

$$E \left[\frac{-jz^{\nu} \gamma t_{in}}{e} \right] = \frac{-j\pi\nu (T_{i1} + T_{i2})}{e} \frac{\sin \pi\nu (T_{i2} - T_{i1})}{\pi\nu (T_{i2} - T_{i1})} \quad (4-75)$$

so in view of Eqs. (4-60) and (4-61) we can write

$$R(\nu) = \sum_i \left\{ \left[\sum_n E[a_{in}^2] \right] R_i \right\} \quad (4-76)$$

where

$$R_i = \exp \left[-j\pi\nu \frac{zh_i}{c} \left[\frac{1}{G_0(\sigma + \beta/2)} + \frac{1}{G_0(\sigma - \beta/2)} \right] \right] \times \frac{\sin \left\{ \pi\nu \frac{zh_i}{c} \left[\frac{1}{G_0(\sigma + \beta/2)} - \frac{1}{G_0(\sigma - \beta/2)} \right] \right\}}{\pi\nu \frac{zh_i}{c} \left[\frac{1}{G_0(\sigma + \beta/2)} - \frac{1}{G_0(\sigma - \beta/2)} \right]} \quad (4-77)$$

The incident power that reaches the i^{th} layer has already been attenuated by the first $(i-1)$ layers. The power which is scattered from a scatterer in i^{th} layer is also attenuated by the first $(i-1)$ layers before it reaches the receiving antenna. So assuming that the average RCS of all layers are equal the contribution of the lower layers will be much smaller. From Figure 18b it can be easily seen that the distance in which the power gets attenuated is $(h_i - h_1) / \cos \theta'$ where θ' is the refraction angle and from the Snell's law is equal to

$$\theta' = \arcsin \left\{ \frac{\sin \theta}{\sqrt{\epsilon_r}} \right\} \quad (4-78)$$

where

$$\begin{aligned} \theta &= \text{angle of incidence} \\ \epsilon_r &= \text{relative dielectric constant of the target} \end{aligned}$$

So if we assume that the attenuation function is exponential, then

$$\frac{E[a_{in}^2]}{E[a_{in}^2]} = \exp \left[\frac{-z(h_i - h_1)}{\delta \cos \theta'} \right] \quad (4-79)$$

where δ is the skin depth and a function of the dielectric properties of the target. By substituting Eq. (4-79) in Eq. (4-76), we obtain

$$\begin{aligned} R(\rho) &= \sum_i \left\{ \sum_n E[a_{in}^2] \exp \left[\frac{-z(h_i - h_1)}{\delta \cos \theta'} \right] \times R_i \right\} = \\ &= \sum_n E[a_{in}^2] \sum_i \left\{ \exp \left[\frac{-z(h_i - h_1)}{\delta \cos \theta'} \right] \times R_i \right\} \end{aligned} \quad (4-80)$$

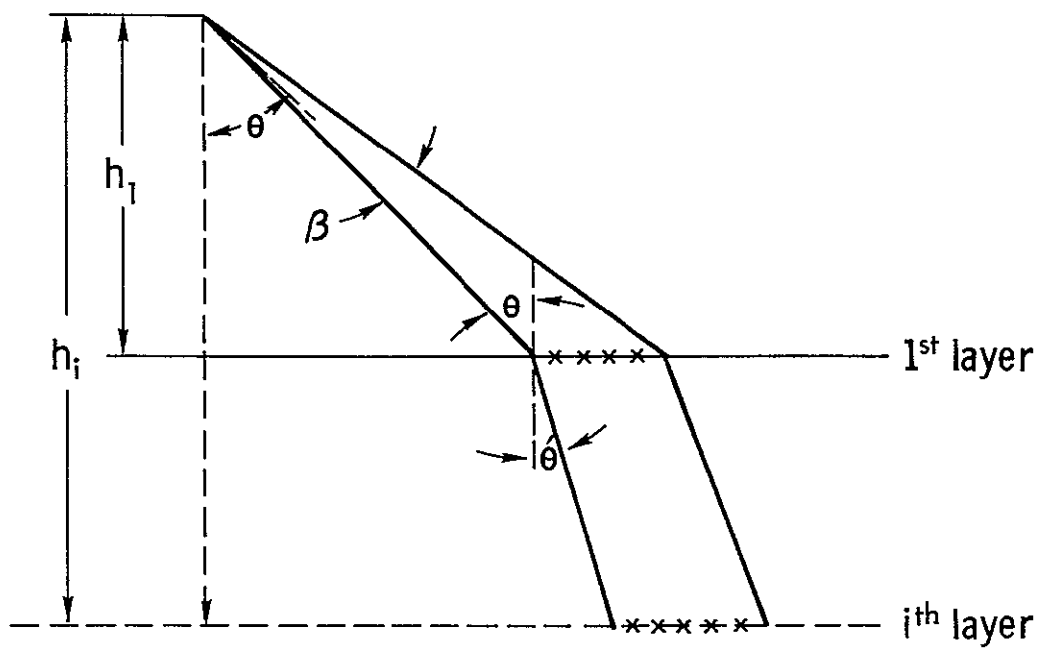


Figure 18b. Uniform scatterer model with penetration.

By substituting Eq. (4-77) into Eq. (4-80)

$$R(\nu) = \left\{ \sum E [a_{in}^2] \right\} \left\{ \sum_i \exp \left[-j \pi \nu \frac{z h_i}{c} \left[\frac{1}{\cos(\theta + \beta/2)} + \frac{1}{\cos(\theta - \beta/2)} \right] \right] \right\} \times$$

$$\times \frac{\sin \left\{ \pi \nu \frac{z h_i}{c} \left[\frac{1}{\cos(\theta + \beta/2)} - \frac{1}{\cos(\theta - \beta/2)} \right] \right\}}{\pi \nu \frac{z h_i}{c} \left[\frac{1}{\cos(\theta + \beta/2)} - \frac{1}{\cos(\theta - \beta/2)} \right]} \exp \left[\frac{-2(h_i - h_1)}{\delta \cos \theta'} \right] \quad (4-81)$$

Because the distance between source and surface is large, the skin depth is very small, and the refraction angle as defined in Eq. (4-78) is small, so the area of illumination for different layers is almost constant. Taking h_i to be equal to h_1 except in the exponent, we obtain

$$R(\nu) = \left\{ \sum E [a_{in}^2] \right\} \frac{\sin \pi \nu \frac{z h_1}{c} \left[\frac{1}{\cos(\theta + \beta/2)} - \frac{1}{\cos(\theta - \beta/2)} \right]}{\pi \nu \frac{z h_1}{c} \left[\frac{1}{\cos(\theta + \beta/2)} - \frac{1}{\cos(\theta - \beta/2)} \right]} \times$$

$$\times \sum_i \exp \left[-j \pi \nu \frac{z h_i}{c} \left[\frac{1}{\cos(\theta + \beta/2)} + \frac{1}{\cos(\theta - \beta/2)} \right] - \frac{2(h_i - h_1)}{\delta \cos \theta'} \right] \quad (4-82)$$

The above sum can be approximated by the following integral

$$\sum_{i=1}^N \exp[-jAh_i - B(h_i - h_1)] = \int_{h_1}^{h_{\max}} \frac{N}{h_{\max} - h_1} e^{-jAh_i - B(h_i - h_1)} dh_i$$

$$= \frac{N}{(h_{\max} - h_1)(jA + B)} \left[\frac{e^{-jAh_1}}{e^{-jAh_{\max} - B(h_{\max} - h_1)}} - e^{-jAh_{\max} - B(h_{\max} - h_1)} \right]$$

(4-83)

$$= N \frac{1 - \exp[-(jA + B)(h_{\max} - h_1)]}{(h_{\max} - h_1)(jA + B)} e^{-jAh_1}$$

Equation (4-82) will be

$$R(\nu) = \exp\left[-j\pi\nu \frac{zh_1}{c} \left(\frac{1}{\cos(\theta + \beta_2)} + \frac{1}{\cos(\theta - \beta_2)} \right)\right] \times N \times \sum_n E[a_n^2]$$

$$\times \frac{\sin \pi\nu \frac{zh_1}{c} \left[\frac{1}{\cos(\theta + \beta_2)} - \frac{1}{\cos(\theta - \beta_2)} \right]}{\pi\nu \frac{zh_1}{c} \left[\frac{1}{\cos(\theta + \beta_2)} - \frac{1}{\cos(\theta - \beta_2)} \right]}$$

(4-84)

$$\times \frac{1}{h_{\max} - h_1} \times \frac{1}{\frac{2\pi\nu}{c} \left[\frac{1}{\cos(\theta + \beta_2)} + \frac{1}{\cos(\theta - \beta_2)} \right] + \frac{2}{8\cos\theta}}$$

$$\times \left\{ 1 - \exp\left[-(h_{\max} - h_1) \left(-\frac{j2\pi\nu}{c} \left\{ \frac{1}{\cos(\theta + \beta_2)} + \frac{1}{\cos(\theta - \beta_2)} \right\} - \frac{2}{8\cos\theta} \right) \right] \right\}$$

Where

$$N = \text{number of the layers} \quad (4-85)$$

$$N \sum_n E[a_{i,n}^2] = \text{sum of the variance of all scatterers located in all layers} \quad (4-86)$$

In order to calculate the standard deviation of the average return signal we substitute Eq. (4-84) and Eq. (4-52) into Eq. (4-48). We obtain

$$\begin{aligned} \sigma_{wr}^2 &= \int_{-\infty}^{\infty} |R(v)|^2 p(v) dv \\ &= \int_{-f_m}^{f_m} |R(v)|^2 \frac{1}{f_m} \left[1 - \frac{|v|}{f_m} \right] dv \end{aligned} \quad (4-87)$$

where $R(v)$ is defined in Eq. (4-84).

The reduction of the standard deviation due to frequency averaging from Eq. (4-49) will then be:

$$\begin{aligned} I &= \frac{\sigma_{wr}^2 \Big|_{\text{Freq. Average}}}{\sigma_{wr}^2 \Big|_{\text{no Average}}} \\ &= \frac{\int_{-f_m/2}^{f_m/2} |R(v)|^2 \frac{1}{f_m} \left[1 - \frac{|v|}{f_m} \right] dv}{f_m \rightarrow 0 \int_{-f_m/2}^{f_m/2} |R(v)|^2 \frac{1}{f_m} \left[1 - \frac{|v|}{f_m} \right] dv} \quad (4-88) \\ &= \frac{1}{|R(0)|^2} \int_{-f_m/2}^{f_m/2} |R(v)|^2 \frac{1}{f_m} \left[1 - \frac{|v|}{f_m} \right] dv \end{aligned}$$

From Eq. (4-84)

$$R(0) = N \sum E[a_{1n}^2] \frac{1}{h_{\max} - h_1} * \frac{1}{\frac{2}{8 \cos \theta'}} * \left\{ 1 - \exp \left[- \frac{2(h_{\max} - h_1)}{8 \cos \theta'} \right] \right\} \quad (4-89)$$

So Eq. (4-88) will be

$$\begin{aligned} I &= \left(\frac{(2/8 \cos \theta')^2}{1 - \exp \left[\frac{-2(h_{\max} - h_1)}{8 \cos \theta'} \right]} \right)^2 \int_{-f_m}^{f_m} \left(\frac{\sin \pi \nu T}{\pi \nu T} \right)^2 * \\ &* \frac{1}{\left(\frac{2\pi \nu}{c} \left[\frac{1}{\cos(\theta + \theta/2)} + \frac{1}{\cos(\theta - \theta/2)} \right] + \frac{2}{8 \cos \theta'} \right)^2} * \left\{ 1 - \exp \left[\left(\frac{-12\pi \nu}{c} * \right. \right. \right. \\ & * \left. \left. \left. \left[\frac{1}{\cos(\theta + \theta/2)} + \frac{1}{\cos(\theta - \theta/2)} \right] - \frac{2}{8 \cos \theta'} \right) * (h_{\max} - h_1) \right] \right\}^2 d\nu. \quad (4-90) \end{aligned}$$

where

$$T \triangleq \frac{2h_1}{c} \left[\frac{1}{\cos(\theta + \theta/2)} - \frac{1}{\cos(\theta - \theta/2)} \right]$$

is the time span of the target. Now if we let the depth of the target go to infinity, i.e.

$$h_{\max} \rightarrow \infty$$

Then Eq. (4-90) will be

$$I = \int_{-f_m}^{f_m} \left(\frac{A_m \pi \nu T}{\pi \nu T} \right)^2 \times \frac{1}{\left[1 + \frac{\pi \nu \delta \cos \theta'}{c} \left(\frac{1}{\cos(\theta + \beta/2)} + \frac{1}{\cos(\theta - \beta/2)} \right) \right]^2} \times \frac{1}{f_m} \left[1 - \frac{|\nu|}{f_m} \right] d\nu \quad (4-91)$$

where

- T = the time span of the target
- δ = skin depth
- c = speed of light
- θ = angle of incidence
- β = antenna beamwidth
- ν = sweep frequency
- f_m = sweep band of the signal
- I = improvement factor
- θ' = refraction angle

Because the requirements leading to Eq. (4-59) are correct for the layer assumption so for the measured data the reduction ratio of variance due to frequency averaging

$$I = \frac{\sigma^2}{\mu^2} \quad (4-92)$$

where

- σ = variance of the measured data
- μ = mean of the measured data

4.2.2 Number of Independent Samples Based on Facet Model

In this section we assume that the target consists of a collection of facets of different sizes, and the return from different facets are independent.

In the previous section it was shown that the target effect can be represented in the form of:

$$c(f) = \sum a_n e^{-j2\pi f t_n} \quad (4-22)$$

The mean and the variance of the return power can be expressed in terms of $c(f)$ as follows:

$$E[w_r] = E[|c(f)|^2] \quad (4-54)$$

$$\begin{aligned} \sigma_{w_r}^2 &= E[w_r^2] - E^2[w_r] \\ &= \int_{-\infty}^{\infty} \left\{ E[|c(f)|^2 |c(f-\gamma)|^2] - E^2[|c(f)|^2] \right\} p(\gamma) d\gamma \quad (4-44) \end{aligned}$$

It was also shown for the uniform scatterer model, that in the absence of frequency averaging, the variance of the return power is equal to its mean, i.e.

$$\begin{aligned} \sigma_{w_r}^2 &= E[|c(f)|^4] - E^2[|c(f)|^2] = \\ &= E^2[|c(f)|^2] = E^2[w_r] \quad (4-93) \end{aligned}$$

Based on this assumption for calculating the reduction factor of the variance of the return power due to frequency averaging, instead of conducting two experiments, one with frequency averaging and the second at a single frequency, and calculating the variance of each set of the data, we only need to know the mean and the variance

of the first set. The reason is that because we are sweeping over a narrow band, compared with the center frequency, so the mean with frequency averaging will be equal to the mean that one would get from the second experiment. On the other hand from Eq. (4-93) the mean square is equal to the variance for the single frequency case. Hence based on the uniform scatterer model, if we conduct one experiment with frequency averaging then the reduction factor of the variance can be obtained by dividing the mean square of the data by its variance. That is:

$$N = \frac{E^2 [w_r]}{\sigma_{w_r}^2} \quad (4-94)$$

where N is the number of independent samples.

The experimental data shown in Section 4.3 are from reference [3] and are calculated based on this assumption.

In this section we will first show that when the target is assumed consists of a collection of facets, the assumption of the equality of the mean and the variance of the return power in the single frequency case does not hold--this is especially true for the case that the product of the sweep band and the time span of the target, $f_m T$, is small, i.e. at small incidence angles. So we will conclude that the calculated number of independent samples as shown in Figure 21 are not correct; because they are based on Eq. (4-94).

In the second part we will calculate the number of independent samples based on the facet model assumption and show that the results for small incidence angles are almost the same as the results predicted by the uniform scatterer model assumption. For large incidence angles the number of the independent samples predicted by the facet model is smaller than the number predicted by the uniform scatterer model and is closer to the number calculated based on the experimental data Figure 21.

4.2.2.1 Mean and Variance of the Return

In what follows we will first calculate $E[|c(f)|^2 |c(f-\nu)|^2]$ then by putting $\nu = 0$, we will obtain $E[|c(f)|^4]$. We will then calculate the mean of the return power, i.e. $E[|c(f)|^2]$ and will show that, unlike the uniform scatterer model, the mean square is larger than the variance, i.e.

$$E^2 [|c(f)|^2] > E [|c(f)|^4] - E^2 [|c(f)|^2] \quad (4-95)$$

or

$$2 E^2 [|c(f)|^2] - E [|c(f)|^4] > 0 \quad (4-96)$$

from Eq. (4-22)

$$E [|c(f)|^2 |c(f-\nu)|^2] = E \left[\sum_n \sum_m \sum_p \sum_q a_n a_m a_p a_q e^{-j2\pi f t_n} e^{j2\pi f t_m} e^{-j2\pi(f-\nu) t_p} e^{j2\pi(f-\nu) t_q} \right]$$

Because it is assumed that a_n and t_n are independent and t_n is uniformly distributed, we get

$$E [|c(f)|^2 |c(f-\nu)|^2] = \sum_{n \neq m \neq p \neq q} N(N-1)(N-2)(N-3) \langle a_n \rangle^4 \left(\frac{\sin \pi f T}{\pi f T} \right)^2 \left(\frac{\sin \pi (f-\nu) T}{\pi (f-\nu) T} \right)^2 \quad (a)$$

$$+ \sum_{n=m \neq p \neq q} N(N-1)(N-2) \langle a_n^2 \rangle \langle a_n \rangle^2 \left(\frac{\sin \pi (f-\nu) T}{\pi (f-\nu) T} \right)^2 \quad (b)$$

$$+ \sum_{n=p \neq m \neq q} N(N-1)(N-2) \langle a_n^2 \rangle \langle a_n \rangle^2 \frac{\sin \pi (2f-\nu) T}{\pi (2f-\nu) T} \frac{\sin \pi f T}{\pi f T} \frac{\sin \pi (f-\nu) T}{\pi (f-\nu) T} \quad (c)$$

$$+ \sum_{n=q \neq m \neq p} N(N-1)(N-2) \langle a_n^2 \rangle \langle a_n \rangle^2 \frac{\sin \pi \nu T}{\pi \nu T} \frac{\sin \pi f T}{\pi f T} \frac{\sin \pi (f-\nu) T}{\pi (f-\nu) T} \quad (d)$$

$$+ \sum_{m=p \neq n \neq q} N(N-1)(N-2) \langle a_n^2 \rangle \langle a_n \rangle^2 \frac{\sin \pi \nu T}{\pi \nu T} \frac{\sin \pi f T}{\pi f T} \frac{\sin \pi (f-\nu) T}{\pi (f-\nu) T} \quad (e)$$

$$m = q \neq n \neq p$$

$$+ N(N-1)(N-2) \langle a_n^2 \rangle \langle a_n \rangle^2 \frac{\sin \pi f T}{\pi f T} \frac{\sin \pi (f-v) T}{\pi (f-v) T} \frac{\sin \pi (2f-v) T}{\pi (2f-v) T} \quad (f)$$

$$p = q \neq n \neq m$$

$$+ N(N-1)(N-2) \langle a_n^2 \rangle \langle a_n \rangle^2 \left(\frac{\sin \pi f T}{\pi f T} \right)^2 \quad (g)$$

$$n = m \neq p = q$$

$$+ N(N-1) \langle a_n^2 \rangle^2 \quad (h)$$

$$n = p \neq m = q$$

$$+ N(N-1) \langle a_n^2 \rangle^2 \left(\frac{\sin \pi (2f-v) T}{\pi (2f-v) T} \right)^2 \quad (i)$$

$$n = q \neq p = m$$

$$+ N(N-1) \langle a_n^2 \rangle^2 \left(\frac{\sin \pi v T}{\pi v T} \right)^2 \quad (j)$$

$$n = m = p \neq q$$

$$+ N(N-1) \langle a_n^3 \rangle \langle a_n \rangle \left(\frac{\sin \pi (f-v) T}{\pi (f-v) T} \right)^2 \quad (k)$$

$$n = m = q \neq p$$

$$+ N(N-1) \langle a_n^3 \rangle \langle a_n \rangle \left(\frac{\sin \pi (f-v) T}{\pi (f-v) T} \right)^2 \quad (l)$$

$$m = p = q \neq n$$

$$+ N(N-1) \langle a_n^3 \rangle \langle a_n \rangle \left(\frac{\sin \pi f T}{\pi f T} \right)^2 \quad (m)$$

$$n = p = q \neq m$$

$$+ N(N-1) \langle a_n^3 \rangle \langle a_n \rangle \left(\frac{\sin \pi f T}{\pi f T} \right)^2 \quad (n)$$

$$n = m = p = q$$

$$+ N \langle a_n^4 \rangle \quad (o)$$

Now we will calculate $E[|c(f)|^2] E[|c(f-\nu)|^2]$ and by substituting $\nu = 0$ we get the mean square.

$$\begin{aligned}
 E[|c(f)|^2] E[|c(f-\nu)|^2] &= E\left\{ \sum_n \sum_m a_n a_m e^{-j2\pi f t_n} e^{j2\pi f t_m} \right\} E\left\{ \sum_n \sum_m a_n a_m \right. \\
 &\quad \left. e^{-j2\pi(f-\nu)t_n} e^{j2\pi(f-\nu)t_m} \right\} = \\
 &= N^2 \langle a_n^2 \rangle^2 + \\
 &+ N^2(N-1) \langle a_n^2 \rangle \langle a_n \rangle^2 \left(\frac{\sin \pi(f-\nu)T}{\pi(f-\nu)T} \right)^2 + \\
 &+ N^2(N-1) \langle a_n^2 \rangle \langle a_n \rangle^2 \left(\frac{\sin \pi f T}{\pi f T} \right)^2 + \\
 &+ N^2(N-1)^2 \langle a_n \rangle^4 \left(\frac{\sin \pi f T}{\pi f T} \right)^2 \left(\frac{\sin \pi(f-\nu)T}{\pi(f-\nu)T} \right)^2
 \end{aligned} \tag{4-98}$$

Now we want to prove that in general mean square is larger than the variance, i.e.

$$(\text{mean})^2 - \text{variance} > 0$$

or

$$E^2[|c(f)|^2] - \left\{ E[|c(f)|^4] - E^2[|c(f)|^2] \right\} > 0 \tag{4-99}$$

or

$$2 E^2[|c(f)|^2] - E[|c(f)|^4] > 0 \tag{4-100}$$

If we substitute $\nu = 0$ in Eqs. (4-97) and (4-98), and assuming that N is large and

$$\left(\frac{\sin \pi f T}{\pi f T}\right)^2 \ll \left(\frac{\sin \pi \nu T}{\pi \nu T}\right)^2 = 1$$

We obtain

$$\begin{aligned} 2 E^2 [|c(f)|^2] - E [|c(f)|^4] &= N \langle a_n^2 \rangle^2 \left\{ N^3 \left(\frac{\sin \pi f T}{\pi f T}\right)^4 \right. \\ &- 2 N^2 \frac{\sin 2\pi f T}{2\pi f T} \left(\frac{\sin \pi f T}{\pi f T}\right)^2 \frac{\langle a_n \rangle^2}{\langle a_n^2 \rangle} - 4 N \frac{\langle a_n^3 \rangle \langle a_n \rangle}{\langle a_n^2 \rangle^2} \left(\frac{\sin \pi f T}{\pi f T}\right)^2 \\ &\left. - N \left(\frac{\sin 2\pi f T}{2\pi f T}\right)^2 + \frac{\langle a_n^4 \rangle}{\langle a_n^2 \rangle^2} \right\} \end{aligned} \quad (4-101)$$

As will be shown $\langle a_n \rangle$, $\langle a_n^2 \rangle$, $\langle a_n^3 \rangle$, and $\langle a_n^4 \rangle$ have comparable magnitude, so for the small incidence angles where the time span of the target, T , is very small fT will not be large and consequently $\left(\frac{\sin(\pi f T)}{\pi f T}\right)^2$ is not very small, and because N is large, the first term in Eq. (4-101) will dominate. So

$$2 E^2 [|c(f)|^2] - E [|c(f)|^4] \cong \langle a_n^2 \rangle^2 N^4 \left(\frac{\sin \pi f T}{\pi f T}\right)^4 > 0 \quad (4-102)$$

In other words the mean is larger than the variance.

4.2.2.2 Number of Independent Samples

We want to calculate the reduction in the variance from Eq. (4-44). From Eqs. (4-97) and (4-98) the integrand in Eq. (4-44) will be:

$$\begin{aligned}
 E \left[|c(f)|^2 |c(f-\nu)|^2 \right] - E^2 \left[|c(f)|^2 \right] &\cong 2N^3 \langle a_n^2 \rangle \langle a_n \rangle^2 \times \\
 &\times \left(\frac{\sin \pi \nu T}{\pi \nu T} \right) \left(\frac{\sin \pi f T}{\pi f T} \right) \left(\frac{\sin \pi (f-\nu) T}{\pi (f-\nu) T} \right) + N^2 \langle a_n^2 \rangle^2 \left(\frac{\sin \pi \nu T}{\pi \nu T} \right)^2 + N \\
 &\times \langle a_n^4 \rangle \tag{4-103}
 \end{aligned}$$

From Eqs. (4-44) and from the definition of the number of the independent samples

$$I = \frac{\sigma_{wr}^2 \Big| \text{no Averaging}}{\sigma_{wv}^2 \Big| \text{Freq. Averaging}}$$

We obtain

$$\begin{aligned}
 I = \frac{2N^3 \langle a_n^2 \rangle \langle a_n \rangle^2 \left(\frac{\sin \pi f T}{\pi f T} \right)^2 + N^2 \langle a_n^2 \rangle^2 + N \langle a_n^4 \rangle}{2N^3 \langle a_n^2 \rangle \langle a_n \rangle^2 \left(\frac{\sin \pi f T}{\pi f T} \right)^2 \int \frac{\sin \pi \nu T}{\pi \nu T} p(\nu) d\nu + N^2 \langle a_n^2 \rangle^2 \int \left(\frac{\sin \pi \nu T}{\pi \nu T} \right)^2 p(\nu) d\nu + N \langle a_n^4 \rangle}
 \end{aligned} \tag{4-104}$$

where $p(\nu)$ is defined in Eq. (4-52). When the product of sweep band and time span of the illuminated area is small i.e. $\nu T \ll 1$, the answer to both integrals will be one, so I , as expected, will be equal to unity. But when the product is not small and since $f \gg \nu$, fT will be large and $\left(\frac{\sin \pi f T}{\pi f T} \right)^2 \rightarrow 0$, so I will be equal to

$$I = \frac{N^2 \langle a_n^2 \rangle^2 + N \langle a_n^4 \rangle}{N^2 \langle a_n^2 \rangle^2 \int \left(\frac{\Delta \pi \nu T}{\pi T} \right)^2 p(\nu) d\nu + N \langle a_n^4 \rangle} \quad (4-105)$$

or letting $I' = \left[\int \left(\frac{\Delta \pi \nu T}{\pi T} \right)^2 p(\nu) d\nu \right]^{-1}$ and dividing the numerator and the denominator by $N^2 \langle a_n^2 \rangle^2$

$$I = \frac{1 + \frac{N \langle a_n^4 \rangle}{N^2 \langle a_n^2 \rangle^2}}{\frac{1}{I'} + \frac{N \langle a_n^4 \rangle}{N^2 \langle a_n^2 \rangle^2}} \quad (4-106)$$

where I' is the number of independent samples predicted by uniform scatterer assumption (see Section 4.2.1). If we substitute $N \langle \quad \rangle$ by summation in Eq. (4-106) we obtain

$$I = \frac{1 + \frac{\sum E[a_n^4]}{\{\sum E[a_n^2]\}^2}}{\frac{1}{I'} + \frac{\sum E[a_n^4]}{\{\sum E[a_n^2]\}^2}} \quad (4-107)$$

It should be mentioned that the summation $\sum_{n=1}^N$ is for all facets—large, medium, and small—so in order to calculate the second term in the denominator we break it and group each size separately

$$\sum_{n=1}^N E[a_n^2] = \sum_{n=1}^{n_l} E[a_n^2] + \sum_{m=1}^{n_m} E[a_m^2] + \sum_{p=1}^{n_s} E[a_p^2]$$

$$\sum_{n=1}^N E[a_n^4] = \sum_{n=1}^{n_l} E[a_n^4] + \sum_{m=1}^{n_m} E[a_m^4] + \sum_{p=1}^{n_s} E[a_p^4] \quad (4-109)$$

where

$$\begin{aligned} n_l &= \text{number of large facets} \\ n_m &= \text{number of medium facets} \\ n_s &= \text{number of small facets} \\ N &= n_l + n_m + n_s \end{aligned}$$

Now we calculate N , n_l , n_m , and n_s .

Time delay due to each facet with a length L from Figure 19 is $\frac{2L}{c} \sin \theta_n$ where θ_n is the local incidence angle. The average value of this delay will be:

$$\begin{aligned} \left\langle \frac{2L}{c} \sin \theta_n \right\rangle &= \left\langle \frac{2L}{c} (\sin \theta - s \cos \theta) \right\rangle = \\ &= \int_0^{\infty} \int_{-\infty}^{\infty} \frac{2L}{c} (\sin \theta - s \cos \theta) P(L) P(s) ds dL = \end{aligned}$$

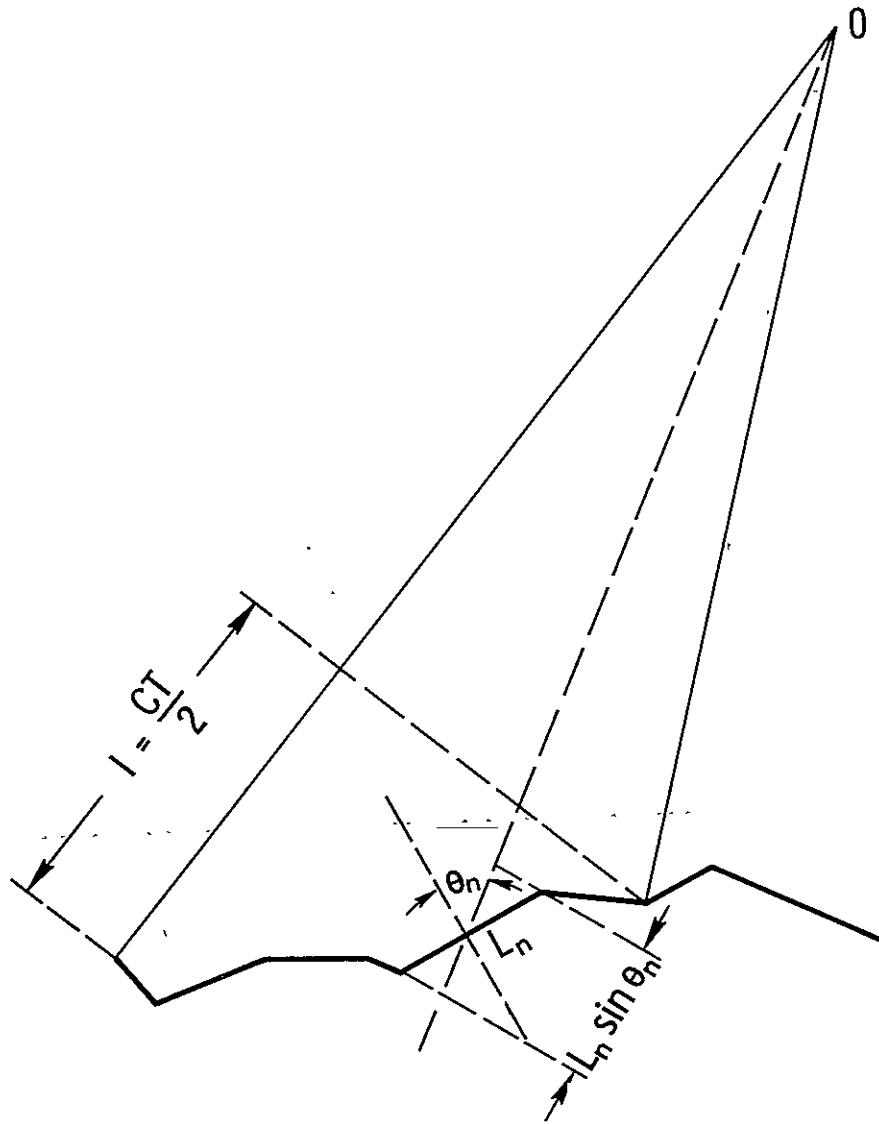


Figure 19. Time delay based on facet model.

$$\begin{aligned}
E[a_n^4] &= A^2 \frac{2}{\sigma\sqrt{2\pi}} \int_{\lambda}^{\infty} \sin^4 KL \sin \sigma e^{-\frac{L^2}{2\sigma^2}} dL \\
&= A^2 \frac{2}{\sigma\sqrt{2\pi}} \int_{\lambda}^{\infty} \frac{3 - 4 \cos(2KL \sin \sigma) + \cos(4KL \sin \sigma)}{8} e^{-\frac{L^2}{2\sigma^2}} dL \\
&= \text{Real} \left\{ A^2 \left[\frac{3}{8} \left(1 - \text{erf} \left(\frac{\lambda}{\sigma\sqrt{2}} \right) \right) - \frac{1}{2} \exp \left[- \left(K \sin \sigma \sigma\sqrt{2} \right)^2 \right] \right] \times \frac{2}{\sqrt{\pi}} \right. \\
&\quad \times \left. \left[\int_{\frac{\lambda}{\sigma\sqrt{2}} + jK \sin \sigma \sigma\sqrt{2}}^{\infty} e^{-z^2} dz + \frac{1}{8} e^{-\left(2K \sin \sigma \sigma\sqrt{2} \right)^2} \times \frac{2}{\sqrt{\pi}} \times \int_{\frac{\lambda}{\sigma\sqrt{2}} + j2K \sin \sigma \sigma\sqrt{2}}^{\infty} e^{-z^2} dz \right] \right\} \quad (4-118)
\end{aligned}$$

At nadir:

$$E[a_n^2] = 2\sigma^2 \left\{ \frac{2\lambda}{\sigma\sqrt{2\pi}} + 1 - \text{erf} \left(\frac{\lambda}{\sigma\sqrt{2}} \right) \right\} \quad (4-119)$$

$$E[a_n^4] = 4\sigma^4 \left\{ \frac{2}{\sqrt{\pi}} \left(\frac{\lambda}{\sigma\sqrt{2}} \right)^3 e^{-\left(\frac{\lambda}{\sigma\sqrt{2}} \right)^2} + \frac{6\lambda}{\sigma\sqrt{2\pi}} e^{-\left(\frac{\lambda}{\sigma\sqrt{2}} \right)^2} + 3 - 3 \text{erf} \left(\frac{\lambda}{\sigma\sqrt{2}} \right) \right\} \quad (4-120)$$

So

$$\frac{E^2[a_n^2]}{E[a_n^4]} \approx \frac{1}{3} \quad (4-121)$$

$$\begin{aligned}
&= \int_0^{\infty} \int_{-\infty}^{\infty} \frac{2L}{c} (\sin\theta - s \cos\theta) \frac{2}{\sqrt{L} \sqrt{2\pi}} e^{-\frac{L^2}{2\sigma^2}} \frac{1}{\sqrt{s} \sqrt{2\pi}} e^{-\frac{s^2}{2\sigma_s^2}} ds dL \\
&= \int_0^{\infty} \frac{2L}{c} \sin\theta \frac{2}{\sqrt{L} \sqrt{2\pi}} e^{-\frac{L^2}{2\sigma^2}} dL \\
&= \frac{4\sqrt{L} \sin\theta}{\sqrt{2\pi} c}
\end{aligned} \tag{4-110}$$

where

- s = slope
- p(s) = probability distribution of slope
- p(L) = probability distribution of facet length

Since the time delay is equal to the average time delay times the total number of facets, we get

$$\frac{4\sqrt{L} \sin\theta}{\sqrt{2\pi} c} N = T \tag{4-111}$$

or

$$N = \frac{\sqrt{2\pi} c T}{4\sqrt{L} \sin\theta} \tag{4-112}$$

then n_l , n_m , and n_s will be

$$n_l = N \int_{\lambda}^{\infty} e^{-\frac{L^2}{2\sigma^2}} dL = \frac{\sqrt{2\pi} c T}{4\sqrt{L} \sin\theta} \int_{\lambda}^{\infty} e^{-\frac{L^2}{2\sigma^2}} dL \tag{4-113}$$

$$n_m = N \int_{\frac{2\lambda}{5}}^{\lambda} e^{-\frac{L^2}{2\sigma^2 l}} dL = \frac{\sqrt{2\pi} CT}{4 \sigma l \sin \theta} \int_{\frac{2\lambda}{5}}^{\lambda} e^{-\frac{L^2}{2\sigma^2 l}} dL \quad (4-114)$$

$$n_s = N \int_0^{\frac{2\lambda}{5}} e^{-\frac{L^2}{2\sigma^2 l}} dL = \frac{\sqrt{2\pi} CT}{4 \sigma l \sin \theta} \int_{\frac{2\lambda}{5}}^{\lambda} e^{-\frac{L^2}{2\sigma^2 l}} dL \quad (4-115)$$

where, as before, it is assumed that the targets whose size is, smaller than $2\lambda/5$ are considered to be small, larger than λ are considered to be large, and between $2\lambda/5$ and λ are considered to be medium.

In what follows we calculate $E[a_n^2]$ and $E[a_n^4]$ for large, medium, and small size facets and substitute the results in Eq. (4-108) to calculate the number of the independent samples.

i) For large facets note that

$$\begin{aligned} a_n^2 &= \frac{4\pi}{\lambda^2} L^2 \sigma^2 \theta \left(\frac{\sin KL \sin \theta}{KL \sin \theta} \right)^2 \\ &= \frac{4\pi \sigma^2 \theta}{K^2 \lambda^2 \sin^2 \theta} \sin^2 (KL \sin \theta) \\ &= \frac{1}{\pi \tan^2 \theta} \sin^2 (KL \sin \theta) \\ &\triangleq A \sin^2 (KL \sin \theta) \end{aligned} \quad (4-116)$$

Then assuming a Gaussian distribution for facet length, we obtain

$$\begin{aligned}
 E[a_n^2] &= A \frac{2}{\sigma\sqrt{2\pi}} \int_{\lambda}^{\infty} \sin^2 KL \sin \theta e^{-\frac{L^2}{2\sigma^2}} dL \\
 &= \frac{A}{2} \frac{2}{\sigma\sqrt{2\pi}} \int_{\lambda}^{\infty} \{1 - \cos(2KL \sin \theta)\} e^{-\frac{L^2}{2\sigma^2}} dL \\
 &= \frac{A}{2} \frac{2}{\sqrt{\pi}} \int_{\frac{\lambda}{\sigma\sqrt{2}}}^{\infty} \{1 - \cos(2K \sin \theta \sigma\sqrt{2} t)\} e^{-t^2} dt \\
 &= \frac{A}{2} \left\{ 1 - \operatorname{erf}\left(\frac{\lambda}{\sigma\sqrt{2}}\right) - \frac{2}{\sqrt{\pi}} \int_{\frac{\lambda}{\sigma\sqrt{2}}}^{\infty} \cos(2K \sin \theta \sigma\sqrt{2} t) e^{-t^2} dt \right\} \\
 &= \frac{A}{2} \left(1 - \operatorname{erf}\left(\frac{\lambda}{\sigma\sqrt{2}}\right) \right) - \frac{A}{\sqrt{\pi}} \operatorname{Re} \left\{ \int_{\frac{\lambda}{\sigma\sqrt{2}}}^{\infty} e^{-(t^2 - j 2K \sin \theta \sigma\sqrt{2} t)} dt \right\} \\
 &= \frac{A}{2} \left(1 - \operatorname{erf}\left(\frac{\lambda}{\sigma\sqrt{2}}\right) \right) - \frac{A}{\sqrt{\pi}} e^{-\frac{(K \sin \theta \sigma\sqrt{2})^2}{4}} \operatorname{Re} \left\{ \int_{\frac{\lambda}{\sigma\sqrt{2}}}^{\infty} e^{-(t - j K \sin \theta \sigma\sqrt{2})^2} dt \right\} \\
 &= \frac{A}{2} \left(1 - \operatorname{erf}\left(\frac{\lambda}{\sigma\sqrt{2}}\right) \right) - \frac{A}{\sqrt{\pi}} e^{-\frac{(K \sin \theta \sigma\sqrt{2})^2}{4}} \operatorname{Re} \left\{ \int_{\frac{\lambda}{\sigma\sqrt{2}} - j K \sin \theta \sigma\sqrt{2}}^{\infty} e^{-z^2} dz \right\} \quad (4-117)
 \end{aligned}$$

For relatively large incidence angles

$$E[a_n^2] = \frac{1 - \operatorname{erf} \frac{\lambda}{\sigma\sqrt{2}}}{2\pi \tan^2 \theta} \quad (4-122)$$

$$E[a_n^4] = \frac{3 \left(1 - \operatorname{erf} \frac{\lambda}{\sigma\sqrt{2}}\right)^2}{8\pi^2 \tan^4 \theta} \quad (4-123)$$

then

$$\frac{E[a_n^2]^2}{E[a_n^4]} \approx \frac{2}{3} \quad (4-124)$$

ii) Medium size facets

$$a_n^2 = \frac{25}{\lambda^{1/2}} L^{5/4} \left(\frac{\sin KL \sin \theta}{KL \sin \theta} \right)^2 \quad (4-125)$$

So

$$\begin{aligned} E[a_n^2] &= B \frac{2}{\sigma\sqrt{2\pi}} \int_{\frac{2\lambda}{5}}^{\lambda} L^{5/4} \frac{\sin^2 KL \sin \theta}{L^2} e^{-\frac{L^2}{25\sigma^2}} dL \\ &= B \frac{2}{\sigma\sqrt{2\pi}} \int_{\frac{2\lambda}{5}}^{\lambda} \frac{\sin^2 KL \sin \theta}{L^{3/4}} e^{-\frac{L^2}{25\sigma^2}} dL \\ &\approx B \frac{2}{\sigma\sqrt{2\pi}} \frac{e^{-\left(\frac{.7\lambda}{\sigma\sqrt{2}}\right)^2}}{(.7\lambda)^{3/4}} \times \frac{1}{2} \left[.6\lambda - \sin(2K\lambda \sin \theta) - \sin(.8K\lambda \sin \theta) \right] \end{aligned} \quad (4-126)$$

$$E[a_n^4] = B^2 \frac{2}{\sigma\sqrt{2\pi}} \int_{\frac{2\lambda}{5}}^{\lambda} \left(L^{5/4} \frac{\sin^2 K L d\sigma}{L^2} \right)^2 e^{-\frac{L^2}{2\sigma^2}} dL$$

$$\approx B^2 \frac{2}{\sigma\sqrt{2\pi}} \frac{e^{-\left(\frac{.7\lambda}{\sigma\sqrt{2}}\right)^2}}{(.7\lambda)^{3/2}} \left[.6\lambda - \sin 2K\lambda \sin \sigma + \sin .8K\lambda \sin \sigma + (4-127) \right. \\ \left. + \sin 4K\lambda \sin \sigma - \sin 1.6K\lambda \sin \sigma \right]$$

where

$$B \triangleq \frac{25}{\lambda^{1/2} K \sin \sigma} \quad (4-128)$$

and

$$\frac{E^2[a_n^2]}{E[a_n^4]} \approx -1 \quad (4-129)$$

iii) Small facets

From reference [19]

$$a_n^2 = \frac{114}{\lambda^2} L^3 \quad (4-130)$$

So

$$E[a_n^2] = c \frac{2}{\sigma\sqrt{2\pi}} \int_0^{\frac{2\lambda}{5}} L^3 e^{-\frac{L^2}{2\sigma^2}} dL \quad (4-131)$$

$$\approx c \frac{2}{\sigma\sqrt{2\pi}} \frac{(.04\lambda)^4}{4}$$

$$E[a_n^4] = c^2 \frac{2}{\sigma\sqrt{2\pi}} \int_0^{\frac{2\lambda}{5}} L^6 e^{-\frac{L^2}{2\sigma^2}} dL \quad (4-132)$$

$$= c^2 \frac{2}{\sigma\sqrt{2\pi}} \frac{(.04\lambda)^7}{7}$$

where

$$c \triangleq 114/\lambda^4 \quad (4-133)$$

$$\frac{E^2[a_n^2]}{E[a_n^4]} \approx \frac{\lambda}{6.5\delta_l} \quad (4-134)$$

Now if we substitute the results of Eqs. (4-131), (4-132), (4-127), (4-126), (4-118), (4-117), (4-115), (4-114), and (4-113) into Eqs. (4-108) and (4-109) we obtain $\sum_{n=1}^N E[a_n^2]$ and $\sum_{n=1}^N E[a_n^4]$, and by substituting these results in Eq. (4-106) we calculate the number of the independent samples.

In Figure 21 we have shown one typical result of this calculation.

4.2.3 Comparison of the Results with Measured Data

In this section we compare the results obtained in Section 4.2 with measured data.

An experiment was conducted to measure the effect of frequency averaging on the reduction of the variance of the returned power [3]. The results of this experiment for alfalfa and bare ground are shown in Figures 20 and 21.

4.2.3.1 Alfalfa

At incidence angles smaller than 60° alfalfa can be considered a layered medium consisting of uniform scatterers. In Figure 20 we compare the theoretical results obtained assuming no penetration, Eq. (4-56), and the case that we have some penetration, Eq. (4-91), with the result of the experiment. It can be seen that for incidence angles smaller than 60° the penetration model can very well predict the experimental result. For incidence angles larger than 60° the alfalfa behaves like a collection of facets, so the number of the independent samples should be calculated based on the facet model assumption, Eq. (4-107).

4.2.3.2 Bare Ground

In Figure 21 we compare the result obtained based on Waite's [26] derivation and the result obtained based on the facet model theory, Eq. (4-107). It is clear that

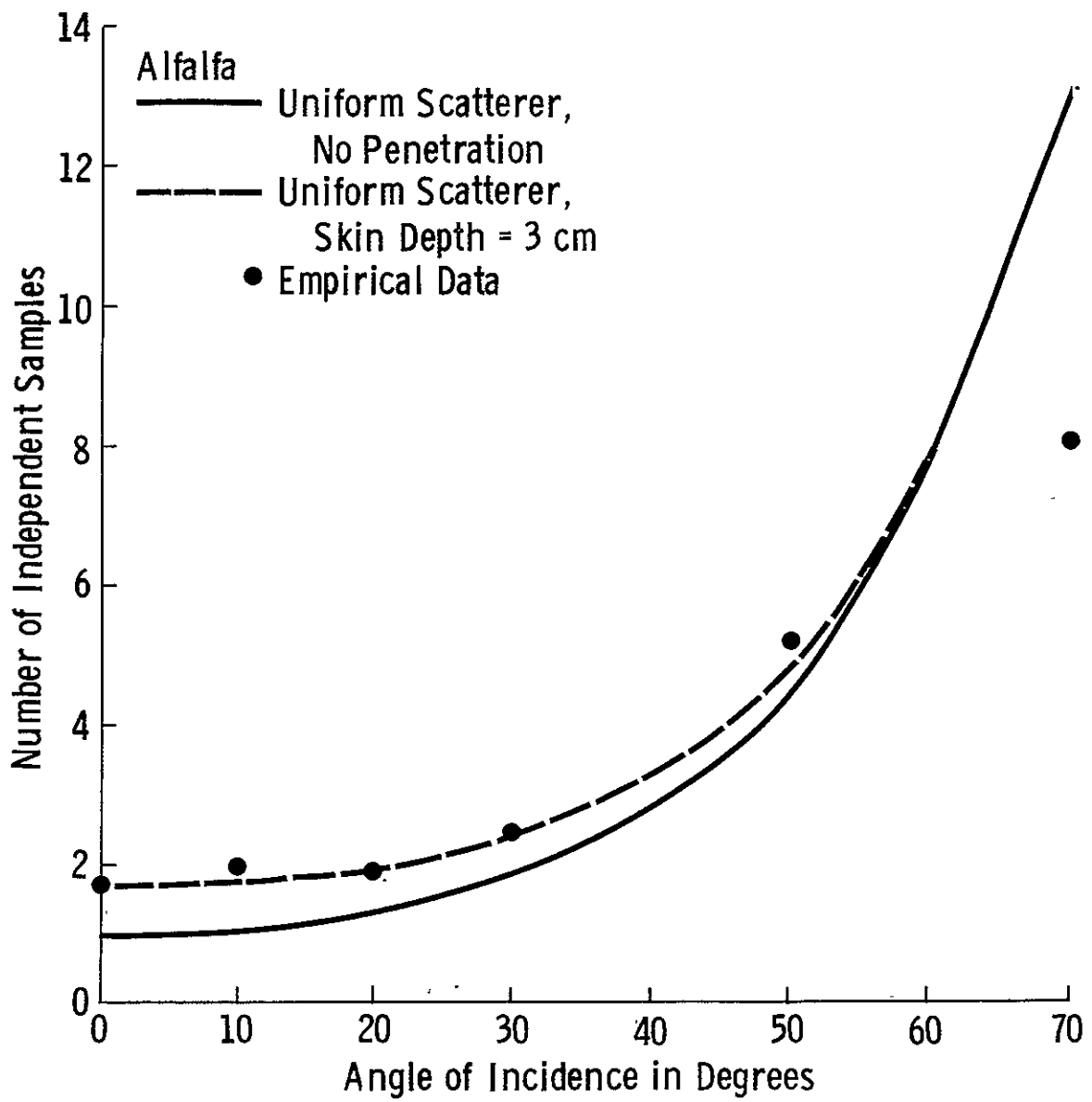


Figure 20. Number of independent samples for alfalfa.

C-2

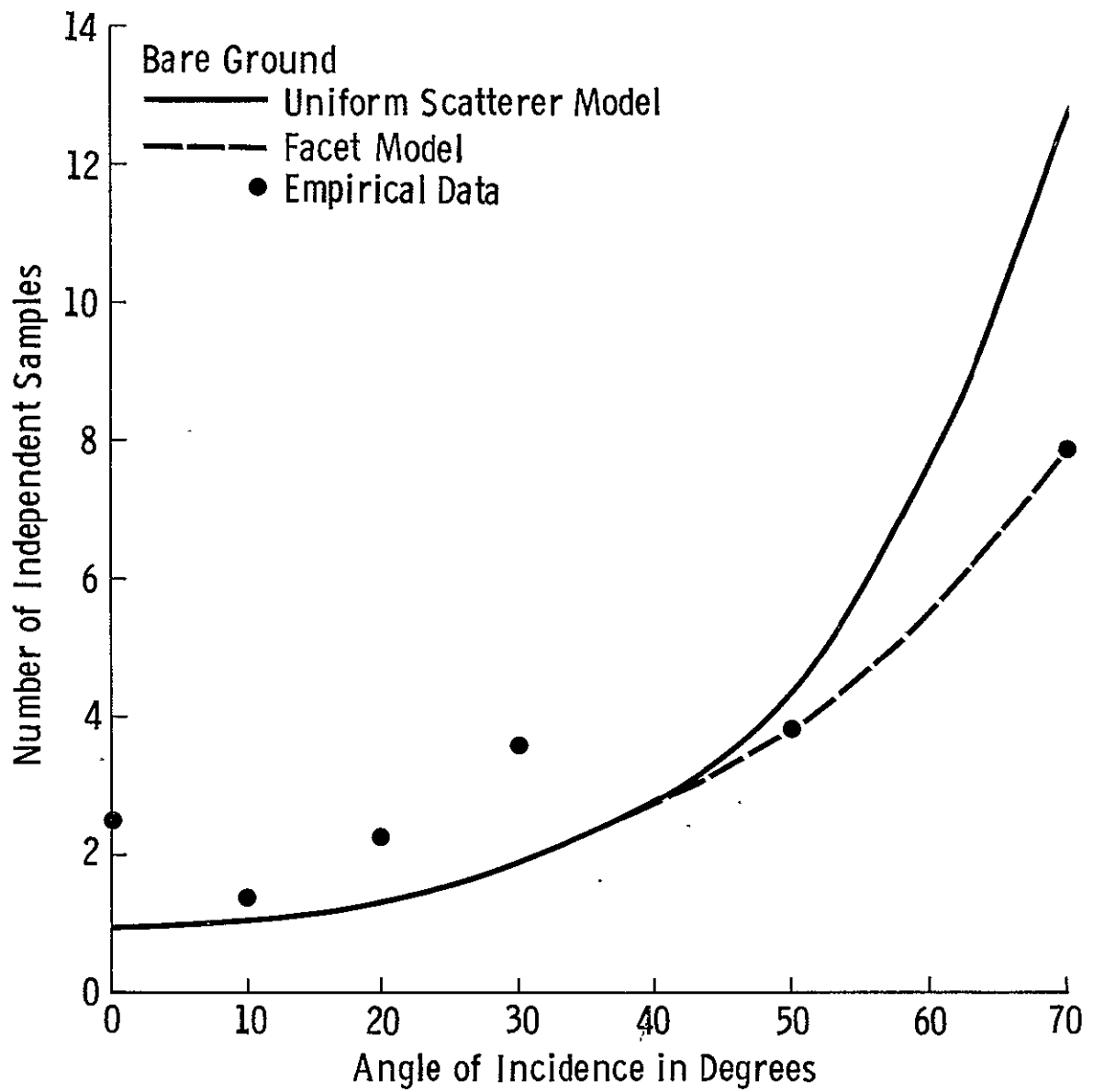


Figure 21. Number of independent samples for bare ground.

at small incidence angles, the facet model does not agree with the calculated number of independent samples based on the experimental data. This may be due to following reasons:

- i) At small incidence angles, as was shown in Section 4.2.2, the return power does not have a Chi-square distribution. Hence the number of the independent samples calculated based on the experimental data, Figure 21, are not correct.
- ii) The theory of the reduction of the variance of the return power based on the facet assumption is not complete and needs more refinement. The derivations in Section 4.2.2 consider only the two dimensional case, although the actual target consists of three dimensional facets. This deficiency can introduce errors, particularly at small incidence angles.

5.0 RESULTS

In this chapter we will compare the theoretical results obtained in Chapter 3 with the experimental data obtained from the bare ground.

Because in general the target is not perfectly conducting, in Section 5.1 we will calculate the reflection coefficient of the target as a function of its dielectric constants.

In Sections 5.2 and 5.3 we will compare the prediction of the model developed in Chapter 3 and Katzin's model [8], with the measured data. It will be shown that the new model predicts results better than Katzin's model.

5.1 Reflection Coefficient

5.1.1 Large Facets

From reference [23] the reflected field from a plane boundary between two media is

$$E_2 = \frac{\mu_2 K_1 \cos \theta - \mu_1 \sqrt{K_2^2 - K_1^2 \sin^2 \theta}}{\mu_2 K_1 \cos \theta + \mu_1 \sqrt{K_2^2 - K_1^2 \sin^2 \theta}} E_0 \quad (5-1)$$

$$(\vec{n} \times \vec{E}_0 = 0)$$

$$H_2 = \frac{\mu_1 K_2^2 \cos \theta - \mu_2 K_1 \sqrt{K_2^2 - K_1^2 \sin^2 \theta}}{\mu_1 K_2^2 \cos \theta + \mu_2 K_1 \sqrt{K_2^2 - K_1^2 \sin^2 \theta}} H_0 \quad (5-2)$$

$$(\vec{n} \times \vec{H}_0 = 0)$$

where

$$K_1^2 = \mu_1 \epsilon_1 \omega^2 + j \mu_1 \sigma_1 \omega$$

$$K_2^2 = \mu_2 \epsilon_2 \omega^2 + j \mu_2 \sigma_2 \omega$$

ϵ_1 = Complex permittivity of the first medium

ϵ_2 = Complex permittivity of the second medium

μ_1 = Complex permeability of the first medium

μ_2 = Complex permeability of the second medium

For our case $\mu_2 = \mu_1 = 1$, so from Eq. (5-1)

$$R_L \Big|_{HH} = \frac{\cos \theta - \sqrt{\epsilon_r - \sin^2 \theta}}{\cos \theta + \sqrt{\epsilon_r - \sin^2 \theta}} \quad (5-3)$$

and from Eq. (5-2)

$$R_L \Big|_{VV} = \frac{\epsilon_r \cos \theta - \sqrt{\epsilon_r - \sin^2 \theta}}{\epsilon_r \cos \theta + \sqrt{\epsilon_r - \sin^2 \theta}} \quad (5-4)$$

where

$$\epsilon_r = \epsilon' + j\epsilon'' \quad (5-5)$$

In order to calculate the reflection coefficient for the ground we use the moisture and the type of the soil to calculate ϵ' and ϵ'' from Figures 22 [25] and then use these results in Eqs. (5-3) and (5-4). The calculated reflection coefficient for HH and VV polarization are shown in Figure 23.

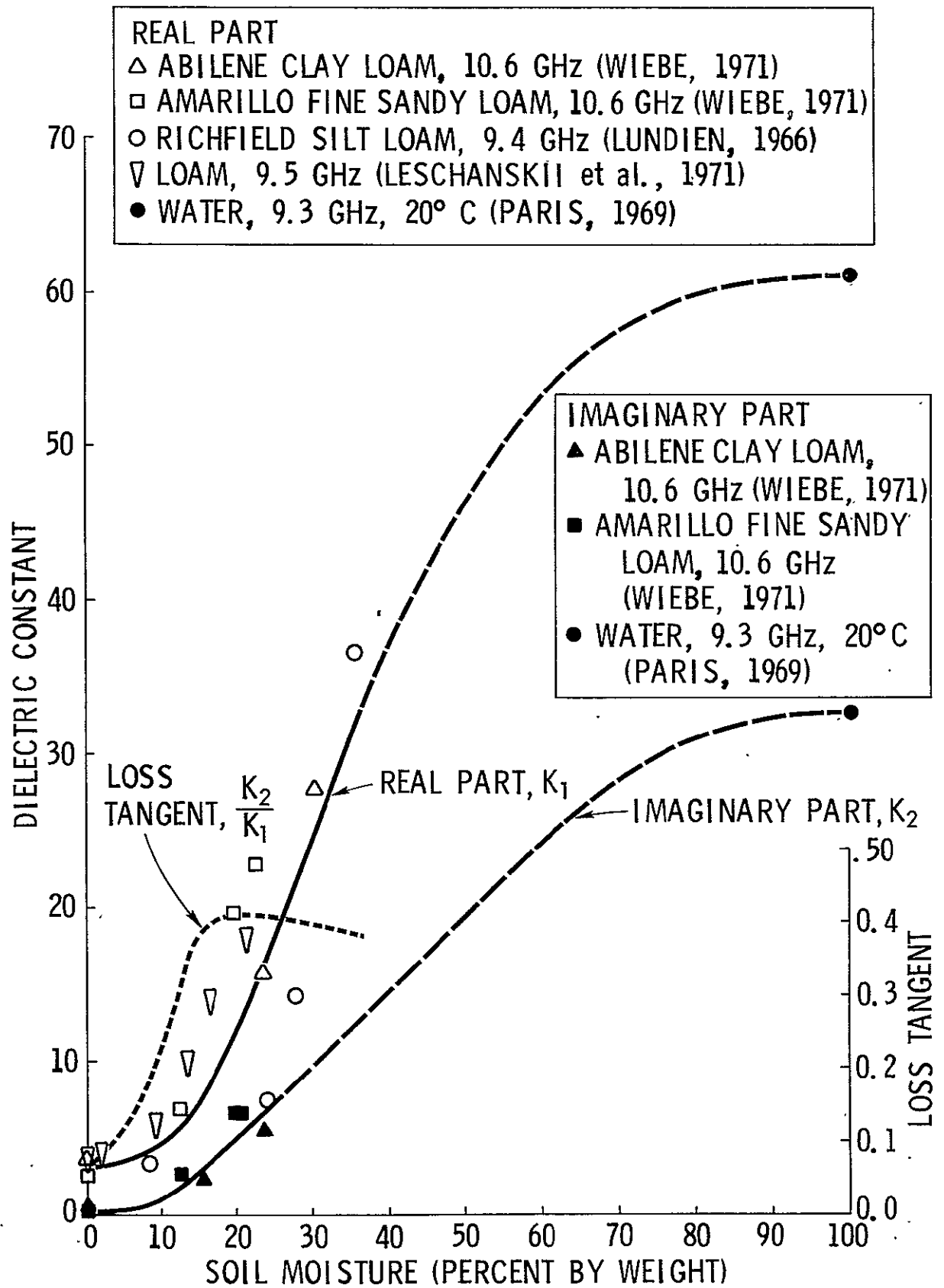


Figure 22. Measured dielectric constant data of loamy soil as a function of moisture content by weight around 10 GHz. Solid curves were drawn to fit the data points and the broken curves were extrapolated [25].

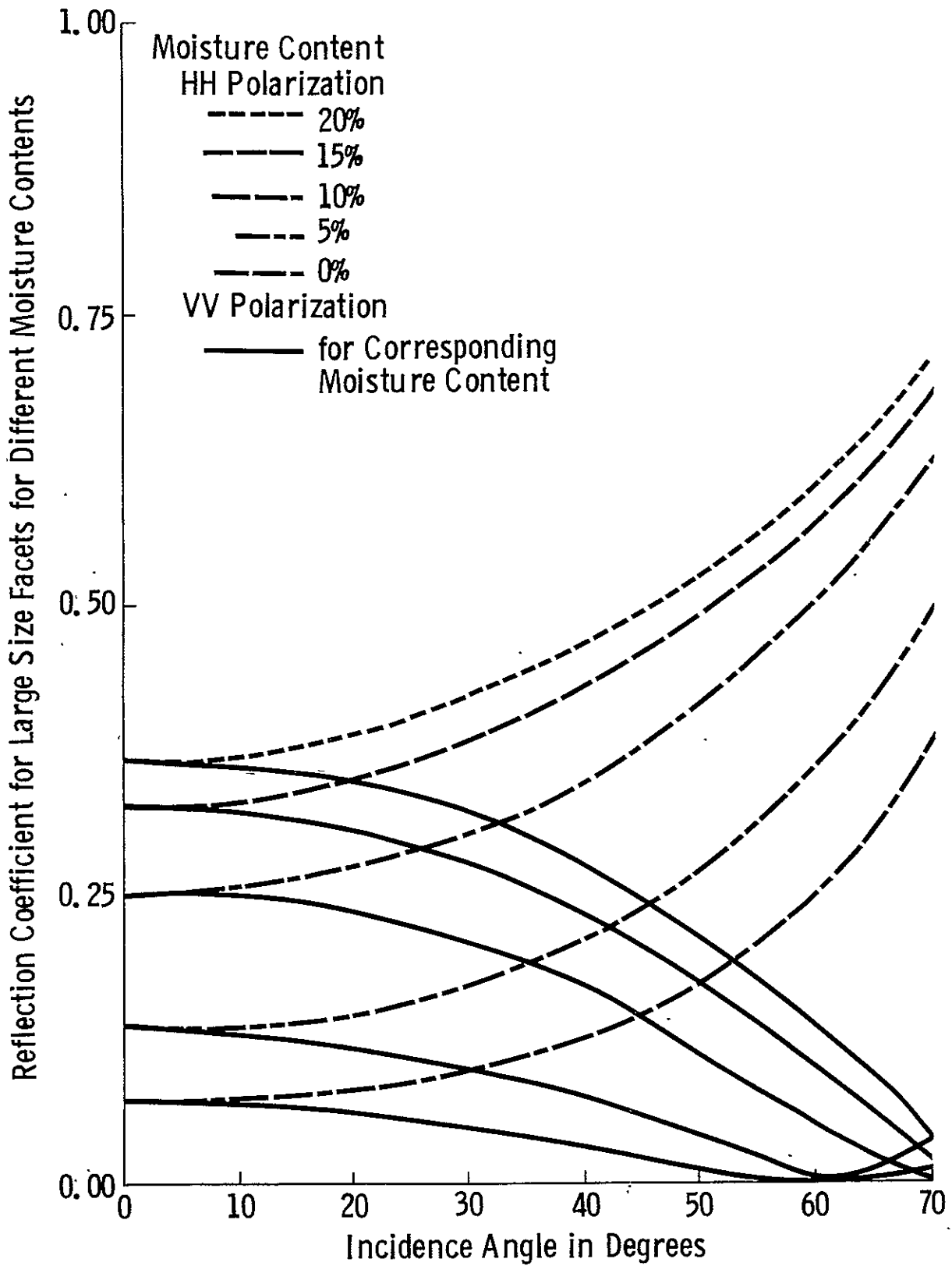


Figure 23. Reflection coefficient for large size facets.

5.1.2 Small Facets

From Eq. (3-37) the dielectric constant enters into the equation in the form of

$$\alpha_{HH} = - \frac{(\mu_r - 1) \left[(\mu_r - 1) \sin^2 \theta + \epsilon_r \mu_r \right] - \mu_r^2 (\epsilon_r - 1)}{\left[\mu_r \cos \theta + \sqrt{\epsilon_r \mu_r - \sin^2 \theta} \right]^2} \quad (5-6)$$

$$\alpha_{VV} = \frac{(\epsilon_r - 1) \left[(\epsilon_r - 1) \sin^2 \theta + \epsilon_r \mu_r \right] - \epsilon_r^2 (\mu_r - 1)}{\left[\epsilon_r \cos \theta + \sqrt{\epsilon_r \mu_r - \sin^2 \theta} \right]^2} \quad (5-7)$$

For the case of bare ground we can always assume that $\mu_r = 1$. Then if we define an effective reflection coefficient, we obtain

$$\begin{aligned} R_s |_{HH} &\triangleq \frac{\alpha_{HH}(\epsilon_r)}{\alpha_{HH}(\infty)} = \frac{1 - \epsilon_r}{\left[\cos \theta + \sqrt{\epsilon_r - \sin^2 \theta} \right]^2} = \frac{\cos \theta - \sqrt{\epsilon_r - \sin^2 \theta}}{\cos \theta + \sqrt{\epsilon_r - \sin^2 \theta}} = \\ &= R_L |_{HH} \end{aligned} \quad (5-8)$$

$$\begin{aligned} R_s |_{VV} &\triangleq \frac{\alpha_{VV}(\epsilon_r)}{\alpha_{VV}(\infty)} = \\ &= \frac{(\epsilon_r - 1) \left[(\epsilon_r - 1) \sin^2 \theta + \epsilon_r \right] / \left[\epsilon_r \cos \theta + \sqrt{\epsilon_r - \sin^2 \theta} \right]^2}{(1 + \sin^2 \theta) / \cos^2 \theta} \end{aligned} \quad (5-9)$$

In Figure 25 $|R_s HH|^2$ and $|R_s VV|^2$ are shown as a function of incidence angle and soil moisture content.

5.1.3. Medium Size Facets

For the medium size facets we assume that the reflection coefficient is the average of the reflection coefficient of the small and the large size facets, i.e.

$$|R_M HH|^2 = \left\{ |R_s HH|^2 + |R_L HH|^2 \right\} / 2 \quad (5-10)$$

or

$$|R_M HH|^2 = |R_s HH|^2 = |R_L HH|^2 \quad (5-11)$$

and

$$|R_M VV|^2 = \left\{ |R_L VV|^2 + |R_s VV|^2 \right\} / 2 \quad (5-12)$$

Figure 24 shows $|R_M HH|^2$ and $|R_M VV|^2$ versus angle of incidence for different soil moistures.

5.2 Comparison of the Results of the Theory With Data

In the following pages we will compare some samples of the measured data with theoretical predictions.

As Figures 26 through 31 show close to nadir in both polarizations, almost all the return comes from the large facets. But at large incidence angles in HH polarization case, the predicted return is determined by the return from medium size facets while in VV polarization it is mainly determined by the return from small facets. To facilitate comparison of theoretical prediction with experimental data

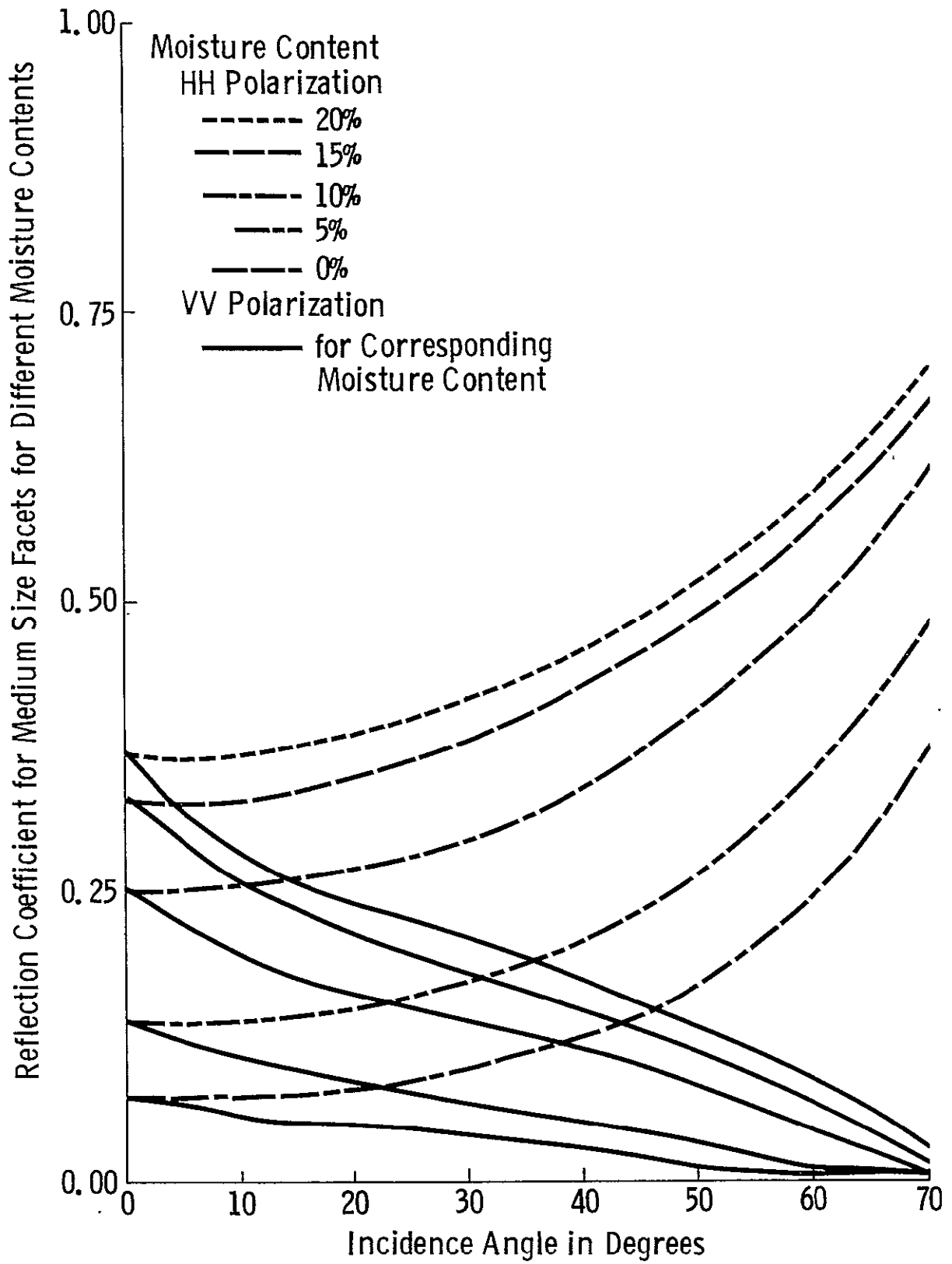


Figure 24. Reflection coefficient for medium size facets.

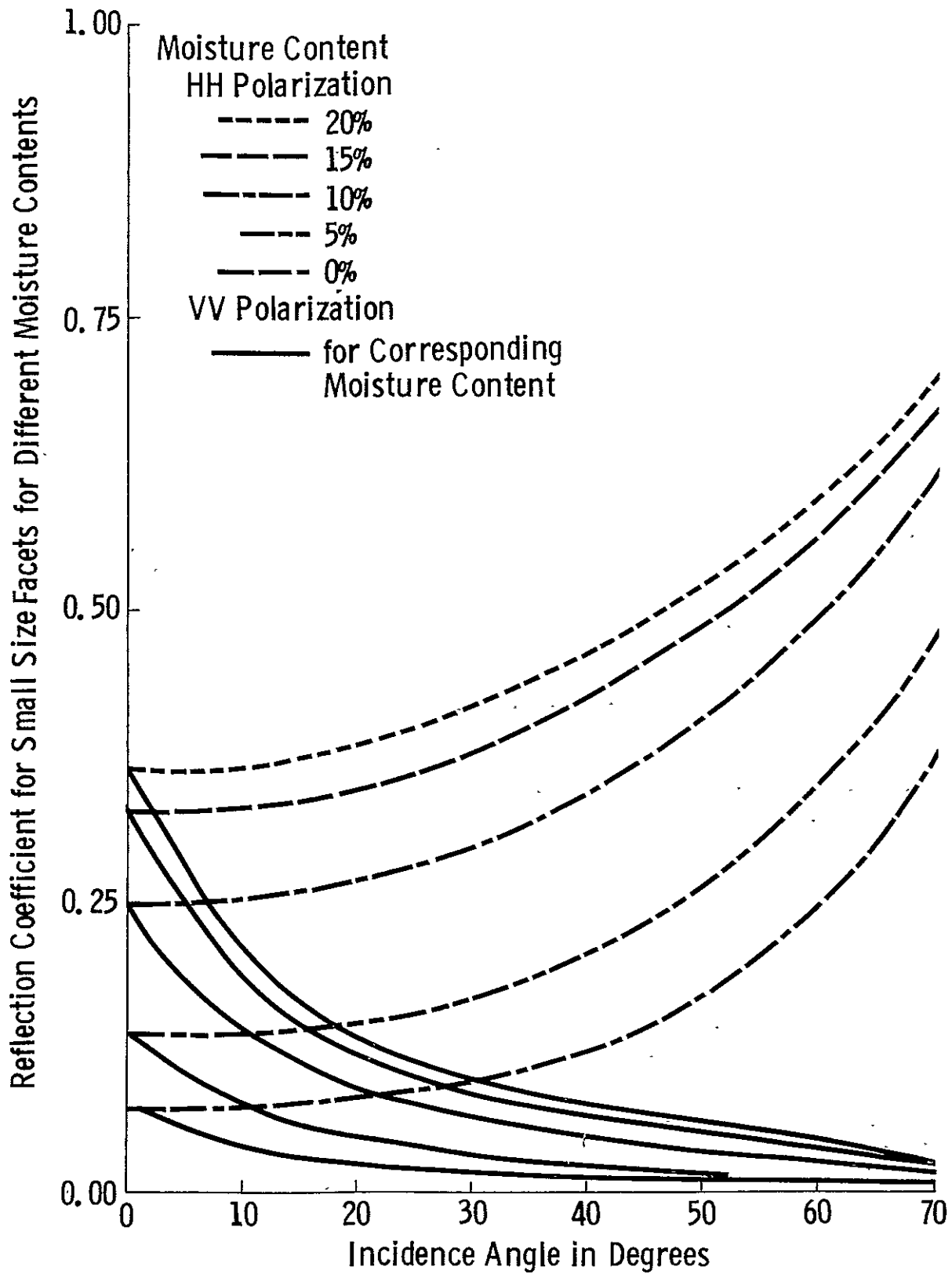


Figure 25. Reflection coefficient for small size facets.

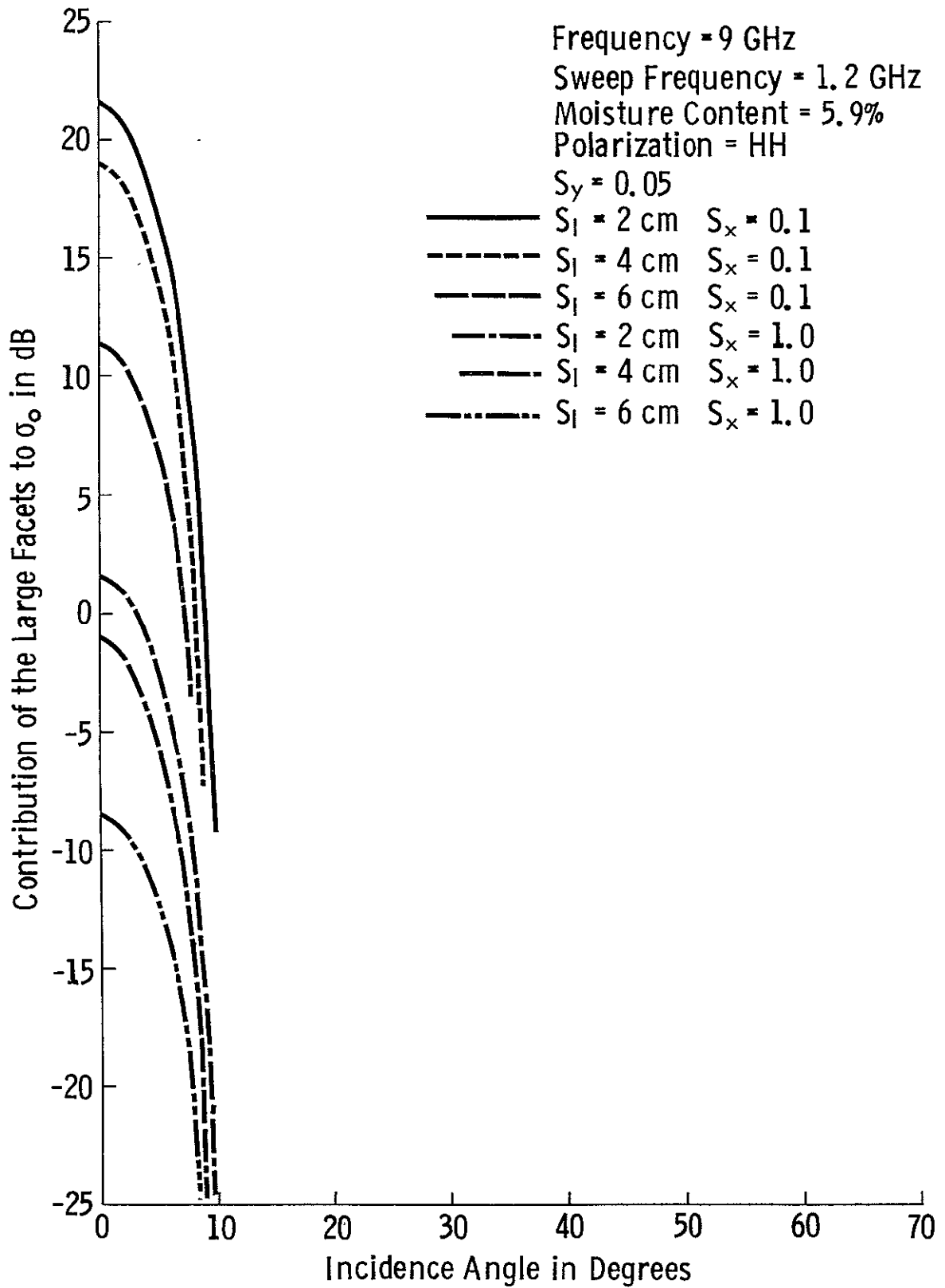


Figure 26. Contribution of the large facets to the return.

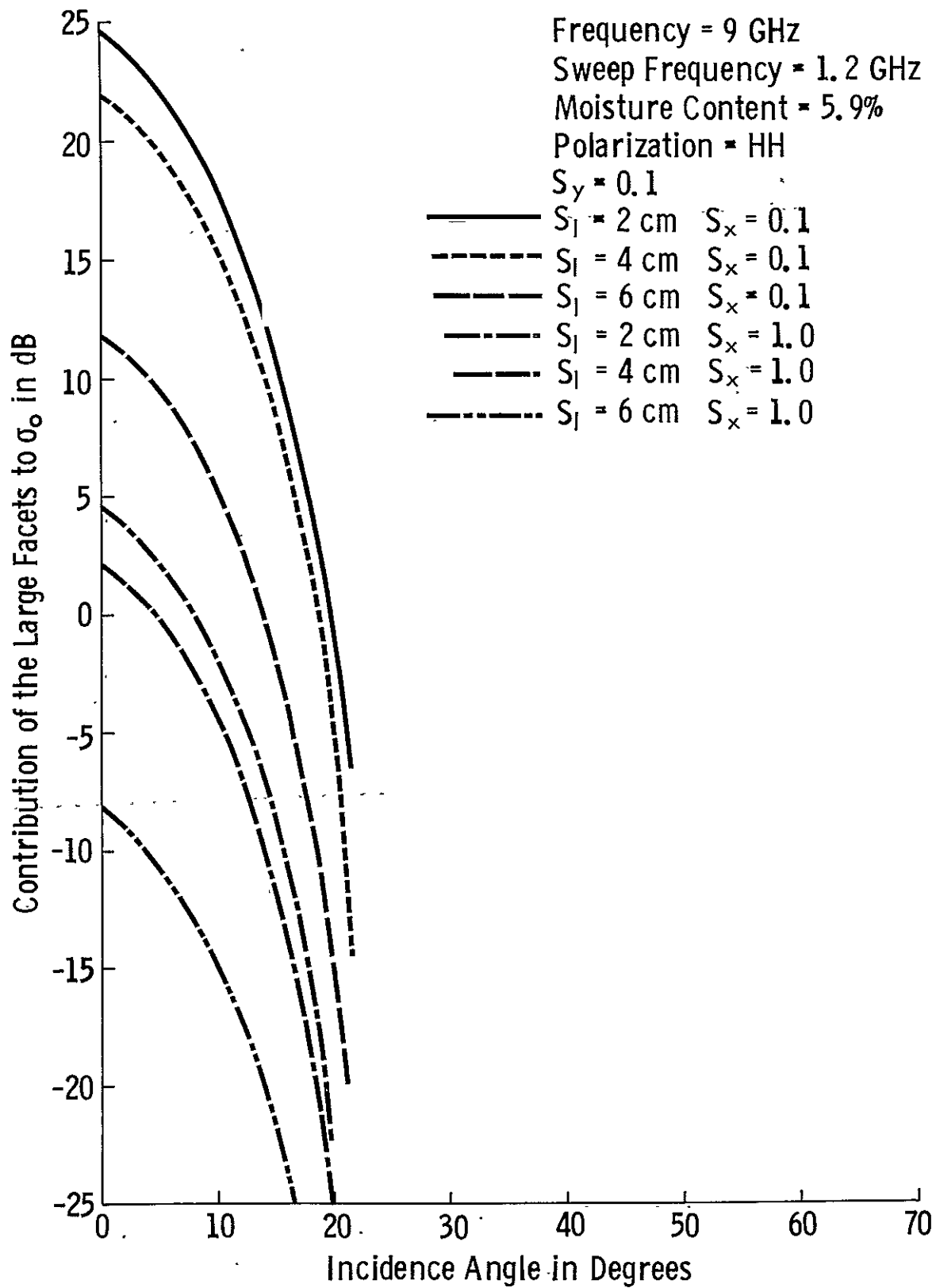
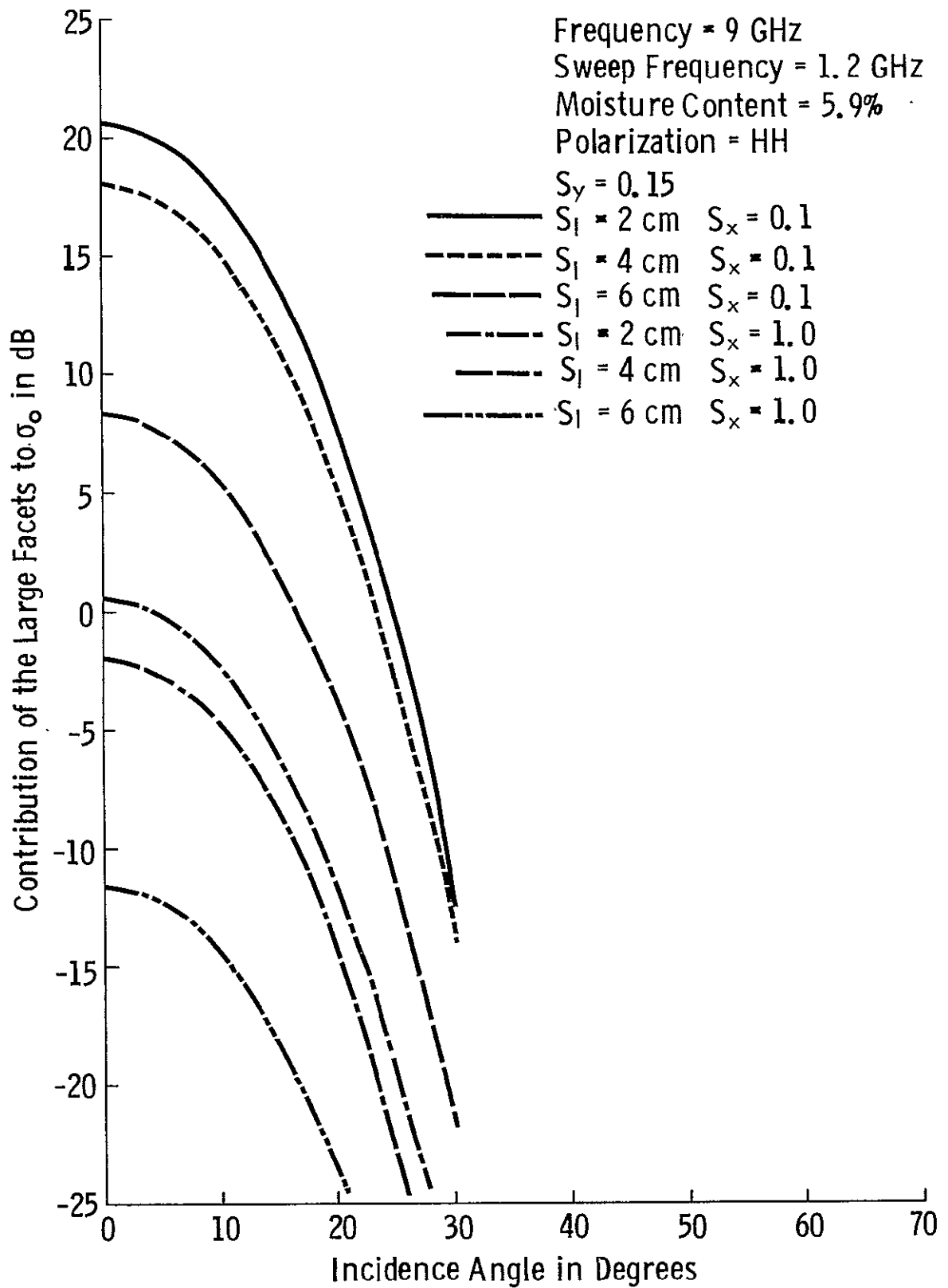


Figure 27. Contribution of the large facets to the return.



e 28. Contribution of the large facets to the return.

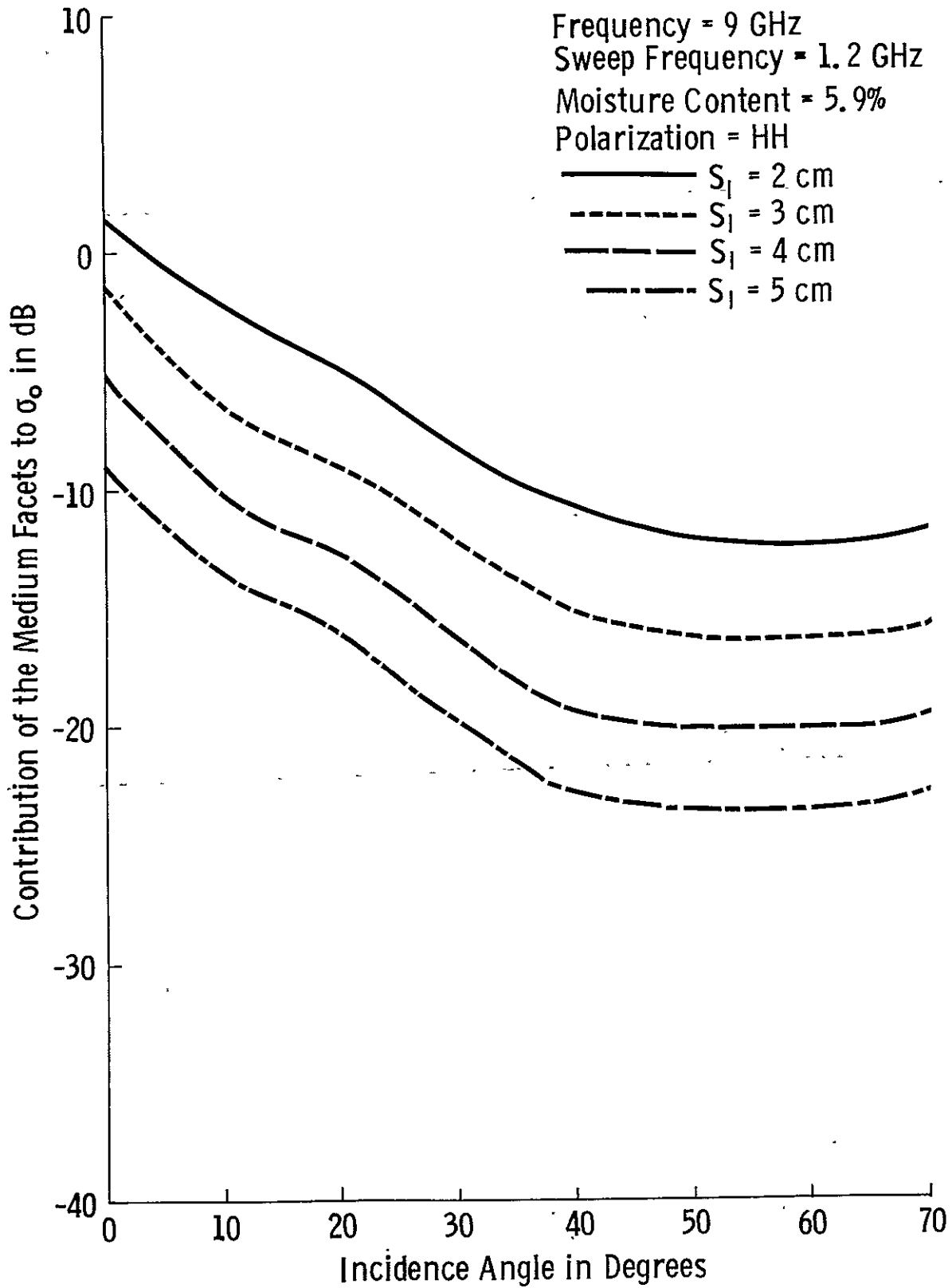


Figure 29. Contribution of medium size facets to the return for HH polarization.

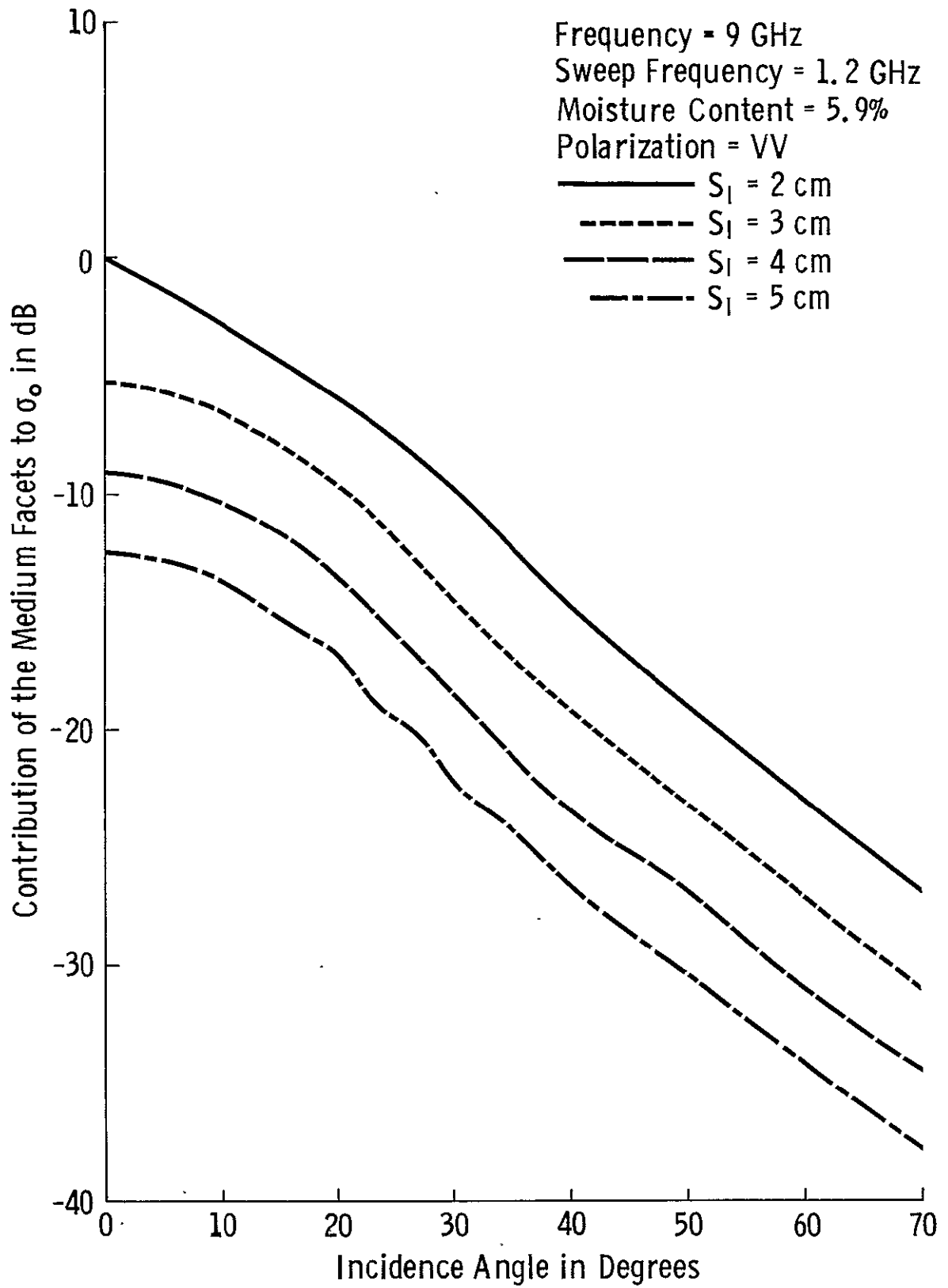


Figure 30. Contribution of medium size facets to the return for VV polarization.

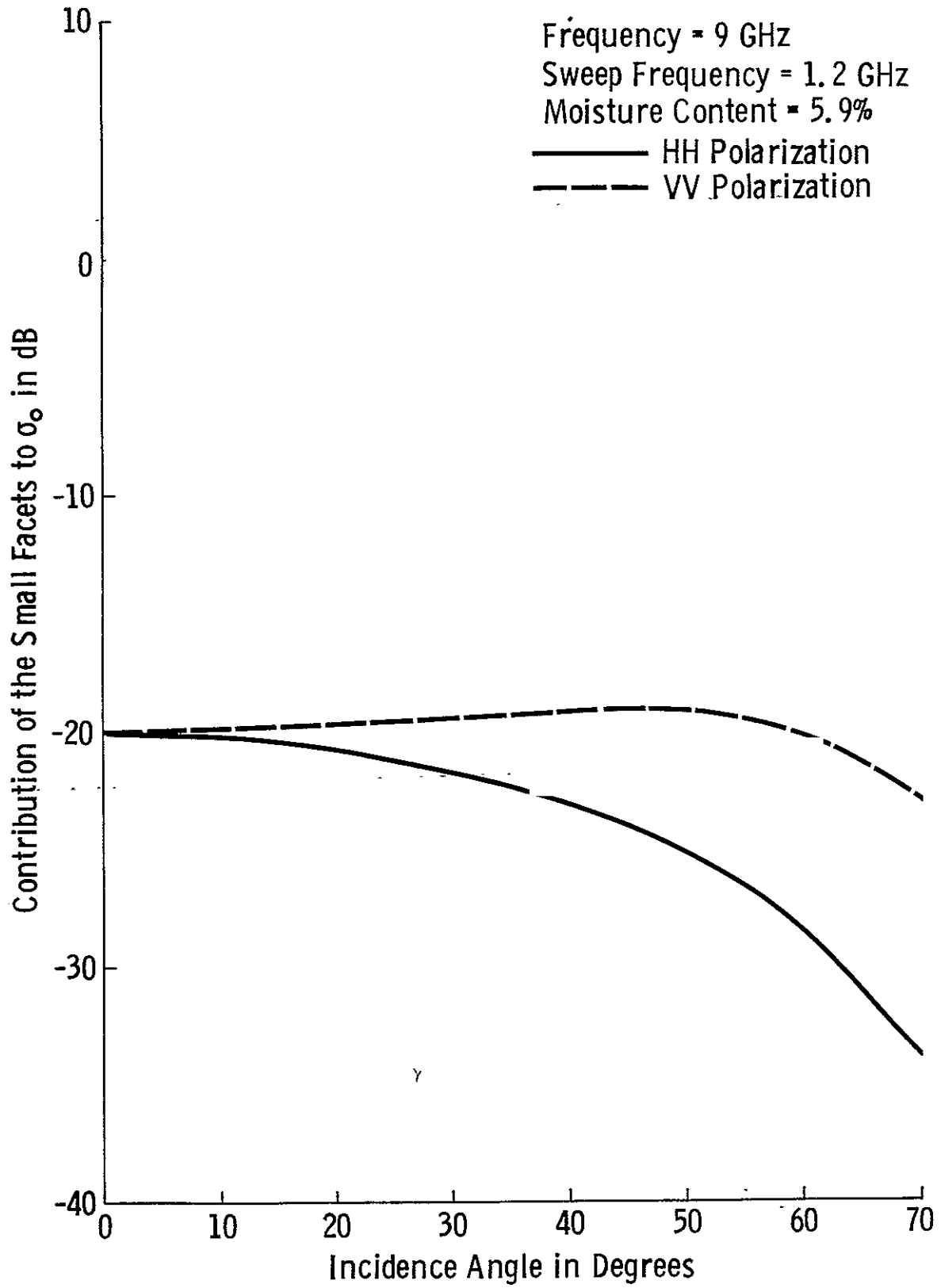


Figure 31. Contribution of small facets to the return.

(Figures 32-47), which represent an average return over a 1.2 GHz bandwidth, the theoretical calculation shown in Figures 26-47 represent the average of the calculated return at the indicated center frequency and the returns at the neighboring frequencies 400 MHz on each side.

In fitting the theory to the data curve we use the level of the curve at large angles in HH polarization to determine the standard deviation of the distribution of the facet size, then use the level and the shape of the curve near zero angle to determine the standard deviations of the slopes. Once these parameters are determined, they are used to predict the return in VV polarization. It should be noted that in large angles in VV polarization the return predicted by the theory is only a function of the frequency and the dielectric constants of the target.

When we increase the frequency the standard deviation of the facet size must stay constant, but because we include smaller facets to the large category, it is possible that the standard deviations of the slopes also increase.

The results of the fittings are shown in Figures 32 through 47, where

S_x = standard deviation of the slope in x direction

S_y = standard deviation of the slope in y direction

S_ℓ = standard deviation of the distribution of the facet size

In order to check the accuracy of the predicted variance of the slope distribution, we calculate the variance of the slope of the ground from the data taken at the time of the radar measurement. After smoothening the surface curve, Figure 48, by the length of the smallest facet in the large category, i.e. λ , the variance of slope was calculated to be 0.07, and this is very close to the predicted value of 0.075 that has been used to calculate the data in Figures 40 through 43.

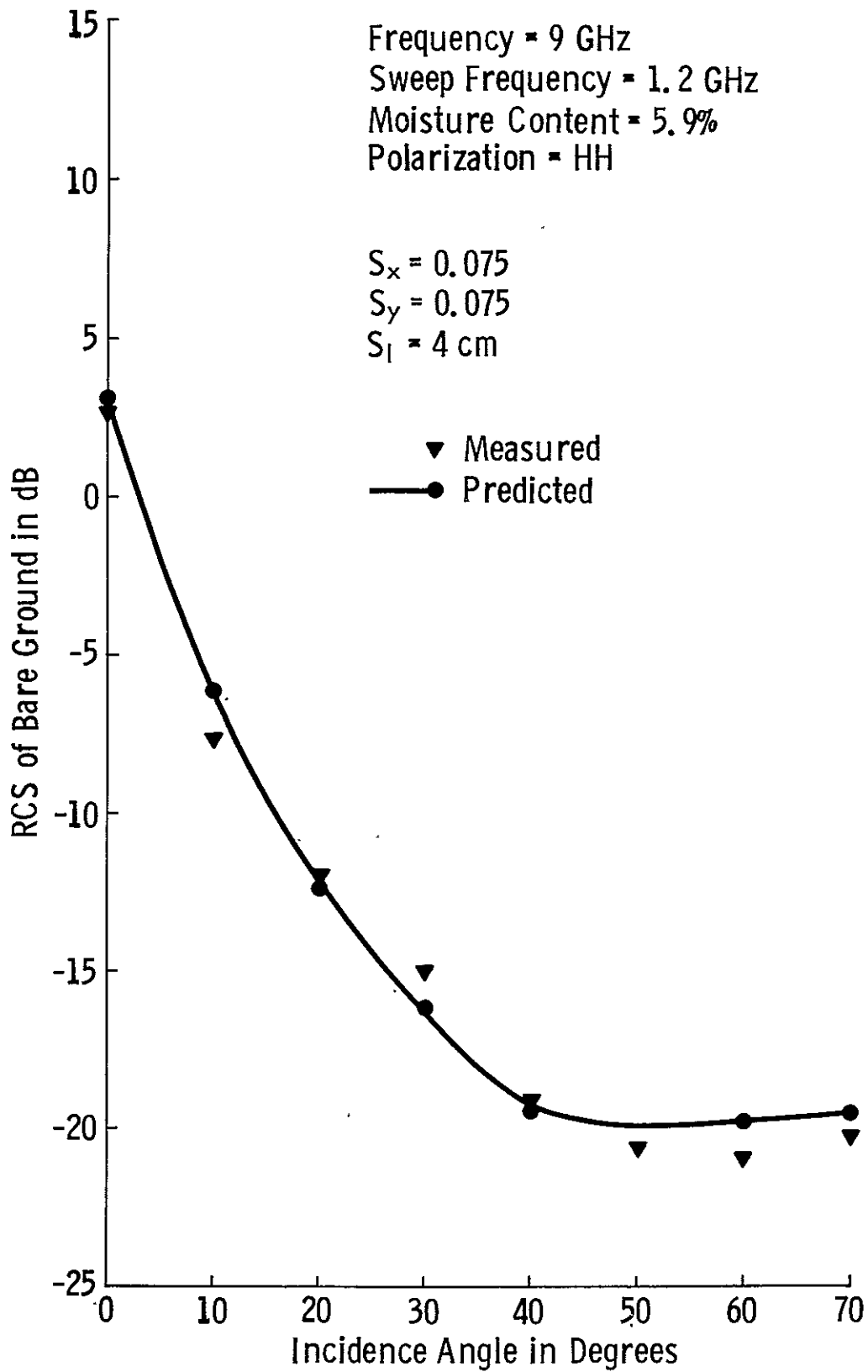


Figure 32. RCS of bare ground; moisture content = 5.9%, frequency = 9 GHz, polarization = HH.

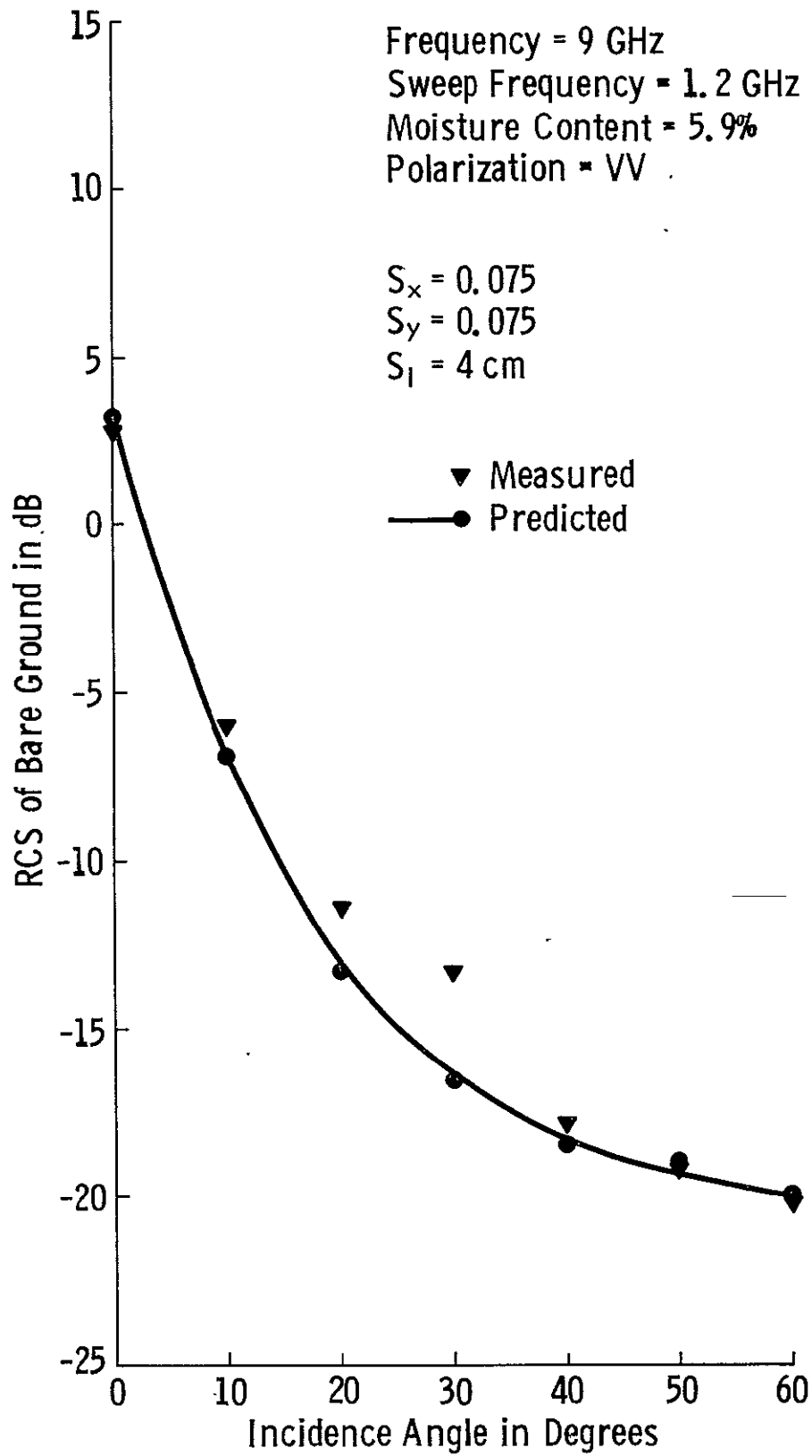


Figure 33. RCS of bare ground; moisture content = 5.9%, frequency = 9 GHz, polarization = VV.

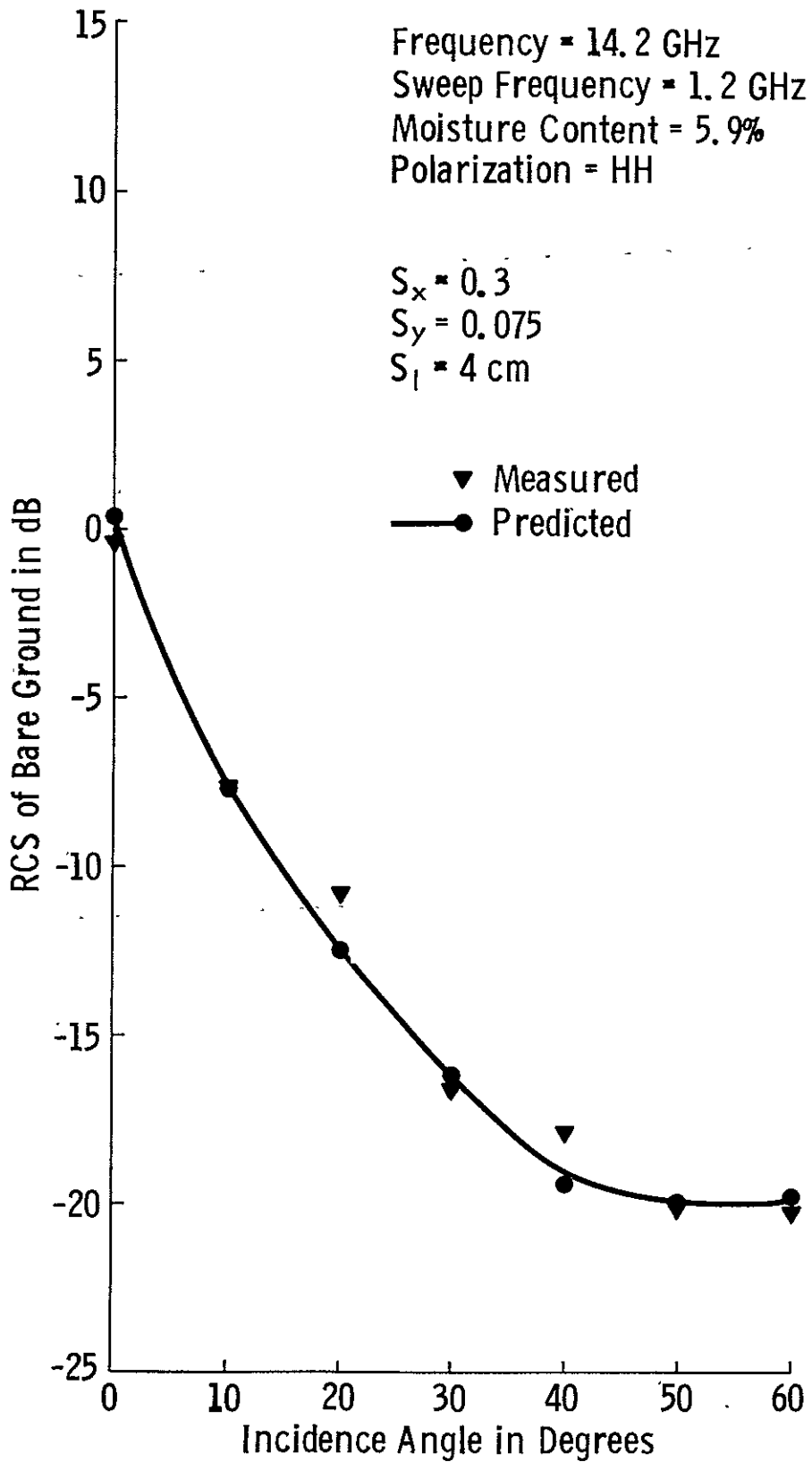


Figure 34. RCS of bare ground; moisture content = 5.9%, frequency = 14.2 GHz, polarization = HH.

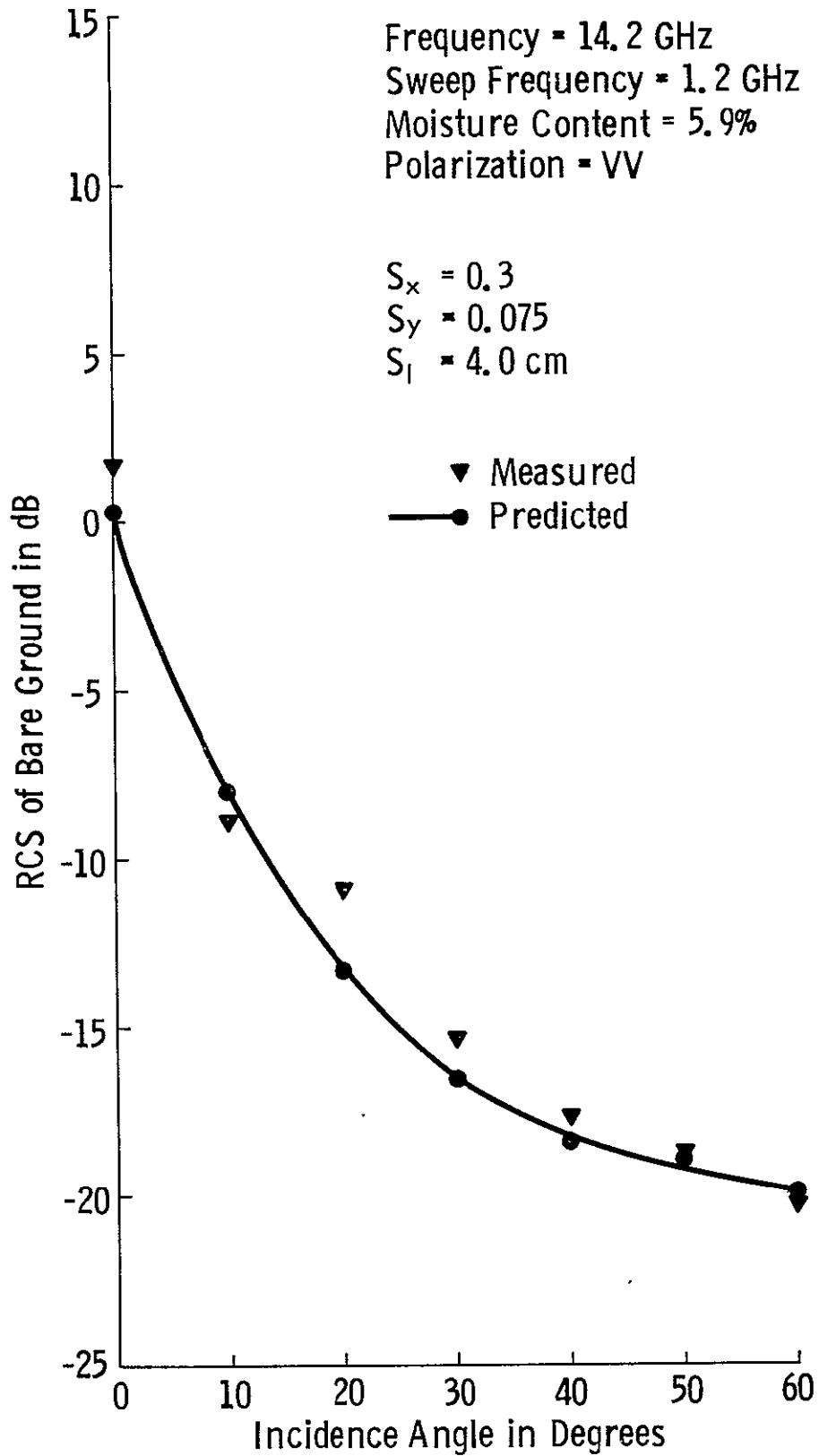


Figure 35. RCS of bare ground; moisture content = 5.9%, frequency = 14.2 GHz, polarization = VV.

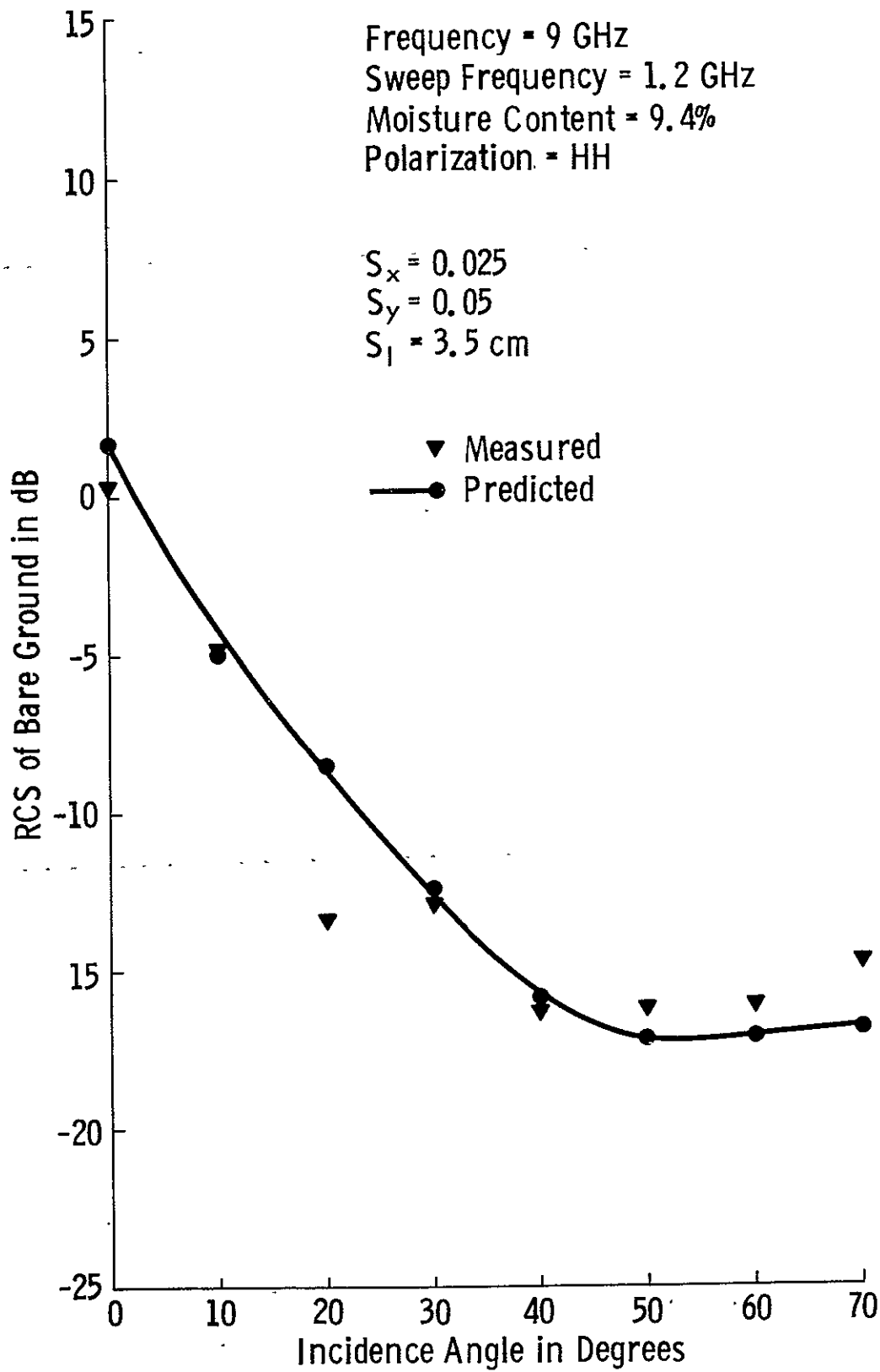


Figure 36. RCS of bare ground; moisture content = 9.4%, frequency = 9 GHz, polarization = HH.

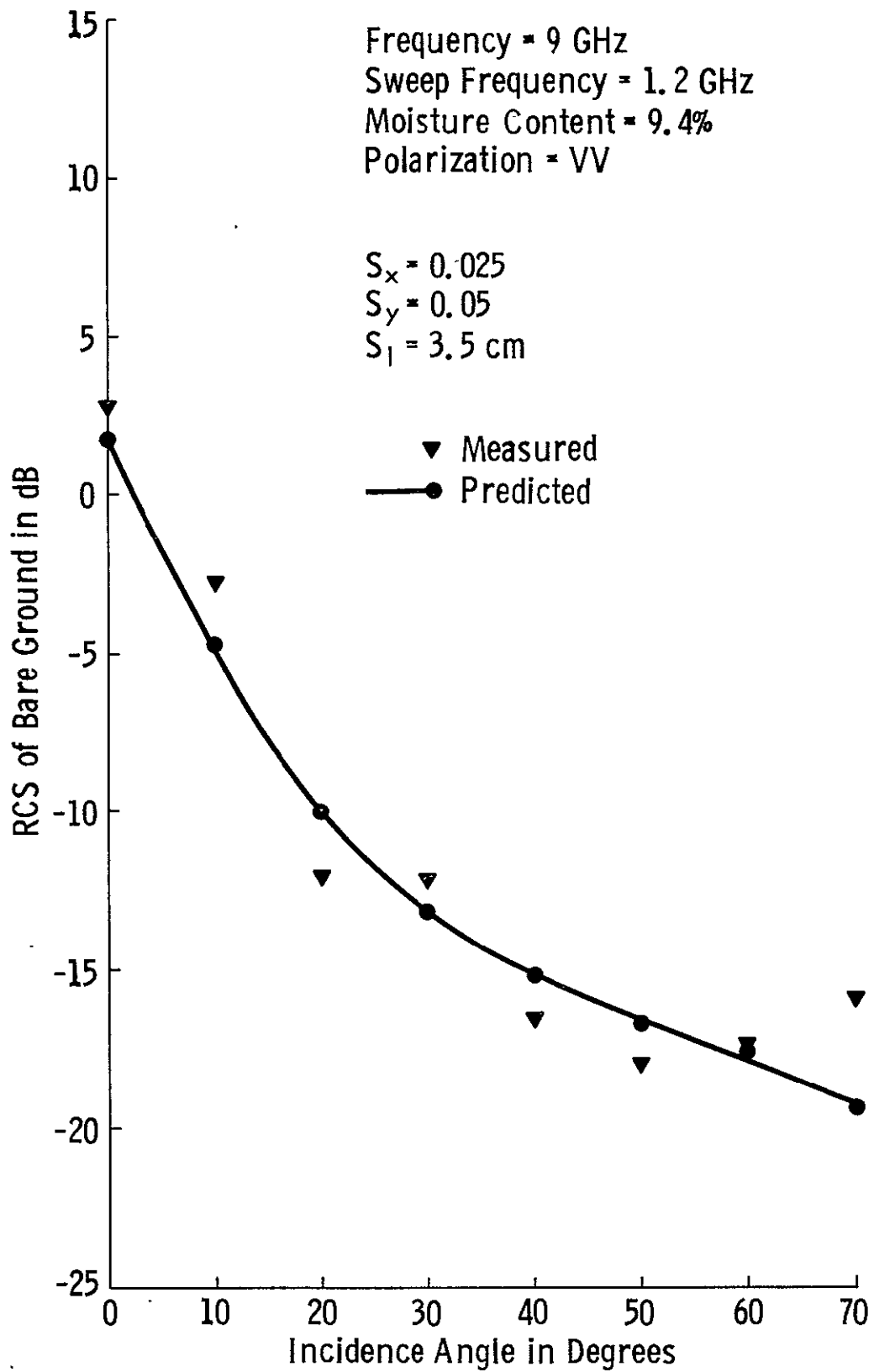


Figure 37. RCS of bare ground; moisture content = 9.4%, frequency = 9 GHz, polarization = VV.

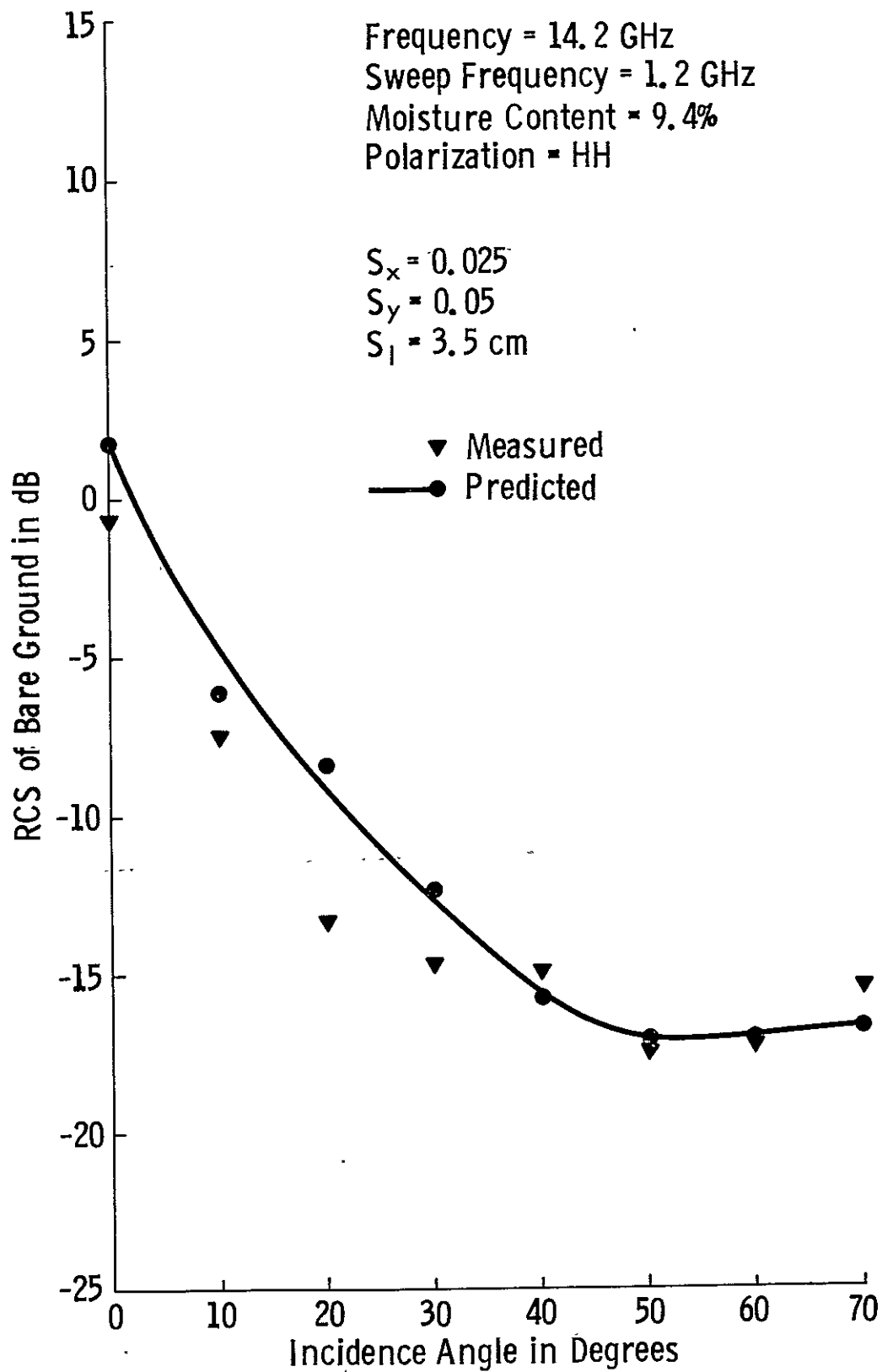


Figure 38. RCS of bare ground; moisture content = 9.4%, frequency = 14.2 GHz, polarization = HH.

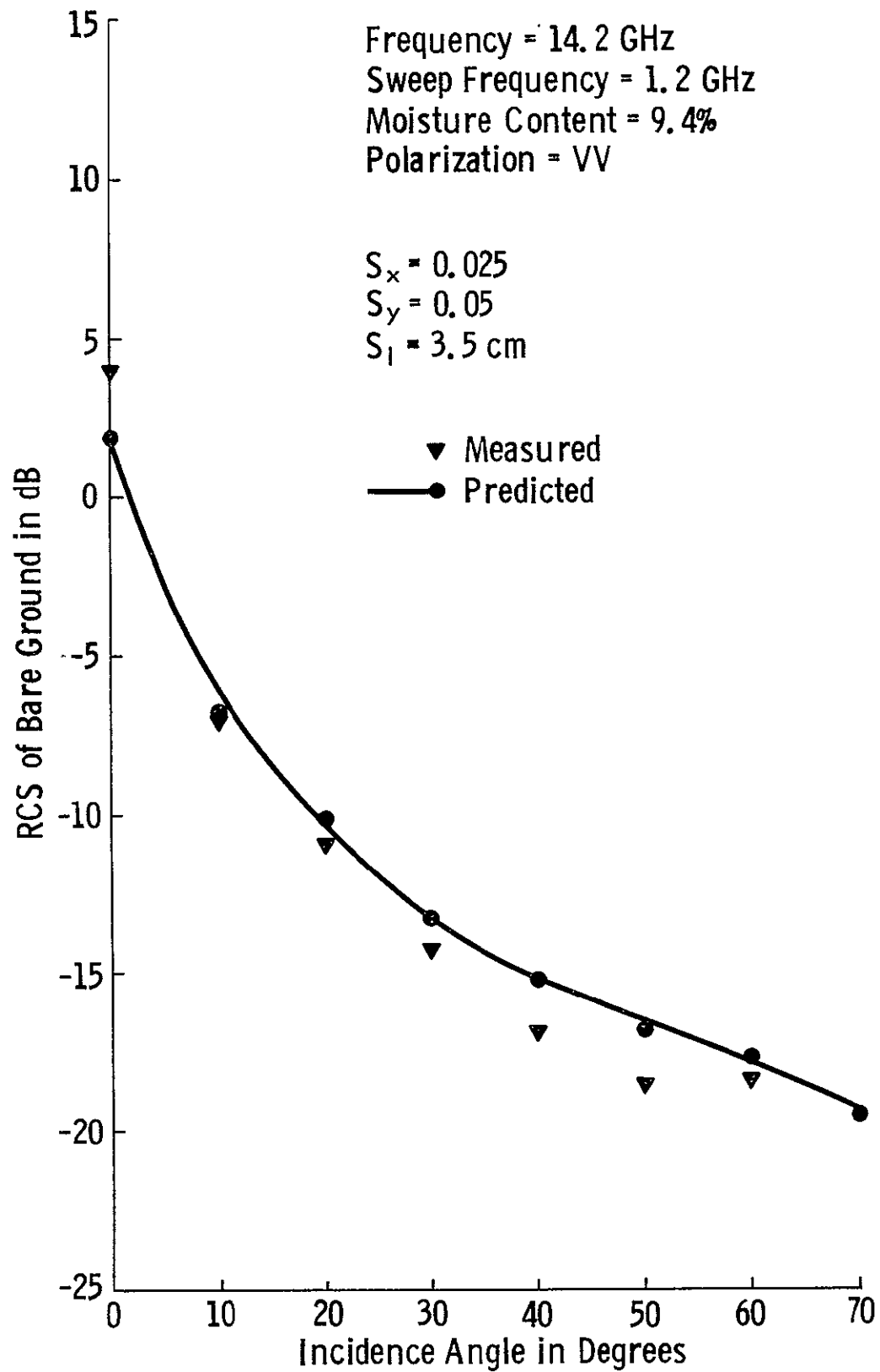


Figure 39. RCS of bare ground; moisture content = 9.4%, frequency = 14.2 GHz, polarization = VV.

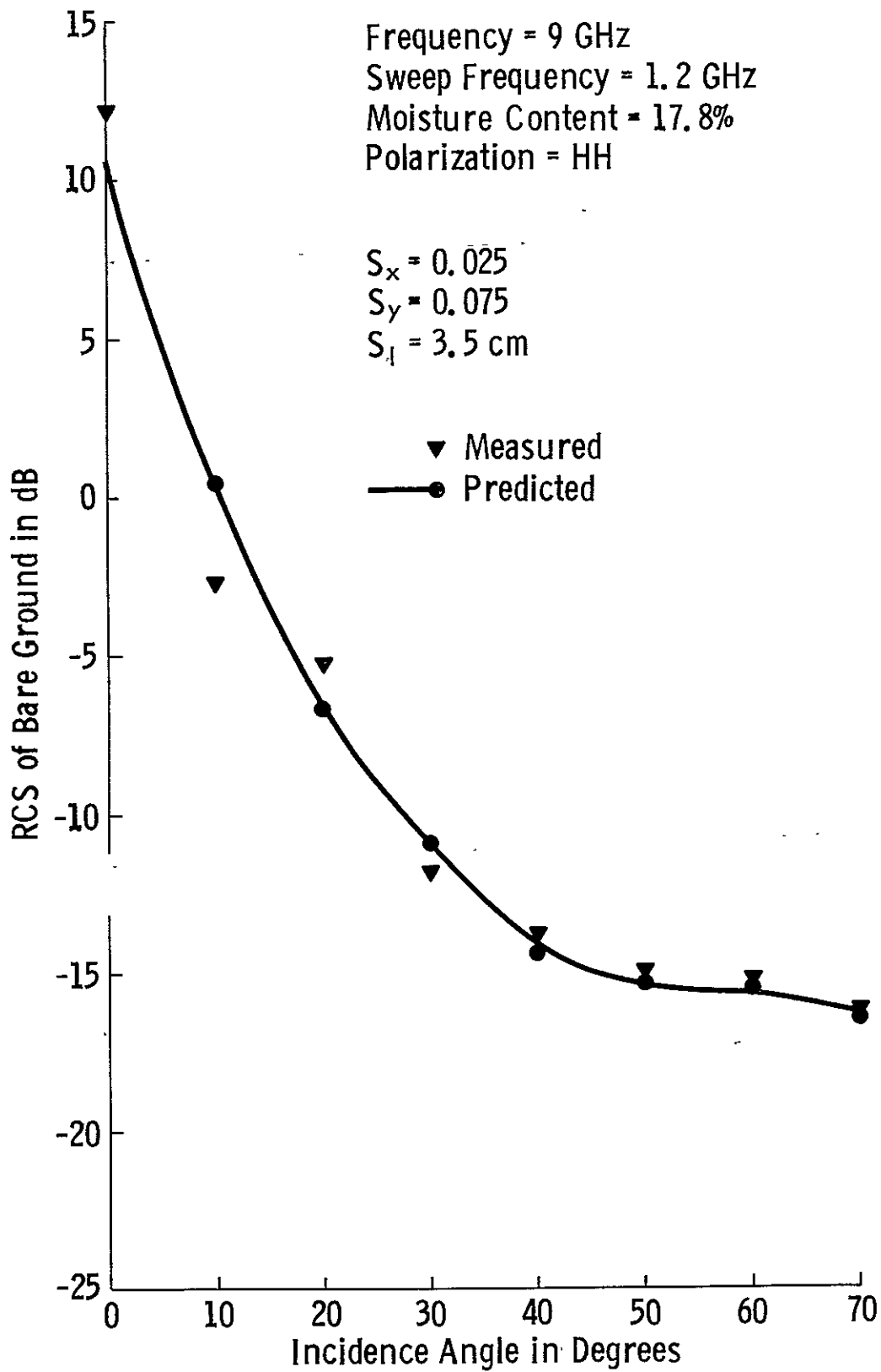


Figure 40. RCS of bare ground; moisture content = 17.8%, frequency = 9 GHz, polarization = HH.

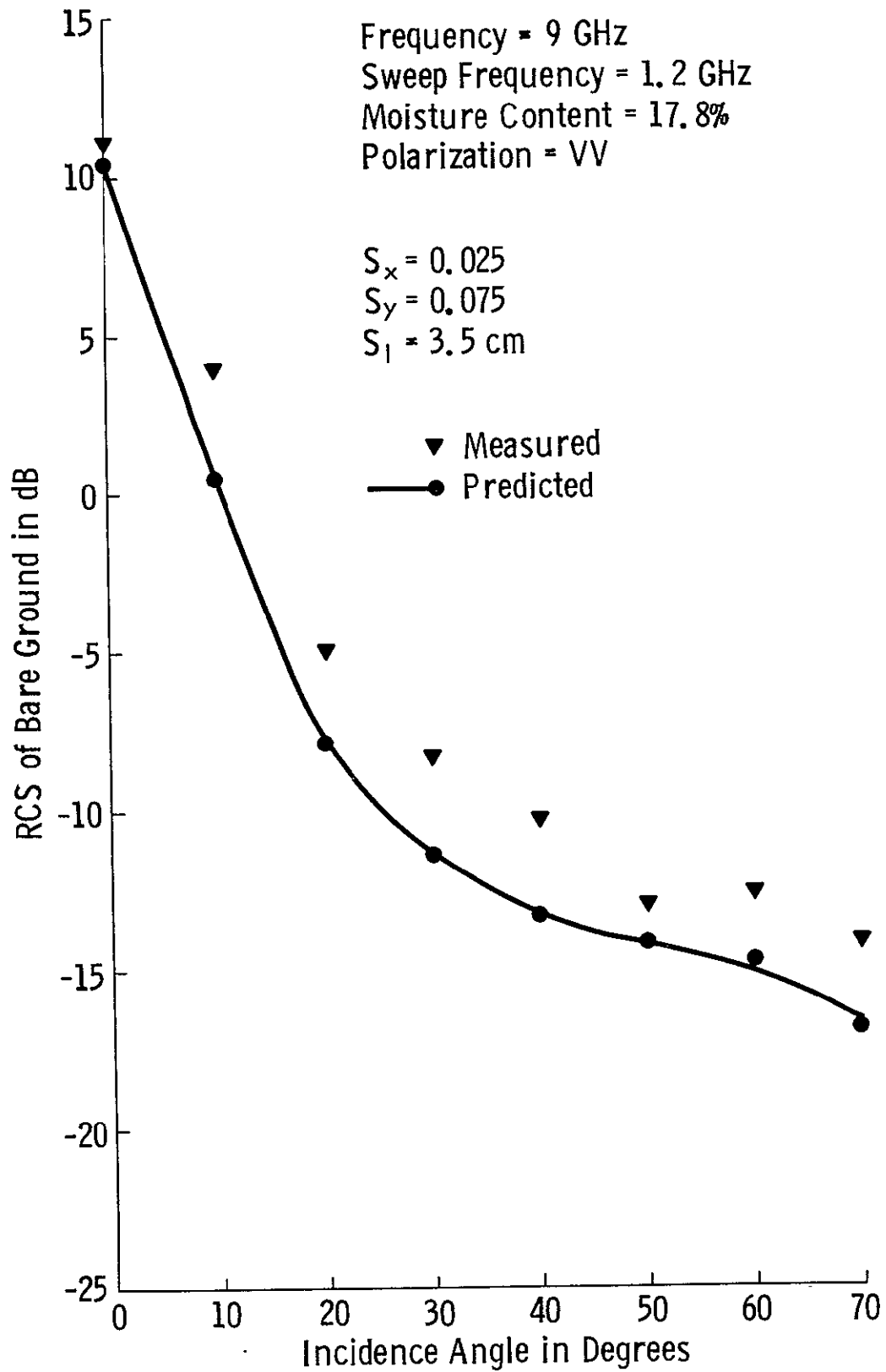


Figure 41. RCS of bare ground; moisture content = 17.8%, frequency = 9 GHz, polarization = VV.

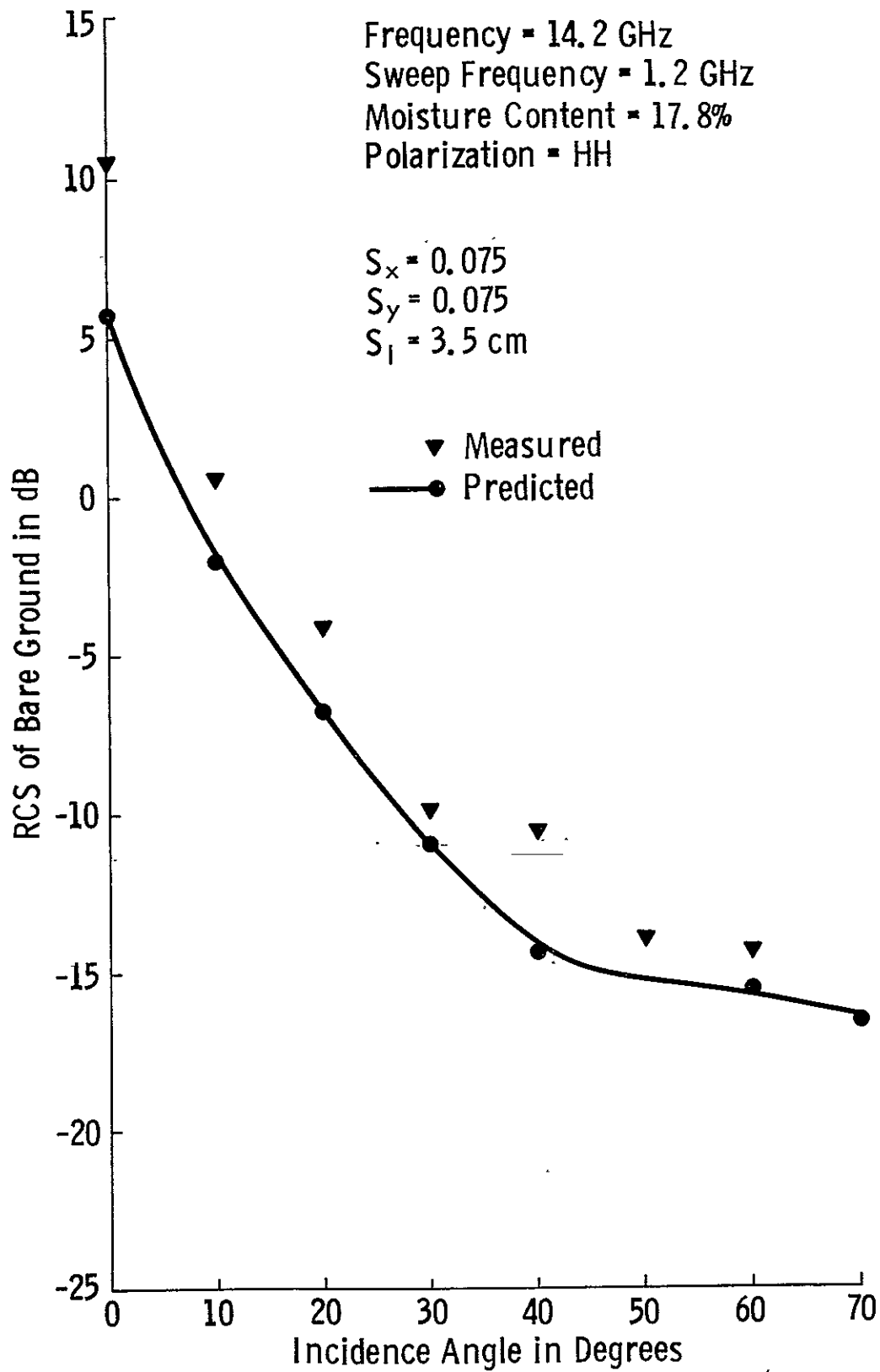


Figure 42. RCS of bare ground; moisture content = 17.8%, frequency = 14.2 GHz, polarization = HH.

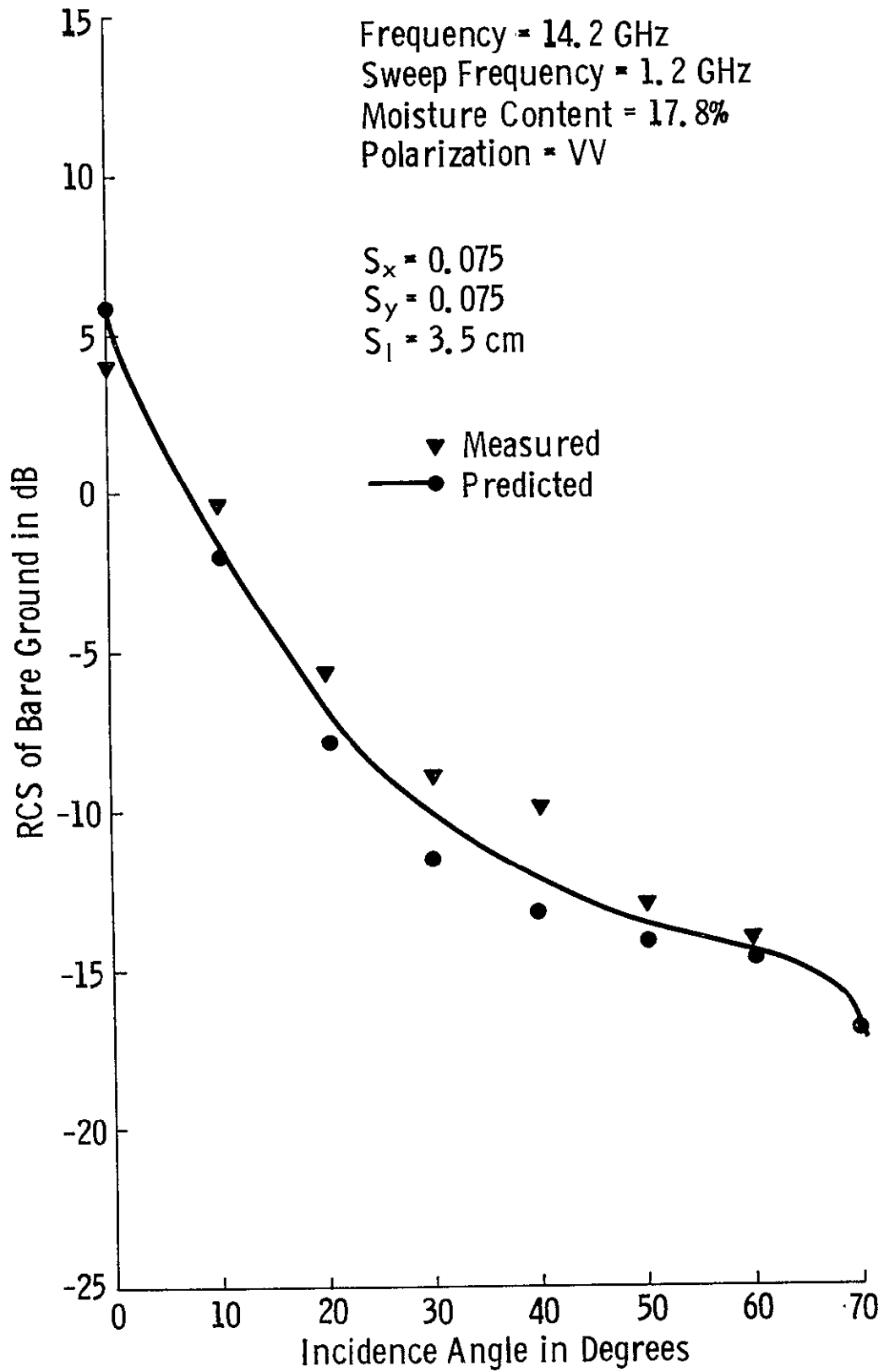


Figure 43. RCS of bare ground; moisture content = 17.8%, frequency = 14.2 GHz, polarization = VV.

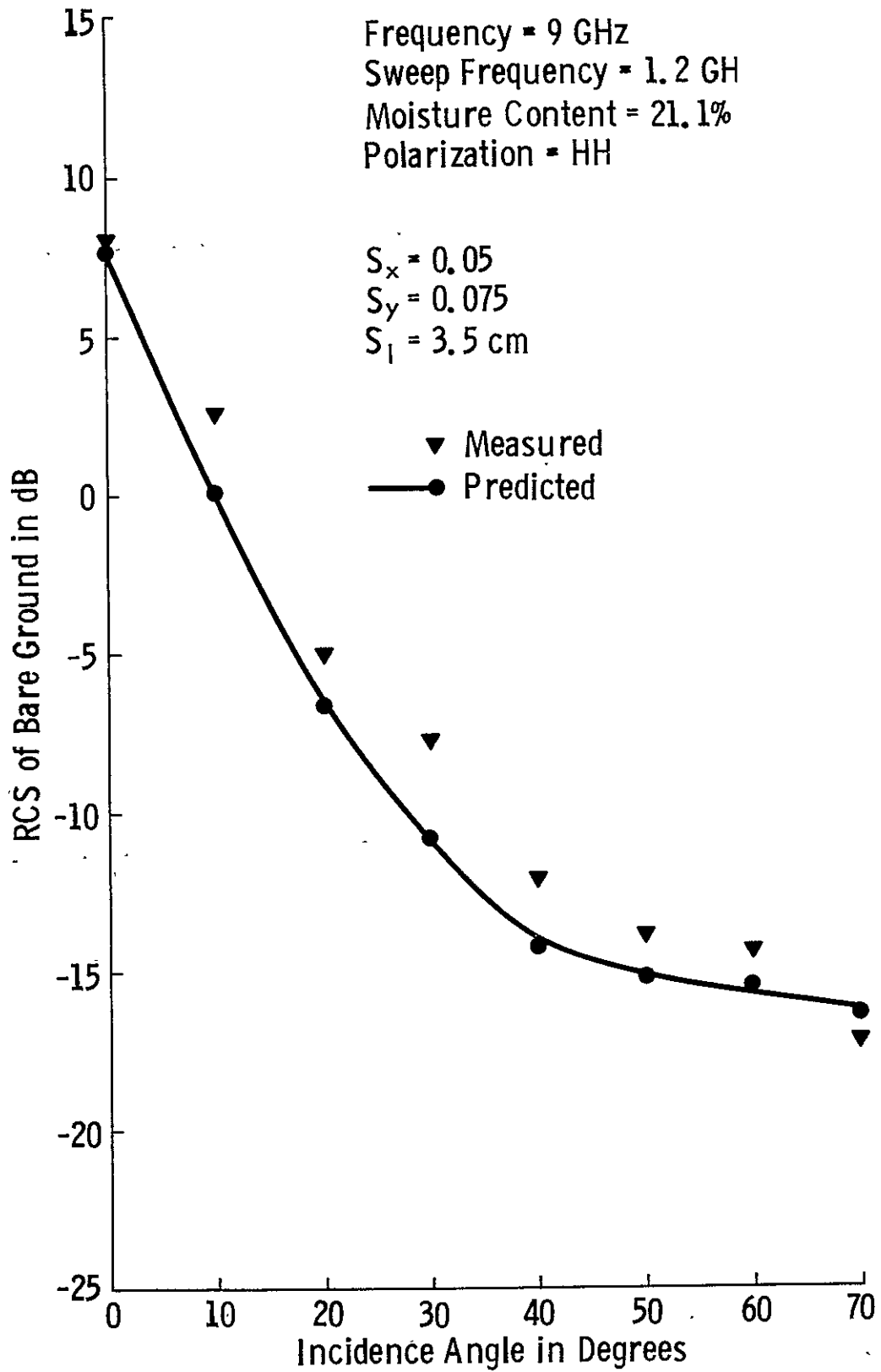


Figure 44. RCS of bare ground; moisture content = 21.1%, frequency = 9 GHz, polarization = HH.

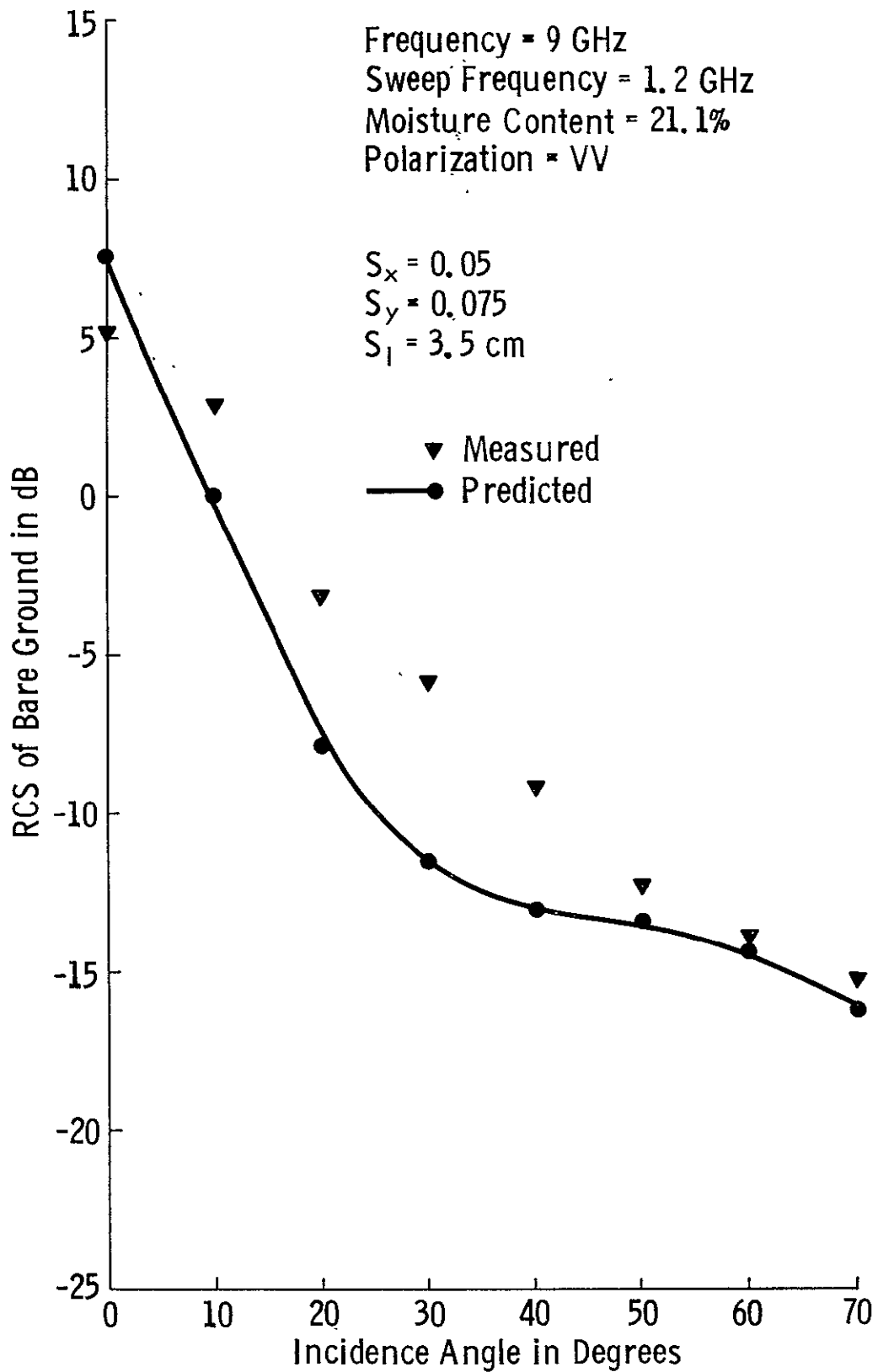


Figure 45. RCS of bare ground; moisture content = 21.1%, frequency = 9 GHz, polarization = VV.

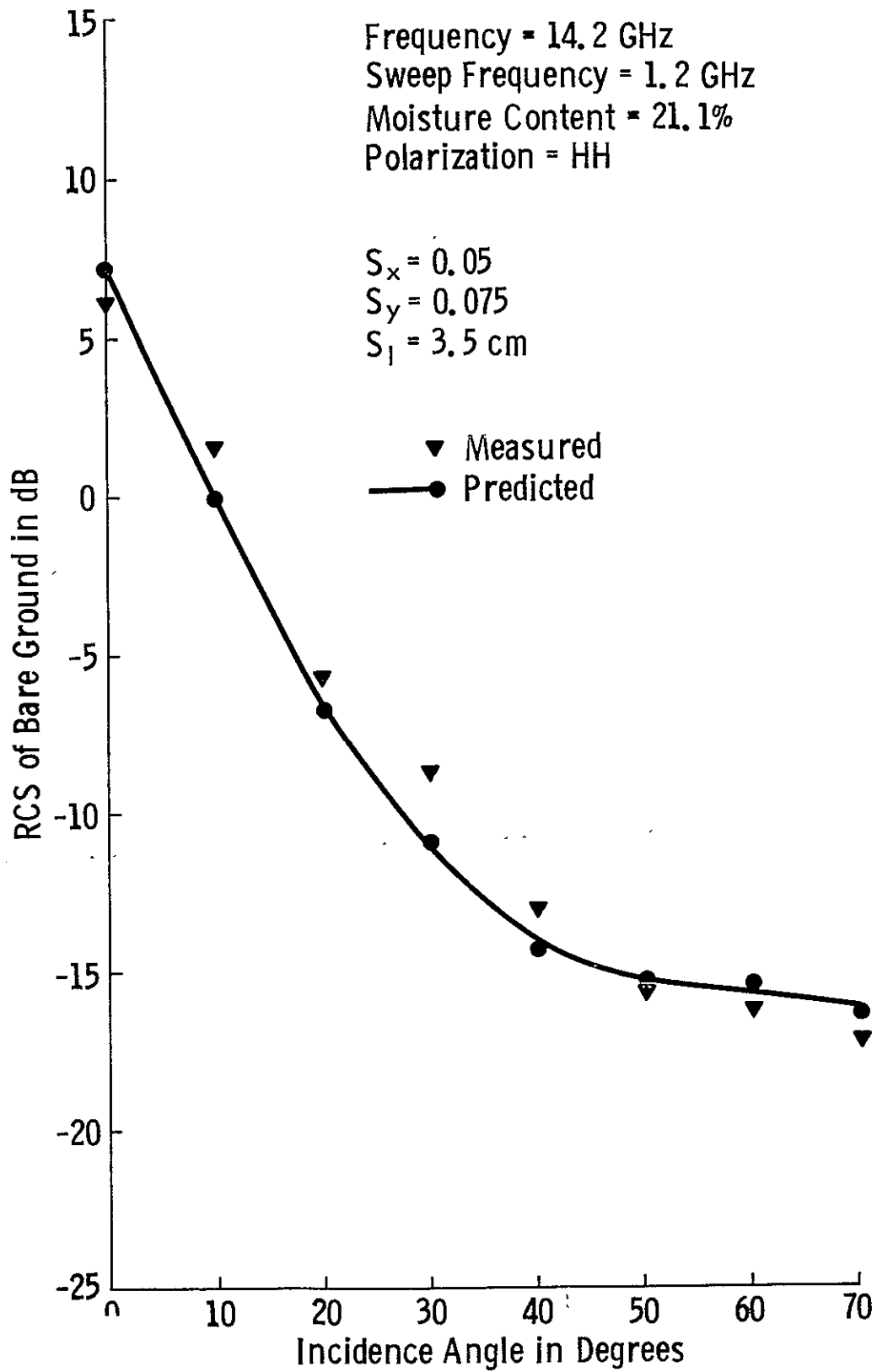


Figure 46. RCS of bare ground; moisture content = 21.1%, frequency = 14.2 GHz, polarization = HH.

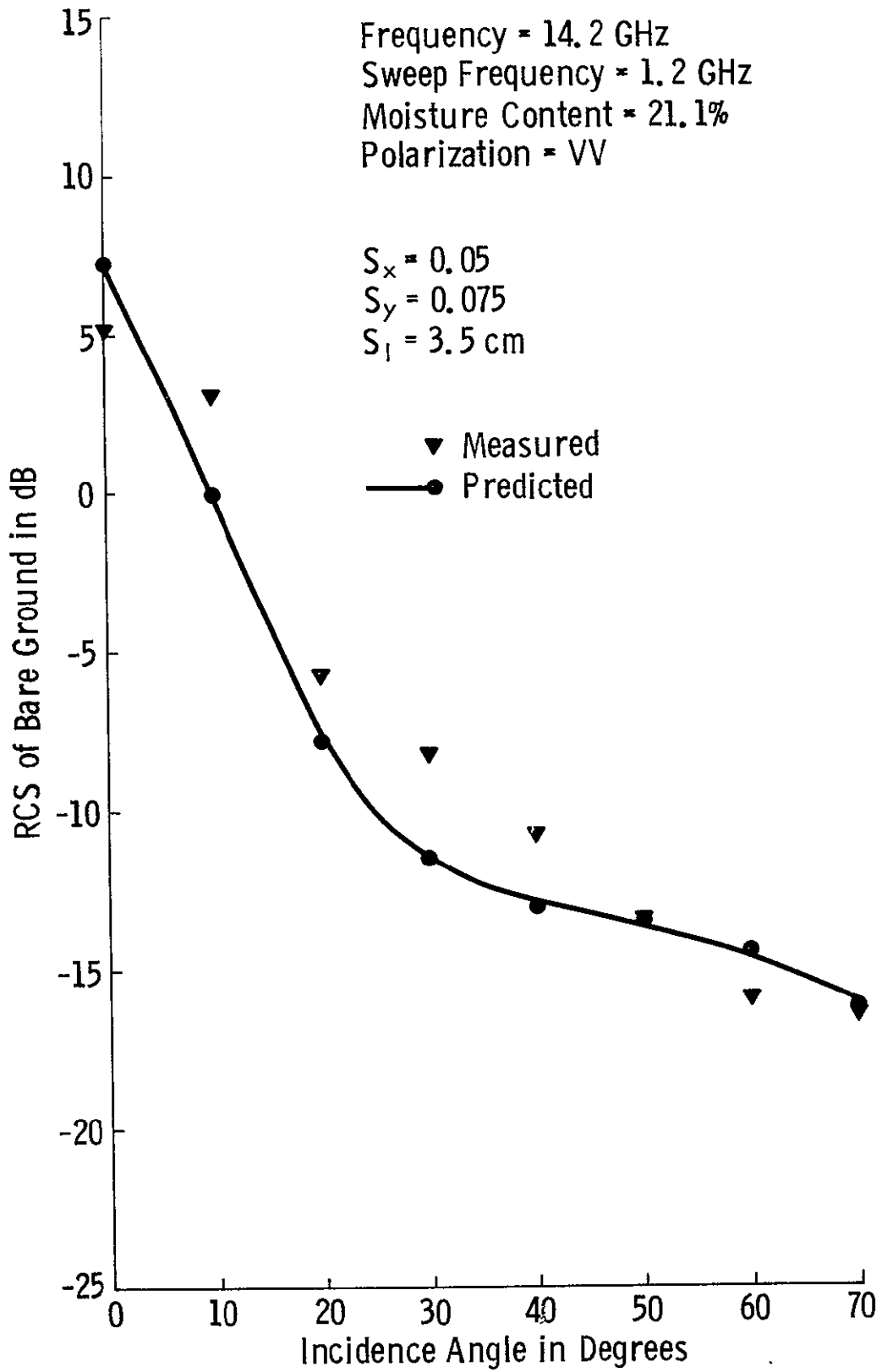


Figure 47. RCS of bare ground; moisture content = 21.1%, frequency = 14.2 GHz, polarization = VV.

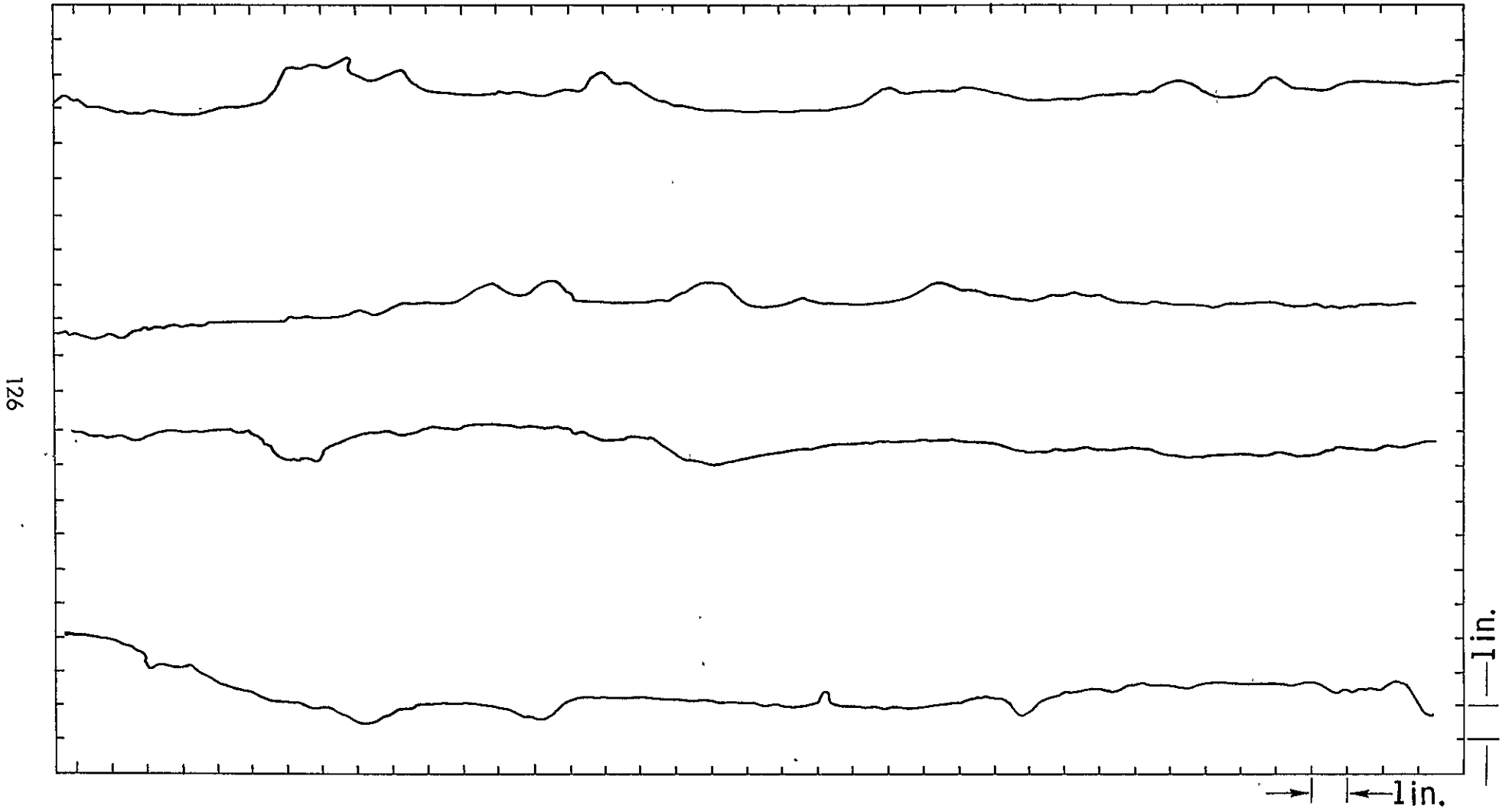


Figure 48. Four samples of ground contour. Moisture content = 17.8%.



Field No. 1
Average Moisture Content = 5.9%
(First 2.5 cm)



Field No. 2
Average Moisture Content = 9.4%
(First 2.5 cm)



Field No. 3
Average Moisture Content = 17.8%
(First 2.5 cm)
Standard Deviation of Slope = 0.07



Field No. 4
Average Moisture Content = 21.1%
(First 2.5 cm)

Plate 1. Photographs of bare fields
at four different dates.

5.3 Comparison of Facet Model with Katzin's Facet Model

As stated earlier Katzin assumes that the target is composed of small and large facets and the return power is the sum of the return from each category.

For large facet

$$\sigma_L = \frac{K^2}{\pi} \int_{A_1}^{A_2} A^2 P(A) \iint_{-\infty}^{\infty} \gamma^2 p(z_x, z_y) \left(\frac{\sin Bl}{Bl} \right)^2 \times \left(\frac{\sin c\mu}{c\mu} \right)^2 dz_x dz_y dA$$

(5-13)

where

$$\gamma = \cos \theta + Z_y \sin \theta$$

$$Bl = Ka Z_x \cos \theta$$

$$c\mu = Kb(-Z_y \cos \theta + \sin \theta)$$

$$K = 2\pi/\lambda$$

$$\lambda = \text{wavelength}$$

$P(A)$ = probability distribution function of the area of the facet.

$P(Z_x, Z_y)$ = joint probability distribution function of the slopes in x and y directions

A_1 = the transition area from small to large which is equal to $.1104\lambda^2$

then by assuming that the slope has a Gaussian distribution:

$$p(z_x, z_y) = \frac{1}{2\pi s_x s_y} \exp\left[-\frac{z_x^2}{2s_x^2} - \frac{z_y^2}{2s_y^2}\right] \quad (5-14)$$

$$\bar{\sigma}_L = \int_{A_1}^{A_2} A^2 p(A) \frac{K^2}{\pi} G dA \quad (5-15)$$

where

$$G \triangleq \frac{\pi}{2 s_x s_y K^2 A} \exp\left[-\frac{\tan^2 \theta}{2 s_y^2}\right] (1 + \tan^4 \theta) \cdot \left[1 - \frac{1}{\sqrt{2\pi} K A^{1/2} \cos \theta}\right] \quad (5-16)$$

In Eq. (5-16) we can define g_1 and g_2 such that:

$$\frac{K^2}{\pi} G \triangleq g_1 A^{-1} + g_2 A^{-3/2} \quad (5-17)$$

where

$$g_1 \triangleq \frac{e^{-\tan^2 \theta / 2s_y^2}}{2s_x s_y} (1 + \tan^4 \theta) \quad (5-18)$$

$$g_2 \triangleq - \frac{g_1 \lambda}{(2\pi)^{3/2} \sin \theta s_x} \quad (5-19)$$

then from Eq. (5-15)

$$\sigma_L = \int_{A_1}^{A_2} A^2 p(A) [g_1 A^{-1} + g_2 A^{-3/2}] dA \quad (5-20)$$

The return from the small facet is assumed to be in the Rayleigh region, hence

$$\sigma_s = \int_{A_0}^{A_1} g_0 \frac{A^3}{\lambda^4} p(A) dA \quad (5-21)$$

where

$$g_0 \triangleq \frac{4^5}{9} \quad (5-22)$$

A_1 and $P(A)$ are the same as defined in Eq. (5-13).

Then the return from the target will be

$$\begin{aligned}
 \bar{\sigma} &= \bar{\sigma}_S + \bar{\sigma}_L \\
 &= \int_{A_1}^{A_2} A^2 p(A) \left[g_1 A^{-1} + g_2 A^{-3/2} \right] dA \\
 &\quad + \frac{g_0}{\lambda^4} \int_{A_0}^A A^3 p(A) dA
 \end{aligned} \tag{5-23}$$

Now Katzin assumes that the distribution of the facet area is

$$p(A) = N_0 A^{-m} \tag{5-24}$$

If we substitute this relation in Eq. (5-23)

$$\begin{aligned}
 \bar{\sigma} &= N_0 \left\{ \frac{g_0}{\lambda^4} \int_{A_0}^{A_1} A^{-\frac{n-2}{2}} dA + g_1 \int_{A_1}^{A_2} A^{-\frac{n+2}{2}} dA + \right. \\
 &\quad \left. + g_2 \int_{A_1}^{A_2} A^{-\frac{n+3}{2}} dA \right\}
 \end{aligned} \tag{5-25}$$

where

$$n \triangleq 2m-4 \quad (5-26)$$

m is the same as in Eq. (5-24).

For the case that $n \neq 0$ & $n \neq 4$, i.e. $m \neq 2$ & $m \neq 4$, Eq. 5-25 becomes

$$\begin{aligned} \bar{\sigma} = 2N_0 \left\{ \frac{g_0}{4-n} \lambda^{-4} \left(A_1^{\frac{4-n}{2}} - A_0^{\frac{4-n}{2}} \right) + \frac{g_1}{n} \times \left(A_1^{-\frac{n}{2}} - A_2^{-\frac{n}{2}} \right) + \right. \\ \left. + \frac{g_2}{n+1} \left(A_1^{-\frac{n+1}{2}} - A_2^{-\frac{n+1}{2}} \right) \right\} \end{aligned} \quad (5-27)$$

When $n = 0$, then

$$\begin{aligned} \bar{\sigma} = 2N_0 \left\{ \frac{g_0}{4} \lambda^{-4} (A_1^2 - A_0^2) + g_1 \ln \frac{A_2}{A_1} + \right. \\ \left. + g_2 \left(A_1^{-1/2} - A_2^{-1/2} \right) \right\} \end{aligned} \quad (5-28)$$

and when $n = 4$

$$\begin{aligned} \bar{\sigma} = 2N_0 \left\{ g_0 \lambda^{-4} \ln \frac{A_1}{A_0} + \frac{g_1}{4} (A_1^{-2} - A_2^{-2}) + \right. \\ \left. \frac{g_2}{5} \left(A_1^{-5/2} - A_2^{-5/2} \right) \right\} \end{aligned} \quad (5-29)$$

The problem with these equations is that they sometimes give results which are not acceptable. For example in Eq. 5-29 when the smallest facet of the target goes to zero σ goes to infinity, or in some cases one gets a negative number for σ from Eqs. (5-27) and (5-28).

One other problem is that Katzin does not take into consideration the case that the target is not perfectly conducting, so in order to compare his results with the measured data we have to only look at the shape of the curves not their level.

In what follows we have calculated Eqs. (5-27), (5-28), and (5-29) for different values of the parameters; frequency, the size of largest facet, the size of smallest facet, shape of the facet distribution function, and standard deviations of the slope in x and y direction. If we compare these results as shown in Figures 49 and 50 with the value of the measured RCS which have been shown in Figures 32 through 47, we see that Katzin's model predicts the return from the bare ground very poorly. One important point is that for incidence angle range 20° - 50° the measured data has a positive curvature, and this is the same as the result predicted by our model, while Katzin's model gives us a negative curvature; so fitting Katzin's model to the data is not possible.

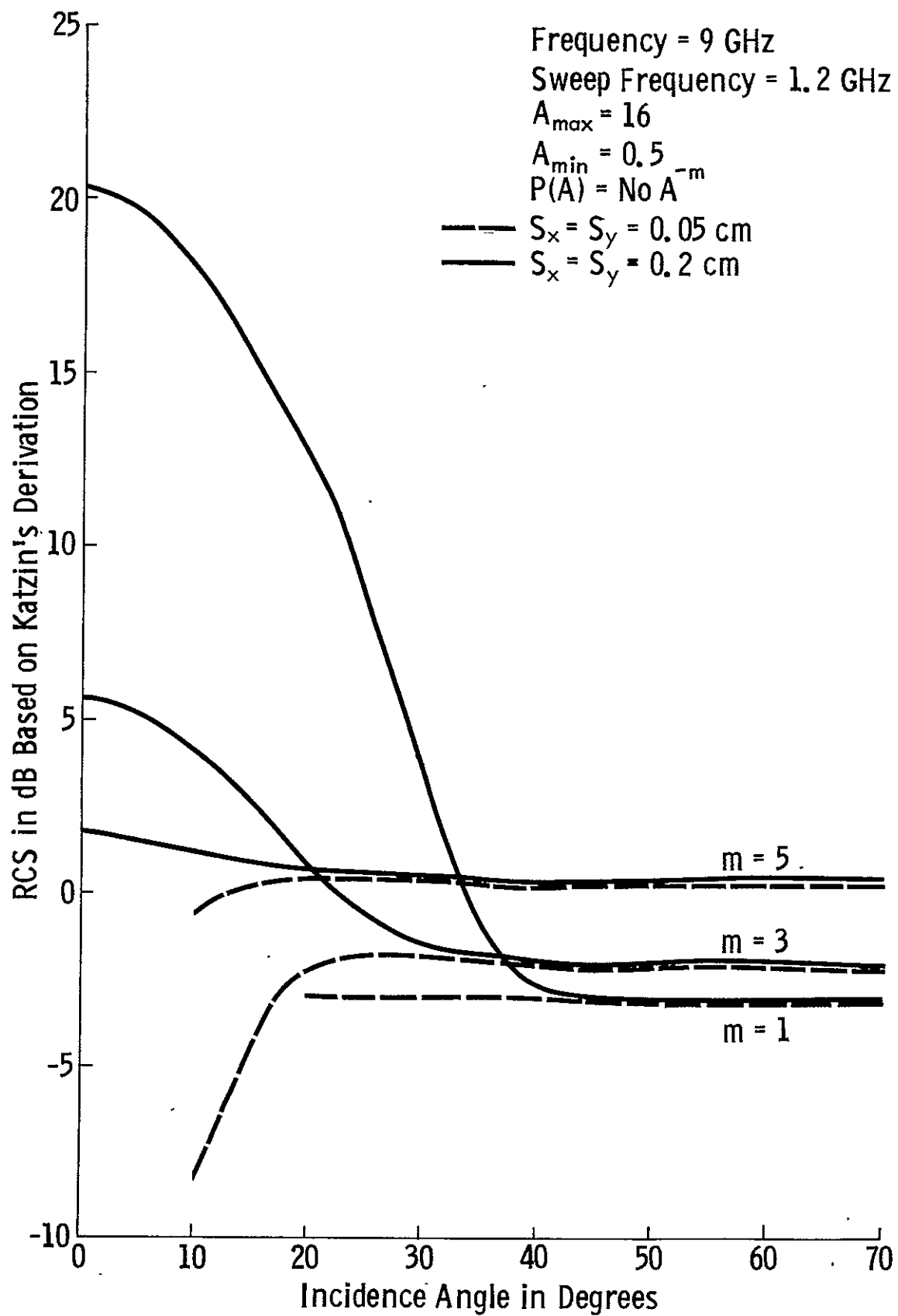


Figure 49. RCS based on Katzin's derivation.

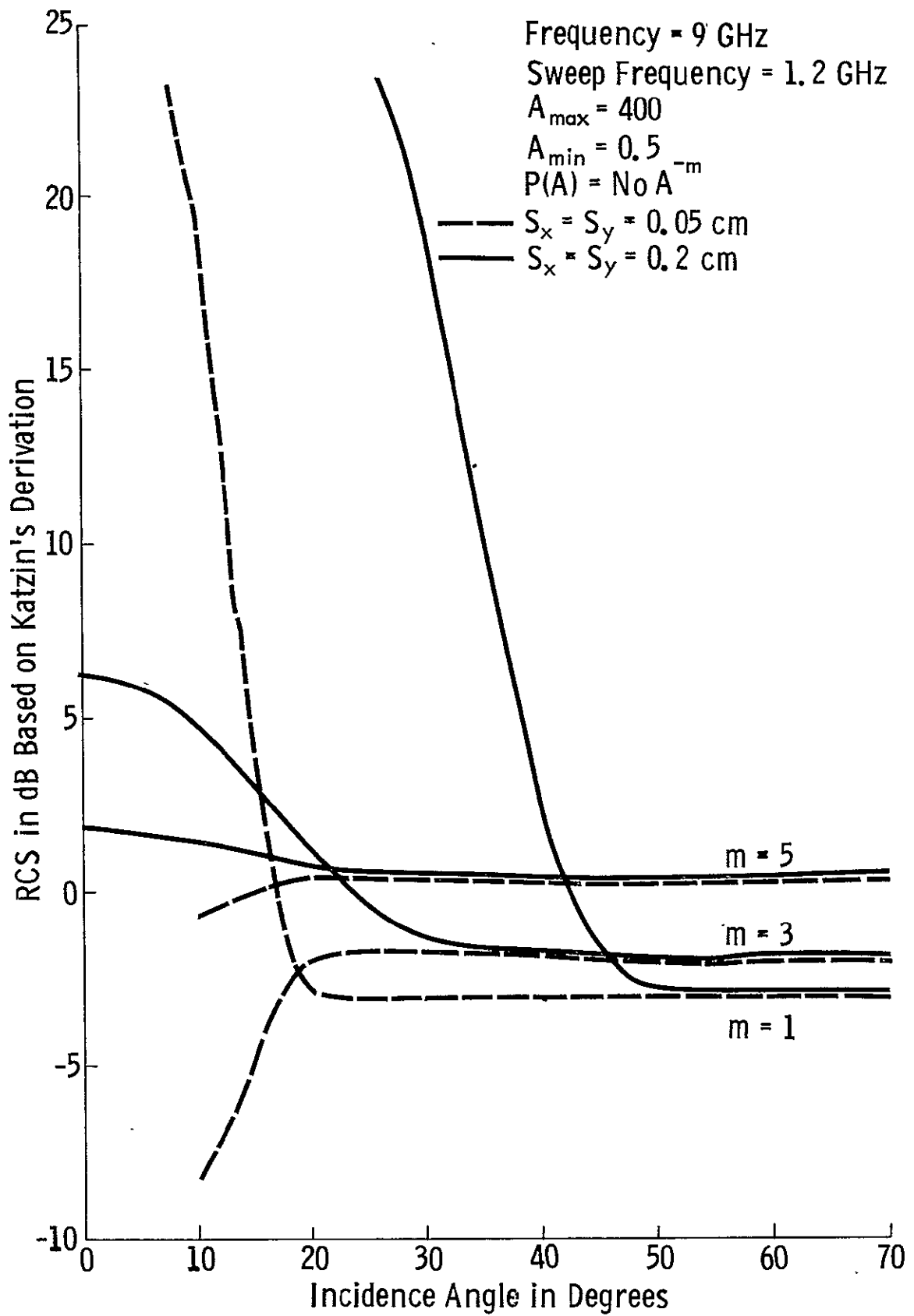


Figure 50. RCS based on Katzin's derivation.

6.0 CONCLUSION

Theoretical work was conducted to investigate the radar return terrain. The target area was modeled as a collection of facets described in terms of facet size and slope distribution.

The facet model was used to calculate the radar cross section of bare ground and the effect of frequency averaging on the reduction of the variance of the return.

Starting with the results obtained by Katzin [8] it was shown that when he divides the facets into two categories, small and large, he actually groups not only the medium size facets but also some of the small facets as large. So we divided the facets into three categories, small, medium and large. Katzin in his derivation assumes some distribution function for the area, because getting an experimental function for area is very difficult we changed the distribution function of the area to the distribution function of the length and width. We also introduced an effective reflection coefficient in our equations in order to be able to compare the result of the theory with the measured data.

We showed that by assuming that the distribution of the slope is Gaussian, and by assuming that the distribution of the length of the facet is in the form of the positive side of a Gaussian distribution, the results are in better agreement with experimental data than Katzin's model.

We also showed that for this calculation we do not need to know the exact correlation length of the small structure on the ground and introduced an effective correlation length which is only a function of the wavelength, i.e. the radar wave has some smoothing effect. The comparison of the theory and the measured data shows that our conclusion is correct.

We showed that at near zero incidence angles in both polarizations the major part of the return is due to large facets but at larger incidence angles it depends on the polarization, i.e. for HH polarization medium size facets have a major role in the return while in VV polarization, the small facets contribute the most.

So by knowing the level of the return at large incidence angles for HH, and VV polarization, and by knowing the shape and level of the return as a function of

angle near nadir we are able to, respectively, calculate standard deviation of the facet size, moisture content, standard deviation of the slope in y direction, and standard deviation in the x direction.

In the second section of the work, namely the prediction of the number of independent samples due to frequency averaging, we started from Waite's, [26] uniform scatterer model and extended it and took into consideration the penetration effect. Comparison with data taken from alfalfa shows good agreement. We then assumed that the target consists of a collection of two dimensional facets and calculated the number of independent samples. Comparison with the data taken from the bare ground reveals that our result is correct for large incidence angles but at small incidence angles, both due to the limited number of available data points and the assumption of the equality of the mean and the variance in a single frequency, the facet model cannot predict the same number of independent samples calculated based on the measured data.

We showed that based on the facet model assumption the reduction in the variance of the returned signal is not only a function of the product of the sweep band and the time span of the target, as small scatterer model indicates, but it is also a function of the surface properties—distributions of the slopes and facet size—, center frequency of the incident wave, and the polarization.

REFERENCES

- [1] Abramowitz, M., Handbook of the Mathematical Functions, I. Stegun (Editor), U. S. Department of Commerce, August, 1966.
- [2] Barrick, D., "Rough Surface Scattering Based on the Specular Point Theory," IEEE Trans. on Antennas and Propagation, vol. 16, no. 4, pp. 449-454, July, 1968.
- [3] Bush, T. F. and F. T. Ulaby, "Fading Characteristics of Panchromatic Radar Backscatter from Selected Agricultural Targets," RSL Technical Report 177-48, University of Kansas Center for Research, Inc., Lawrence, December, 1973.
- [4] Cook, C. and M. Bernfeld, Radar Signals, Academic Press, New York, p. 137, 1967.
- [5] Fung, A. K., "A Review of Rough Surface Scattering Theories," CRES Technical Report 105-10, University of Kansas Center for Research, Inc., Lawrence, May, 1971.
- [6] Janza, F., Sandia Corporation Report SCR-533, 1963.
- [7] Katzin, M., "On Mechanism of Radar Sea Clutter," IRE Proceedings, vol. 44, pp. 44-54, January, 1957.
- [8] Katzin, M., "Sea Clutter at High Depression Angles with Application to the Grand Clutter Problem," Proc. 1959 Radar Return Symposium.
- [9] Kodis, R., "A Note on the Theory of Scattering from an Irregular Surface," IEEE Trans. on Antennas and Propagation, vol. 14, no. 1, pp. 77-82, January, 1966.
- [10] Latti, B., An Introduction to Random Signals and Communication Theory, International Textbook Company.
- [11] Longuet-Higgin, M., "Reflection and Refraction at a Random Moving Surface," Jour. Opt. Soc., vol. 50, pp. 838-855, September, 1960.
- [12] Longuet-Higgin, M., "The Statistical Analysis of Random Moving Surface," Phil. Trans. Roy. Soc. of London, vol. A249, pp. 321, 1956.
- [13] Moore, R., W. Waite, and J. Rouse, Jr., "Panchromatic and Polypanchromatic Radar," Proc. IEEE, vol. 57, no. 4, pp. 590-594, April, 1969.
- [14] Peak, W., "Theory of Radar Return from Terrain," IRE Intl. Conv. Record 7, part 1:27, 1959.
- [15] Papoulis, A., Probability, Random Variables, and Stochastic Processes, McGraw-Hill Book Company.

- [16] Rice, S., "Mathematical Analysis of Random Noise," Bell System Technical Journal, vol. 23, 1944.
- [17] Rice, S., "Reflection of Electromagnetic Waves from Slightly Rough Surface," in: Kline, M. The Theory of Electromagnetic Waves, Dover Company, New York.
- [18] Ruck, T., D. Barrick, W. Stuart, and C. Kirchbaum, Radar Cross Section Handbook, Vol. 1, Plenum Press.
- [19] Ruck, T., D. Barrick, W. Stuart, and C. Kirchbaum, Radar Cross Section Handbook, Vol. 2, Plenum Press.
- [20] Seltzer, J., "A Modified Specular Point Theory for Radar Backscatter," Ph. D. Thesis, Purdue University, 1971.
- [21] Skolnik, M., Introduction to Radar Systems, McGraw-Hill Book Company, New York, p. 264, 1962.
- [22] Spetner, L. and I. Katz, "Two Statistical Models for Radar Terrain Return," IRE Trans. on Antennas and Propagation, vol. 8, pp. 242-246, May, 1960.
- [23] Stratton, J., Electromagnetic Theory, McGraw-Hill Book Company, pp. 493-496, 1941.
- [24] Struik, D., Differential Geometry, pp. 55-88, 1961.
- [25] Ulaby, F. T., J. Cihlar and R. K. Moore, "Active Microwave Measurements of Soil Water Content," Journal of Remote Sensing, January, 1975.
- [26] Waite, W. P., "Broad-Spectrum Electromagnetic Backscatter," CRES Technical Report 133-17, University of Kansas Center for Research, Inc., Lawrence, August, 1970.

APPENDIX A

KATZIN'S ASSUMPTION

From physical optics, the RCS for a large circular disk with a diameter D is given

$$\bar{\sigma} = \frac{4\pi A^2}{\lambda^2} \left[\frac{2 \sin \theta_g \text{J}_1(2\pi D \cos \theta_g / \lambda)^2}{2\pi D \cos \theta_g / \lambda} \right] \quad (\text{A-1})$$

where θ_g is the grazing angle.

Figure A-1 shows that for $x > 8$ $y = \left(\frac{\text{J}_1(x)}{x/2} \right)^2$ has an envelope defined by the equation $y = 8/\pi x^3$. Hence its value on the average over x will be equal to half of the value of the envelope, i.e. $4/\pi x^3$.

So for the case when $2\pi D/\lambda \cos \theta_g > 8$ i.e.

- (i) θ_g is small
- (ii) $D > \lambda$

We can approximate $\left(\frac{\text{J}_1(x)}{x/2} \right)^2$ by $4/\pi x^3$ and obtain the average RCS.

$$\bar{\sigma} = \frac{4\pi A^2}{\lambda^2} \sin^2 \theta_g \times \frac{4}{\pi \left(\frac{2\pi D \cos \theta_g}{\lambda} \right)^3} \quad (\text{A-2})$$

By substituting the relation for the area of a circular disk,

$$\bar{\sigma} = \frac{\sin^2 \theta_g}{\cos^3 \theta_g} \times \frac{1}{4\pi^{3/2}} \lambda A^{1/2} \quad (\text{A-3})$$

or

$$\frac{\bar{\sigma}}{A} = \frac{\sin^2 \theta_g}{4\pi^{3/2} \cos^3 \theta_g} \left(\frac{A}{\lambda^2} \right)^{-1/2} \quad (\text{A-4})$$

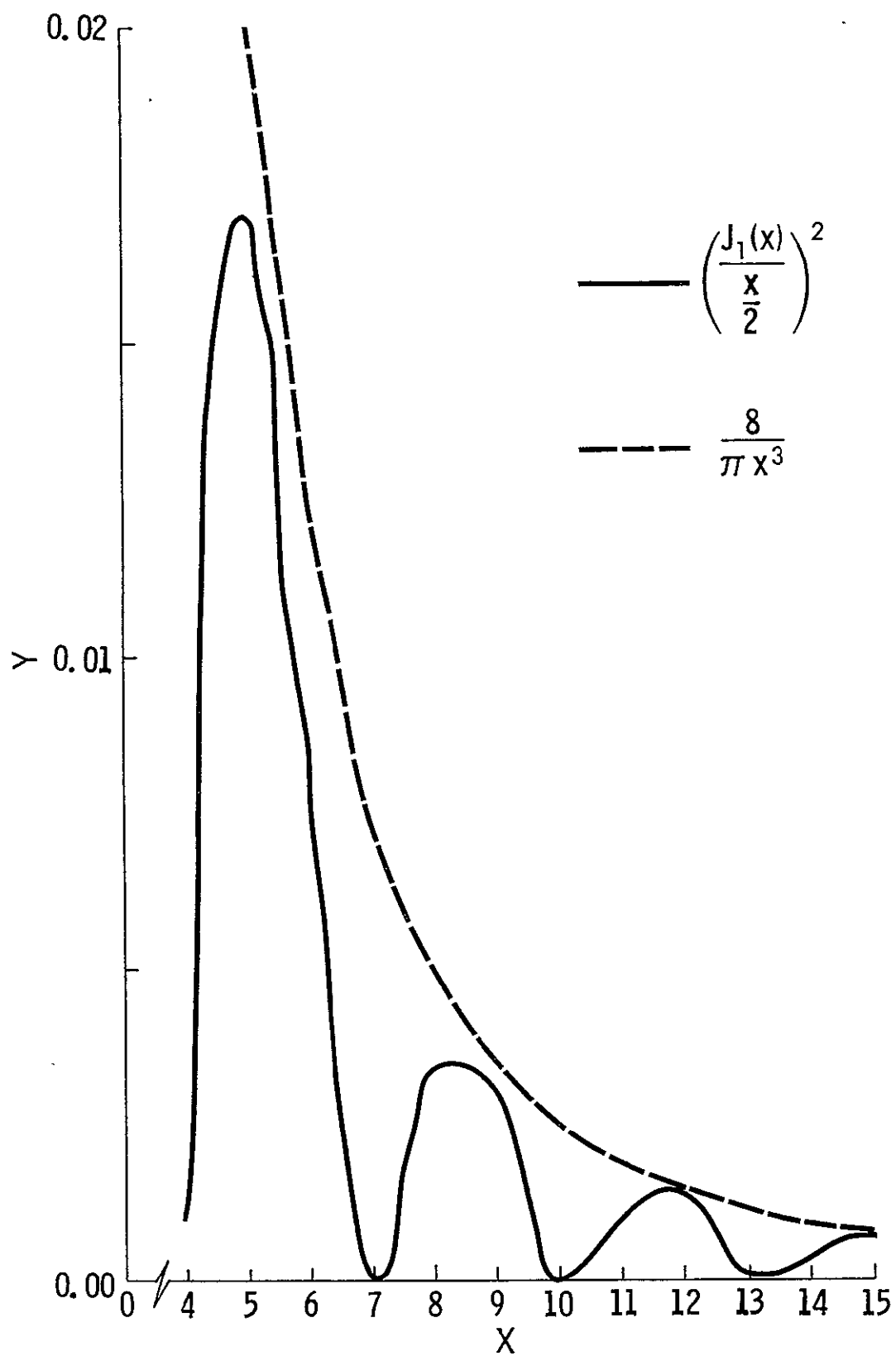


Figure A-1. Radar cross section of a large circular disk.

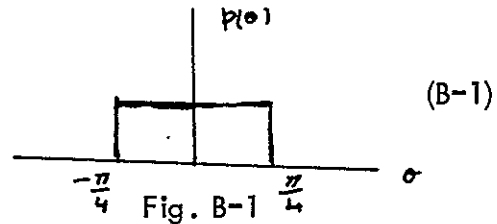
APPENDIX B

RMS HEIGHT FOR SMALL FACETS

We would like to calculate the r.m.s. height of small facets. Because from the assumption of the small perturbation technique $\frac{\partial z}{\partial x} < 1$, we assume that the angle is uniformly distributed between $-\frac{\pi}{4}$ and $\frac{\pi}{4}$, i.e.

$$p(\theta) = \frac{2}{\pi} \quad \frac{\pi}{4} \geq \theta \geq -\frac{\pi}{4}$$

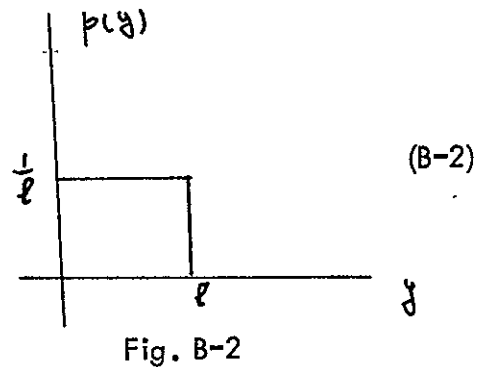
$$= 0 \quad \text{otherwise}$$



then because the distribution of the length of the facet is assumed to be Gaussian and because the length of the facets is small compared to the standard deviation of the facet distribution then we assume that it is uniform, i.e.

$$p(y) = \frac{1}{l} \quad l \geq y \geq 0$$

$$= 0 \quad \text{otherwise}$$



We know that

$$h = y \sin \alpha$$

(B-3)

If we assume that

$$x \triangleq \sin \theta \tag{B-4}$$

$$h = \gamma x$$

then,

$$p(x) = \frac{p(\theta)}{\left| \frac{dx}{d\theta} \right|} \Big|_{\theta = \arcsin x} \tag{B-5}$$

$$= \frac{\frac{2}{\pi}}{\sqrt{1-x^2}} \quad \frac{1}{\sqrt{2}} \geq x \geq -\frac{1}{\sqrt{2}}$$

$$P[h < \alpha] = \int_{-\frac{1}{\sqrt{2}}}^{\frac{\alpha}{l}} p_x(x) \int_{\frac{\alpha}{x}}^l p(y) dy dx \tag{B-6}$$

$$= \int_{-\frac{1}{\sqrt{2}}}^{\frac{\alpha}{l}} \frac{2/\pi}{\sqrt{1-x^2}} \int_{\frac{\alpha}{x}}^l \frac{1}{l} dy dx$$

$$= \frac{2}{\pi l} \int_{-\frac{1}{\sqrt{2}}}^{\frac{\alpha}{l}} \frac{l - \frac{\alpha}{x}}{\sqrt{1-x^2}} dx$$

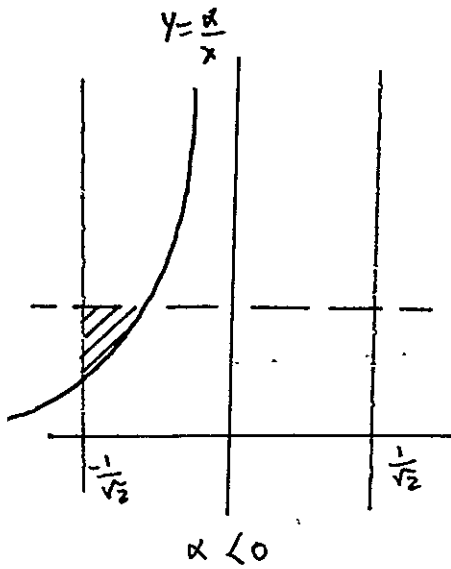


Figure B-3

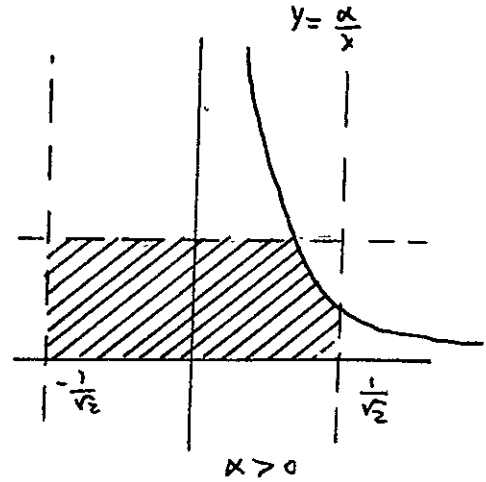


Figure B-4

$$\begin{aligned}
 f(\alpha) &= \frac{dP[h(\alpha)]}{d\alpha} = \frac{P[h(\alpha+\Delta\alpha)] - P[h(\alpha)]}{\Delta\alpha \rightarrow 0} \\
 \alpha < 0 &= \frac{d}{d\alpha} \left[\frac{2}{\pi l} \int_{-\frac{1}{\sqrt{2}}}^{\frac{\alpha+\Delta\alpha}{l}} \frac{l - \frac{\alpha+\Delta\alpha}{x}}{\sqrt{1-x^2}} dx - \frac{2}{\pi l} \int_{-\frac{1}{\sqrt{2}}}^{\frac{\alpha}{l}} \frac{l - \frac{\alpha}{x}}{\sqrt{1-x^2}} dx \right] \\
 &= \frac{2}{\pi l \Delta\alpha} \left[\int_{\frac{\alpha}{l}}^{\frac{\alpha+\Delta\alpha}{l}} \frac{l - \frac{\alpha}{x}}{\sqrt{1-x^2}} dx - \int_{-\frac{1}{\sqrt{2}}}^{\frac{\alpha+\Delta\alpha}{l}} \frac{\Delta\alpha/x}{\sqrt{1-x^2}} dx \right] \\
 &= \frac{2}{\pi l} \int_{-\frac{\alpha}{l}}^{\frac{1}{\sqrt{2}}} \frac{dx}{x\sqrt{1-x^2}} \tag{B-7}
 \end{aligned}$$

For the case that $\alpha > 0$ the result will be in the same form and the only change will be to substitute α in place of $-\alpha$. So the probability density for will be

$$p(\alpha) = \frac{2}{\pi l} \int_{\frac{|\alpha|}{l}}^{\frac{1}{\sqrt{2}}} \frac{dx}{x\sqrt{1-x^2}} \quad \frac{l}{\sqrt{2}} \geq \alpha \geq -\frac{l}{\sqrt{2}} \quad (\text{B-8})$$

$$\langle h^2 \rangle = \int_{-\infty}^{\infty} \alpha^2 p(\alpha) d\alpha = \int_{-\frac{l}{\sqrt{2}}}^{\frac{l}{\sqrt{2}}} \int_{\frac{|\alpha|}{l}}^{\frac{1}{\sqrt{2}}} \frac{2}{\pi l} \frac{\alpha^2}{x\sqrt{1-x^2}} dz d\alpha \quad (\text{B-9})$$

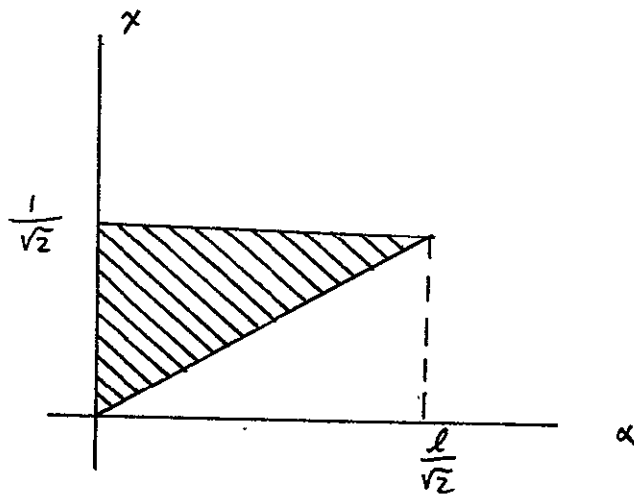


Figure B-5

Because what we are doing is actually integrating over shaded area in Figure B-5 so we can change the order of integration and will have

$$\begin{aligned}
 \langle h^2 \rangle &= \frac{4}{\pi l} \int_0^{\frac{1}{\sqrt{2}}} \frac{1}{x \sqrt{1-x^2}} \int_0^{lx} x^2 dx dx \\
 &= \frac{4}{\pi l} \int_0^{\frac{1}{\sqrt{2}}} \frac{l^3 x^3}{3x \sqrt{1-x^2}} dx \\
 &= \frac{4l^2}{3\pi} \int_0^{\frac{1}{\sqrt{2}}} \frac{x^2}{\sqrt{1-x^2}} dx
 \end{aligned}
 \tag{B-10}$$

If we substitute

$$\begin{aligned}
 x &\triangleq \sin \theta \\
 \langle h^2 \rangle &= \frac{4l^2}{3\pi} \int_0^{\frac{\pi}{4}} \frac{\sin^2 \theta \cos \theta d\theta}{\cos \theta} \\
 &= \frac{4l^2}{3\pi} \int_0^{\frac{\pi}{4}} \sin^2 \theta d\theta \\
 &= l^2 \cdot \frac{\frac{\pi}{2} - 1}{3\pi}
 \end{aligned}
 \tag{B-11}$$

$$\begin{aligned} \text{r.m.s of } h &= l \sqrt{\frac{\frac{\lambda}{2} - 1}{3\pi}} \approx \frac{l}{4} \\ &= \frac{2\lambda/5}{4} = \frac{\lambda}{10} \end{aligned}$$

(B-12)

APPENDIX C

CORRELATION RADIUS OF SMALL FACETS

We would like to calculate the correlation radius for the small facets.
The auto-correlation function of the surface is defined to be

$$R(\tau) = \langle x(t) x(t+\tau) \rangle \quad (\text{C-1})$$

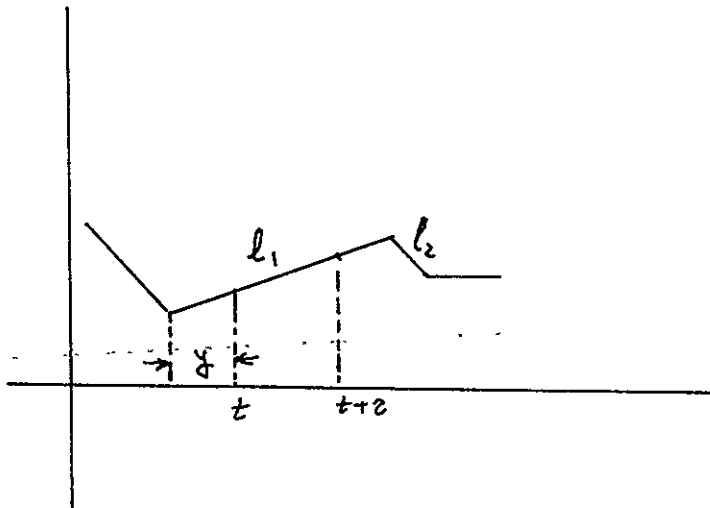


Figure C-1

From Fig. C-1 if the distance of τ is in a way that t and $t+\tau$ are not on the same facet then from the basic assumption of the facet model, indicating that the facets are independent, we know that

$$\langle x(t) x(t+\tau) \rangle = 0. \quad (\text{C-2})$$

So in order to contribute to the average of Eq. (C-1)

$$z \leq l_1 - y \quad (C-3)$$

where

l_1 = length of the facet

y = the distance between point t and the first point of the facet

Because the distribution of y over the facet l_1 is uniform, i.e.

$$P(y) = \frac{1}{l_1} \quad l_1 > y > 0 \quad (C-4)$$
$$= 0 \quad \text{otherwise}$$

then

$$P[z \leq l_1 - y] = \frac{1}{l_1} [l_1 - z] \quad (C-5)$$

l_1 is the length of the facet and has a Gaussian distribution, i.e.

$$p(l_1) = \frac{1}{\sigma \sqrt{2\pi}} \exp\left[-\frac{l_1^2}{2\sigma^2}\right] \quad (C-6)$$

So by using Eqs. (C-5) and (C-6) in Eq. (C-1)

$$R(z) \sim \int_z^{\beta} \frac{1}{l_1} [l_1 - z] e^{-\frac{l_1^2}{2\sigma^2}} dl_1 \quad (C-7)$$

where z is the correlation distance and β is the size of the largest facet in the small facet category. By assumption stated in Chapter 3

$$\beta = \frac{2\lambda}{5}$$

So from Eq. (C-7) by putting $z = l_1 / \sigma\sqrt{2}$

$$R(z) \sim \int_{\frac{z}{\sigma\sqrt{2}}}^{\frac{2\lambda/5}{\sigma\sqrt{2}}} \left[1 - \frac{z}{\sigma\sqrt{2} z} \right] e^{-z^2} dz \quad (C-8)$$

Because

$$\frac{2\lambda}{5} / \sigma\sqrt{2} \quad (C-9)$$

$$e^{-z^2} = 1 - z^2 \quad (C-10)$$

then from Eq. (C-8)

$$R(z) \sim \int_{\frac{z}{\sigma\sqrt{2}}}^{\frac{2\lambda/5}{\sigma\sqrt{2}}} \left[1 - \frac{e}{z\sigma\sqrt{2}} \right] [1-z^2] dz \quad (\text{C-11})$$

or

$$R(z) \sim B - A - A \ln \frac{B}{A} + \frac{A}{2} (B^2 - A^2) - \frac{1}{3} (B^3 - A^3) \quad (\text{C-12})$$

where

$$B \triangleq \frac{2\lambda/5}{\sigma\sqrt{2}} \quad (\text{C-13})$$

$$A \triangleq \frac{e}{\sigma\sqrt{2}} \quad (\text{C-14})$$

then because both A and B are small

$$R(z) = B - A - A \ln \frac{B}{A} \quad (\text{C-15})$$

From Eqs. (C-13), (C-14), (C-15) we determine z in a way that

$$\frac{R(z)}{R(0)} = e^{-1} \quad (\text{C-16})$$

or

$$\frac{B - A - A \ln \frac{B}{A}}{B} = e^{-1} \quad (\text{C-17})$$

or

$$1 - \frac{A}{B} - \frac{A}{B} \ln \frac{B}{A} = e^{-1} \quad (\text{C-18})$$

and from Eqs. (C-13) and (C-14)

$$1 - \frac{z}{2\lambda/5} - \frac{z}{2\lambda/5} \ln \frac{2\lambda/5}{z} = e \quad (\text{C-19})$$

If we put

$$z = \frac{2\lambda}{15} \quad (\text{C-20})$$

then the left hand side of Eq. (C-19) will be

$$\text{LHS} = 1 - \frac{1}{3} - \frac{1}{3} \ln 3 = .37 = e^{-1} \quad (\text{C-21})$$

so

$$z = \frac{2\lambda}{15} \quad (\text{C-22})$$

z in Eq. (C-22) is the effective correlation radius of the surface when it is looked at by a wavelength equal to λ .

APPENDIX D

EVALUATION OF THE INTEGRAL FOR LARGE FACETS

In discussing the return from large facets we have to calculate the integrals in the form of

$$w_1 = \frac{1}{p^2} \int_{-\infty}^{\infty} e^{-a^2 u^2} \frac{\sin^2 p(c+bu)}{(c+bu)^2} du \quad (D-1)$$

$$w_2 = \frac{1}{p^2} \int_{-\infty}^{\infty} u^2 e^{-a^2 u^2} \frac{\sin^2 p(c+bu)}{(c+bu)^2} du \quad (D-2)$$

$$w_3 = \frac{1}{p^2} \int_{-\infty}^{\infty} u^4 e^{-a^2 u^2} \frac{\sin^2 p(c+bu)}{(c+bu)^2} du \quad (D-3)$$

We first assume that

$$I = \int_{-\infty}^{\infty} e^{-a^2 u^2} \frac{\sin^2 p(c+bu)}{(c+bu)^2} du \quad (D-4)$$

If we integrate both sides vs. p twice the result will be equal to

$$\frac{d^2 I}{dp^2} = 2 \int_{-\infty}^{\infty} e^{-a^2 u^2} \sin 2p(c+bu) du \quad (D-5)$$

If we expand the cos term

$$\frac{d^2 I}{dp^2} = 2 \left\{ \int_{-\infty}^{\infty} e^{-a^2 u^2} \cos 2pc \cos 2pbu \, du - \int_{-\infty}^{\infty} e^{-a^2 u^2} \sin 2pc \sin 2pbu \, du \right\} \quad (D-6)$$

Because the integrand of the second integral is an odd function of u the result is zero. So

$$\begin{aligned} \frac{d^2 I}{dp^2} &= 2 \cos 2pc \int_{-\infty}^{\infty} e^{-a^2 u^2} \cos 2pbu \, du \\ &= 4 \cos 2pc \int_0^{\infty} e^{-a^2 u^2} \cos 2pbu \, du \end{aligned} \quad (D-7)$$

From the table [1]

$$\int_0^{\infty} e^{-px^2} \cos qx \, dx = \frac{1}{2} e^{-q^2/4p} \sqrt{\pi/p} \quad (D-8)$$

so

$$\frac{d^2 I}{dp^2} = 4 \cos 2pc \left[\frac{1}{2} e^{-\frac{4p^2 b^2}{4a^2}} \sqrt{\frac{\pi}{a^2}} \right] \quad (D-9)$$

By substituting the exponential for the cos function

$$\frac{d^2 I}{dp^2} = \frac{2\sqrt{\pi}}{a} \operatorname{Real} \left\{ \exp \left[- \left(\frac{pb}{a} + \frac{iac}{b} \right)^2 - \left(\frac{ac}{b} \right)^2 \right] \right\} \quad (\text{D-10})$$

By defining

$$x \triangleq \frac{pb}{a} \quad (\text{D-11})$$

$$y \triangleq \frac{ac}{b}$$

$$z \triangleq x + iy$$

Eq. (D-10) becomes

$$\frac{d^2 I}{dp^2} = \frac{2\sqrt{\pi}}{a} e^{-y^2} \operatorname{Real} \left[\exp(-z^2) \right] \quad (\text{D-12})$$

From here

$$\frac{dI}{dp} = \frac{a}{b} \frac{2\sqrt{\pi}}{a} e^{y^2} \operatorname{Real} \left[\int e^{-z^2} dz \right] \quad (\text{D-13})$$

From the table [1]

$$\frac{dI}{d\rho} = \text{Real} \left[\frac{2\sqrt{\pi}}{b} e^{y^2} \sum_{n=0}^{\infty} \frac{(-1)^n z^{2n+1}}{n! (2n+1)} \right] + K_1 \quad (\text{D-14})$$

then

$$I = \text{Real} \left\{ \frac{2\sqrt{\pi}a}{b^2} e^{-y^2} \sum_{n=0}^{\infty} \frac{(-1)^n z^{2n+2}}{n! (2n+1)(2n+2)} + K_1 P + K_2 \right\} \quad (\text{D-15})$$

where K_1 and K_2 are independent from P , or from Eq. (D-10)

$$I = \frac{2\sqrt{\pi}a}{b^2} e^{-y^2} \sum_{n=0}^{\infty} \frac{(-1)^n (x^2+y^2)^{n+1} \cos(2n+2)\varphi}{n! (2n+1)(2n+2)} + K_1 P + K_2 \quad (\text{D-16})$$

where

$$\varphi = \arctan \frac{y}{x}$$

Now we will use the boundary condition principle to calculate K_1 and K_2 .

- i) $x=0 \quad y=0$, i.e. looking at a facet with a length zero vertically. In this case the return should be zero.
- ii) $x=0 \quad y \neq 0$, i.e. looking at a facet with a length zero, in an incidence angle θ . In this case the return should also be zero.

From the above boundary conditions

$$I = \frac{2\sqrt{\pi} e^{-y^2} a}{b^2} \left[\sum_{n=0}^{\infty} \frac{(-1)^n (x^2 - y^2)^{n+1} \cos(2n+2)\theta}{n! (2n+1)(2n+2)} + \sum_{n=0}^{\infty} \frac{y^{2n+2}}{n! (2n+1)(2n+2)} \right]$$

(D-17)

and if we write this expression in the compact form

$$I = \frac{2\sqrt{\pi} e^{-y^2} a}{b^2} \left[z \operatorname{erf}(z) + z^* \operatorname{erf}(z^*) - izy \operatorname{erf}(iy) - \frac{z}{\sqrt{\pi}} e^{-\frac{y^2}{2}} (1 - e^{-z^2} \cos 2xy) \right]$$

(D-18)

and from Eq. (D-1)

$$W_1 = \frac{2\sqrt{\pi} e^{-y^2}}{ax^2} \left[z \operatorname{erf}(z) + z^* \operatorname{erf}(z^*) - izy \operatorname{erf}(iy) - \frac{z}{\sqrt{\pi}} e^{-\frac{y^2}{2}} (1 - e^{-z^2} \cos 2xy) \right]$$

(D-19)

where

$$\operatorname{erf}(z) \triangleq \frac{2}{\sqrt{\pi}} \int_0^z e^{-t^2} dt \quad (\text{D-20})$$

Now we want to calculate w_2 vs a^2 . If we differentiate both sides of Eq. (D-1)

$$\frac{\partial w_1}{\partial a^2} = \frac{1}{p^2} \int -u^2 e^{-a^2 u^2} \frac{\sin^2 p(ct+bu)}{(ct+bu)^2} du = -w_2 \quad (\text{D-21})$$

From here

$$w_2 = - \frac{d}{da^2} \left\{ \frac{2\sqrt{\pi} e^{-y^2}}{ax^2} \left[z \operatorname{erf}(z) + z^* \operatorname{erf}(z^*) - izy \operatorname{erf}(iy) - \frac{z}{\sqrt{\pi}} e^{-y^2} \cdot (-1 - e^{-x^2} \cos 2xy) \right] \right\} \quad (\text{D-22})$$

The next problem is to calculate w_3 . From Eq. (D-3) if C is zero, the integrand is an odd function of u so the result will be zero. But if C is not zero because

$$a = \frac{1}{\sqrt{2} \times \text{standard deviation of slope}} \quad (\text{D-23})$$

is very large the exponential will be very small before u gets large enough to have a significant value for $\frac{\sin^2 p(ct+bu)}{(ct+bu)^2}$.

So the result of the integral will be very small, i.e.

$$w_3 \approx 0.$$

CRINC LABORATORIES

Chemical Engineering Low Temperature Laboratory

Remote Sensing Laboratory

Flight Research Laboratory

Chemical Engineering Heat Transfer Laboratory

Nuclear Engineering Laboratory

Environmental Health Engineering Laboratory

Information Processing Laboratory

Water Resources Institute

Technical Transfer Laboratory

Air Pollution Laboratory

Satellite Applications Laboratory

CRINC